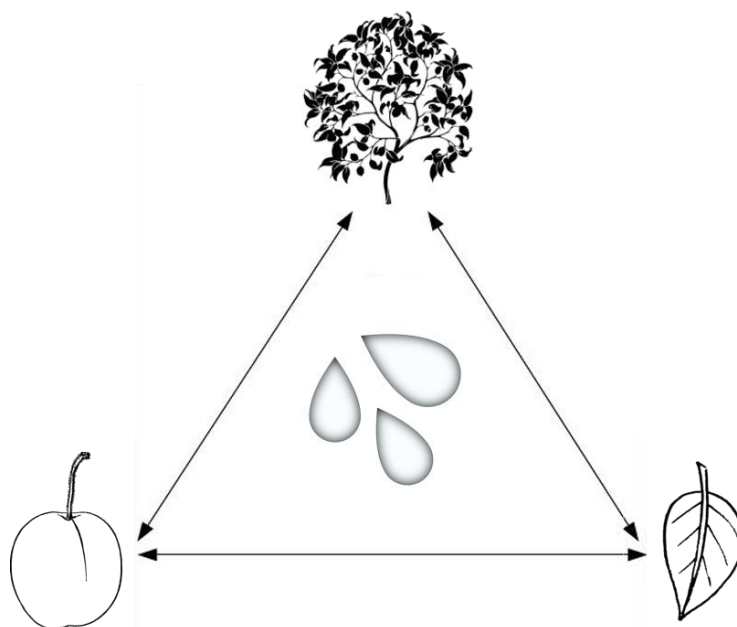




UNIVERSITÀ DEGLI STUDI DI PALERMO

Dottorato in Scienze Agrarie, Forestali e Ambientali
Dipartimento Scienze Agrarie, Alimentari e Forestali
Settore Scientifico Disciplinare AGR/03

FRUIT AND LEAF SENSING FOR THE CONTINUOUS MONITORING OF TREE WATER STATUS IN HIGH-DENSITY ORCHARD SYSTEMS



PhD candidate
ALESSIO SCALISI

PhD coordinator
PROF. VINCENZO BAGARELLO

Supervisor
PROF. RICCARDO LO BIANCO

Co-supervisor
PROF. FRANCESCO P. MARRA

XXXI PHD CYCLE
YEAR 2019

PREFACE

This dissertation is submitted for the degree of Doctor of Philosophy at the University of Palermo, Department of Agricultural, Food and Forest Sciences. The experiments described were conducted under the supervision of Prof. Riccardo Lo Bianco and Prof. Francesco P. Marra, between November 2015 and October 2018. At the Department level, further supervision was provided by Prof. Tiziano Caruso. Dr. Dario Stefanelli and Dr. Mark O'Connell tutored experiments conducted at the research station of Agriculture Victoria (Tatura, VIC, Australia) to support a period of study carried out in Australia.

This dissertation is original and its results were not submitted for any other degree, diploma or other qualification at other institutions and/or universities. By the time of submission, part of this work has been published in journals or proceedings, other papers based on the findings have been either submitted and accepted, or only submitted for publication. Published or accepted review and research papers are exhaustively cited and acknowledged throughout the text.

The following list contains published or accepted papers used in this work at the time of the submission of this dissertation:

- Scalisi A., Bresilla K., Simões Grilo F. (2017). Continuous determination of fruit tree water-status by plant-based sensors. *Italus Hortus* 24 (2), 39-50.
<https://doi.org/10.26353/j.itahort/2017.2.3950>
- Scalisi A., O'Connell M., Lo Bianco R., Stefanelli D. Continuous detection of new plant water status indicators in stage I of nectarine fruit growth. Accepted by *Acta Hortic* (August 2018, presented at Water and Nutrient Relations and Management of Horticultural Crops, IHC 2018, Istanbul, Turkey).
- Scalisi A., Marra F.P., Caruso T., Illuminati C., Costa F., Lo Bianco R. Transpiration rates and hydraulic conductance of two olive genotypes with different sensitivity to drought. Accepted by *Acta Hortic* (August 2018, presented at Water and Nutrient Relations and Management of Horticultural Crops, IHC 2018, Istanbul, Turkey).

Alessio Scalisi

November 2018

ACKNOWLEDGEMENTS

Firstly, I would like to express my gratitude to my PhD supervisor, Prof. Riccardo Lo Bianco, for the continuous support to my studies, which started with my first thesis for my BSc obtained in 2011. His support and supervision were also crucial for my MSc thesis held at the University of Bologna, in which he acted as a co-supervisor. Last, but not least, he significantly contributed to the mentoring of my whole PhD and to the critical review of this dissertation and the papers related to this work. Several times, Riccardo has demonstrated to be a friend, supporting and stimulating my work in moments of difficulties.

Besides, I would like to thank my co-supervisor Prof. Francesco P. Marra for critically helping me with the use of equipment and for the positive influence on experimental designs and data analyses. My genuine thanks also go to Prof. Tiziano Caruso for supporting my experiments with funding and for his insightful comments and feedback, arising from his long experience in the field.

I hereby acknowledge also Prof. Luca Corelli Grappadelli and Dr. Brunella Morandi from the University of Bologna, for kindly lending me fruit-based sensors belonging to their research group in Bologna.

In addition, I acknowledge the consideration that Dr. Kenan Aydınoğlu had about me, when structuring a very important project for rural development in southeastern Turkey, which taught me a lot about Turkish horticultural heritage.

Further sincere thanks go to Dr. Dario Stefanelli and Dr. Mark O'Connell, who provided me an opportunity to join their team as intern, and who gave access to the laboratory and research facilities at Agriculture Victoria, for part of my period of research in Australia. Dario and Mark critically supported my experiments and allowed me to widen my expertise in the field of study. The support of other researchers at Agriculture Victoria was extremely important to achieve my results. Specifically, I would like to acknowledge Ian Goodwin, Des Whitfield, Lexie McClymont, Caulin Aumann, Subhash Chandra, Christine Frisina, Janine Jaeger and Madeleine Peavey. Yet, the technical support and assistance of Dave Haberfield, Jim Selman, Andrew and Cameron O'Connell are gratefully acknowledged. Advice and feedback from the Stonefruit Field Laboratory Advisory Committee was appreciated. Experiments in Tatura were supported by a PhD project funded with a scholarship

issued by the Italian Ministry of Education and the University of Palermo, and by the stone fruit experimental orchard project (SF17006 Summerfruit Orchard - Phase II) funded by Hort Innovation using Summerfruit levy and funds from the Australian Government with co-investment from Agriculture Victoria.

I thank my fellow lab mates at the University of Palermo for the stimulating discussions, sample collection, field measurements and field trips and for all the fun we have had in the three years of my PhD. I acknowledge Filipa S. Grilo, Adele Amico Roxas, Silvia Fretto, Giovanna Sala, Giulia Marino, Placido Volo, Laura Macaluso and our MSc thesis students, Claudia Illuminati and Federico Costa. Yet, I would like to thank Athulya Jancy Benny (RMIT University, Melbourne), a BSc student who I have tutored during an internship at Agriculture Victoria, for her intense and commendable work.

Last but not least, I would like to thank my parents and my siblings for all their unconditional support during the three years of my PhD. Special thanks go to my father, who believed in me and in my dreams, contributing significantly to the person I am today.

LIST OF ABBREVIATIONS

<i>AGR</i> = absolute growth rate	Ψ_p = leaf turgor pressure
<i>ANOVA</i> = analysis of variance	Ψ_{stem} = stem water potential
<i>CAM</i> = crassulacean acid metabolism	<i>PAR</i> = photosynthetically active radiation
<i>CHP</i> = compensation heat pulse	<i>PPFD</i> = photosynthetic photon flux density
<i>CWS</i> = crop water supply	<i>PRD</i> = partial root-zone drying
<i>DAFB</i> = days after full bloom	<i>PWS</i> = plant water status
<i>DI</i> = deficit irrigation	<i>RAW</i> = readily available water
<i>DMC</i> = dry matter content	<i>RDI</i> = regulated deficit irrigation
<i>DOY</i> = day of the year	<i>RGR</i> = relative growth rate
<i>DW</i> = dry weight	<i>RH</i> = relative humidity
<i>E</i> = transpiration	<i>RPCR</i> = relative pressure change rate
<i>EAS</i> = effective area of shade	<i>RWC</i> = relative water content
<i>ET₀</i> = reference evapotranspiration	<i>SHB</i> = stem heat balance
<i>ET_c</i> = crop evapotranspiration	<i>SFI</i> = sap flow index
<i>f_{APAR}</i> = fraction of absorbed PAR	<i>SPAC</i> = soil-plant-atmosphere continuum
<i>FD</i> = fruit diameter	<i>T</i> = temperature
<i>FW</i> = fresh weight	<i>T_c</i> = canopy temperature
<i>g_l</i> = leaf hydraulic conductance	<i>TCSA</i> = trunk cross-sectional area
<i>g_s</i> = leaf stomatal conductance	<i>T_N</i> = normalised transpiration rate
<i>HPFM</i> = high pressure flow meter	<i>TW</i> = turgid weight
<i>HPV</i> = heat pulse velocity	<i>UAVs</i> = unmanned aerial vehicles
<i>HSD</i> = Honestly significant difference	<i>VPD</i> = vapour pressure deficit
<i>K</i> = hydraulic conductance	<i>W_{fraction}</i> = fraction of total transpirable water
<i>K_c</i> = crop coefficient	
<i>K_s</i> = sapwood specific conductance	
<i>LPCP</i> = leaf patch clamp pressure	
<i>LVDT</i> = linear variable displacement transducer	
<i>MANOVA</i> = multivariate analysis of variance	
<i>p_p</i> = attenuated pressure of leaf patches	
<i>p_c</i> = leaf cell turgor pressure	
Φ_{PSII} = efficiency of PSII	
Ψ_{fruit} = fruit water potential	
Ψ_{leaf} = leaf water potential	

LIST OF TABLES

Table 2.1. Authors' subjective relevance of sensors discussed in this paper for each plant water indicator. Scale from 1 to 5, where 1= poor relevance, and 5= high relevance....	17
Table 3.1. Leaf area, leaf size and root fresh weight to leaf fresh weight ratio (FW_{root}/FW_{leaf}) in well-watered (WW) and drought-stressed (DS) 'Nocellara del Belice' (NB) and 'Cerasuola' (CE) olive genotypes. Means \pm standard errors are shown. Different letters indicate significant differences by Tukey's multiple range test ($P < 0.05$).	31
Table 3.2. Crop water supply (CWS) in FI (full irrigated, 100 % of crop evapotranspiration), TTI (2/3 of FI), OTI (1/3 of FI) and RF (rainfed) trees at fruit growth stage II and III. Data represent means between 'Nocellara del Belice' and 'Cerasuola'.	44
Table 3.3. Multivariate analyses of variance (MANOVAs) testing the effects of genotype, irrigation and the genotype \times irrigation interaction on the ratios of statistical parameters extrapolated from fruit relative growth rate (RGR) and leaf relative pressure change rate (RPCR) from diel, diurnal and nocturnal intervals. Ratios: minimum RGR / minimum RPCR (MIN), maximum RGR / maximum RPCR (MAX), summation of RGR values at 15-min intervals / summation of RPCR values at 15-min intervals (SUM), RGR difference between MAX and MIN / RPCR difference between MAX and MIN (RANGE), and RGR relative standard deviation (RSD) / RPCR relative standard deviation (RSD). Significance levels and F shown for each MANOVA.	55
Table 4.1. Trunk cross-sectional area (TCSA), multiple/single fruitlet ratio per shoot, and leaf SPAD index of 'September Bright' nectarine trees under different irrigation levels. Data represent means \pm standard errors. Analysis of variance was followed by Tukey's pairwise comparison (different letters indicate significant differences at $P < 0.05$).	67
Table 4.2. Total rainfall, full irrigation to control irrigated trees (FI) and crop water supply to control trees (CWS, i.e. rainfall + irrigation) at each of the fruit growth stages.	83
Table 4.3. Pearson's correlation coefficients for fruit diameter (FD) and attenuated leaf patch clamp pressure (p_p) vs plant water status (PWS) indicators: stem water potential (Ψ_{stem}), leaf water potential (Ψ_{leaf}), leaf hydraulic conductance (g_l) and leaf relative water content (RWC).	94

LIST OF FIGURES

Figure 2.1. Diel curves of attenuated pressure (P_p) of leaf patch clamp pressure probes in olive leaves at high, mid (half-inverted curve) and low turgor (fully inverted) states.	8
Figure 2.2. Leaf patch clamp pressure probe mounted on a 'September Bright' nectarine leaf (A) and mark left on the leaf after a three-day measurement period (B).	9
Figure 2.3. Diel stem absolute growth rate (AGR) in 1-year-old prickly pear (CAM metabolism) and olive (C3 metabolism) plants.	11
Figure 2.4. Sap flow density fluctuations in 25-year-old orange trees and vapour pressure deficit (VPD) variations over 24 hours in spring.	13
Figure 2.5. Fruit gauge mounted on an olive drupe at its growth stage III (A) and on a	

nectarine fruit at its growth stage I (B).....	16
Figure 2.6. Diel fruit diameter and relative growth rate (RGR) variations in an olive drupe at its growth stage III.....	16
Figure 3.1. Temperature (A), relative humidity (RH, B) and vapour pressure deficit (VPD, C) inside the greenhouse during the drought period.	29
Figure 3.2. Normalized transpiration rate (T_N) of 'Nocellara del Belice' (A) and 'Cerasuola' (B) olive genotypes under different fractions of total transpirable water ($W_{fraction}$). Dashed lines (— —) indicate T_N upper and lower limits.	30
Figure 3.3. Dry matter content (DMC) in leaves (A) of 'Nocellara del Belice' and 'Cerasuola' olive under well-watered (WW) and drought-stressed (DS) conditions, and in roots (B) of WW and DS plants. Error bars indicate standard errors of the means. Different letters in panel A indicate significant differences determined with Tukey's multiple range test ($P < 0.05$). P value in panel B from analysis of variance.	31
Figure 3.4. Sapwood-specific hydraulic conductance (K_s) of well-watered (WW) and drought-stressed (DS) stem (cross-patterned bars) and root sections (white bars). Bar graphs represent mean values of pooled data from 'Nocellara del Belice' and 'Cerasuola' olive genotypes. Error bars represent standard errors of the means and different letters indicate significant differences determined with Tukey's multiple range test ($P < 0.05$).	32
Figure 3.5. Schematisation of statistical parameters calculated on diel basis on a fruit relative growth rate (RGR) curve. MIN = minimum value of RGR, MAX = maximum value of RGR, RANGE = MAX-MIN, SUM = summation of RGR values taken at 15-min intervals from 1 (00.00 h) to 96 (23.45 h), RSD = relative standard deviation, where σ is the standard deviation and $ \mu $ is the absolute value of the mean.	42
Figure 3.6. Daily mean temperature (T) and vapour pressure deficit (VPD) (A), and daily crop water supply (CWS = full irrigation (FI) + rainfall) (B) at fruit growth stages II and III.	44
Figure 3.7. Weekly fruit diameter variations in 'Nocellara del Belice' (NB) and 'Olivo di Mandanici' (MN) olive genotypes from 200 to 291 days of the year (DOY). Error bars represent standard deviations of means (n = 60).	45
Figure 3.8. Association between weight and diameter in 'Nocellara del Belice' (NB) and 'Olivo di Mandanici' (MN) fruit sampled from the beginning of stage II to harvest. In NB, $FW = -7.75 + 0.66 \times FD$ ($P < 0.001$, $R^2 = 0.938$). In MN, $FW = -1.74 + 0.28 \times FD$ ($P < 0.001$, $R^2 = 0.968$).	46
Figure 3.9. Daily curve of stomatal conductance (g_s) in 'Nocellara del Belice' (NB) and 'Olivo di Mandanici' (MN) leaves. Data averaged across different irrigation treatments at 209 days of the year. Error bars indicate standard errors of means. *, significantly different for $P < 0.05$; ***, significantly different for $P < 0.001$ by Tukey's test.	47
Figure 3.10. Daily curve of stem water potential (Ψ_{stem}) in 'Nocellara del Belice' (NB) (A and B) and 'Olivo di Mandanici' (MN) (C and D) at 209 and 287 days of the year (DOY). Trees subjected to full irrigation (FI), 2/3 of FI (TTI), 1/3 of FI (OTI) and no irrigation (RF). Error bars represent standard deviations of means (n = 3). Significant differences determined with analysis of variance and Tukey's Honest Significant Difference (HSD, $P < 0.05$).	48
Figure 3.11. Midday stem water potential (Ψ_{stem}) in 'Nocellara del Belice' (NB) (A) and	

'Olivo di Mandanici' (MN) trees (B) under full irrigation (FI), 2/3 of FI (TTI), 1/3 of FI (OTI) and no irrigation (RF) during stage II (from 196 to 252 DOY) and stage III (from 253 to 287 DOY) of fruit growth. Error bars represent standard deviations of means (n = 3). Significant differences determined with analysis of variance and Tukey's Honest Significant Difference (HSD, P < 0.05).	49
Figure 3.12. Fruit diameter (FD), leaf patch clamp pressure (p_p), fruit relative growth rate (RGR) and leaf relative pressure change rate (RPCR) recorded at 15-min intervals for five days during stage II of fruit growth in 'Nocellara del Belice' (NB) (A, B, C, D, respectively) and 'Olivo di Mandanici' (MN) trees (E, F, G, H) under full irrigation (FI), 2/3 of FI (TTI), 1/3 of FI (OTI) and no irrigation (RF). Grey and white areas show night and day time, respectively.	51
Figure 3.13. Fruit diameter (FD), leaf patch clamp pressure (p_p), fruit relative growth rate (RGR) and leaf relative pressure change rate (RPCR) recorded at 15-min intervals for five days during stage III of fruit growth in 'Nocellara del Belice' (NB) (A, B, C, D, respectively) and 'Olivo di Mandanici' (MN) trees (E, F, G, H) under full irrigation (FI), 2/3 of FI (TTI), 1/3 of FI (OTI) and no irrigation (RF). Grey and white areas show night and day time, respectively.	53
Figure 3.14. Scatter plots of diel leaf relative pressure change rate (RPCR) vs fruit relative growth rate (RGR) in 'Nocellara del Belice' (A and B) and 'Olivo di Mandanici' trees (C and D) under full irrigation (FI), 2/3 of FI (TTI), 1/3 of FI (OTI) and no irrigation (RF) at 223 and 287 days of the year (DOY). Midday stem water potential (Ψ_{stem}) reported for each genotype * DOY * irrigation treatment combination. White and black circles represent diurnal and nocturnal measurements, respectively. Axis scales are equal in all panels and consequently omitted.	54
Figure 3.15. Linear relationships of diel $RGR_{RANGE} / RPCR_{RANGE}$ ($RANGE_{diel}$) (A and B), diurnal $RGR_{MIN} / RPCR_{MIN}$ (MIN_{diur}) (C and D) and nocturnal $RGR_{SUM} / RPCR_{SUM}$ (SUM_{noct}) (E and F) with midday stem water potential (Ψ_{stem}). Grey, white and black circles represent diel, diurnal and nocturnal data, respectively, for 'Nocellara del Belice' (NB) and 'Olivo di Mandanici' (MN).	56
Figure 4.1. Temperature and vapour pressure deficit (VPD) trends (A), and daily crop water supply (CWS, B) in control trees (100% of ET_c) of 'September Bright' nectarines at growth stage I (28 to 63 days after full bloom, DAFB).	66
Figure 4.2. Mid-morning leaf stomatal conductance (g_s) of 'September Bright' nectarines under four different irrigation levels, at 44 and 63 days after full bloom (DAFB). Means (n=6) and standard errors are shown. Different letters indicate significant differences determined with analysis of variance and Tukey's pairwise comparison (P < 0.05).	67
Figure 4.3. Midday stem water potential (Ψ_{stem}) of 'September Bright' nectarines under four different irrigation levels at fruit growth stage I. Means (n=8) and standard errors are shown. Statistically significant differences determined with analysis of variance and Tukey's Honest Significant Difference (HSD, P < 0.05).	68
Figure 4.4. Fruit diameter during stage I of 'September Bright' nectarines under four different irrigation levels. Means (n=36) and standard errors are shown. Statistically significant differences determined with analysis of variance and Tukey's Honest Significant Difference (HSD, P < 0.05).	69
Figure 4.5. Fruit diameter (A) and attenuated pressure of leaf patches (p_p , B) weekly	

trends in 'September Bright' nectarines under four different irrigation levels, at fruit growth stage I. Grey and white areas emphasize night and day hours, respectively. Panels C and D show 24-hour absolute changes in fruit diameter ($|\Delta \text{diameter}|$) and p_p ($|\Delta p_p|$), respectively, for the Control and DI_0 treatments, and daily maximum VPD (VPD_{max}).....70

Figure 4.6. Stem water potential (Ψ_{stem} , A), fruit diameter (B) and attenuated pressure of leaf patches (p_p , C) diel trends in 'September Bright' nectarines under four different irrigation levels, at 50 days after full bloom (DAFB). Grey and white areas emphasize night and day hours, respectively. In panel A, significant differences determined with analysis of variance and Tukey's Honest Significant Difference (HSD) at $p < 0.05$. Panels D and E, show linear regression analysis of fruit diameter and p_p vs Ψ_{stem} , respectively.....71

Figure 4.7. Fruit diameter during each fruit growth stages of 'September Bright' nectarines under control irrigation. Time series expressed in days after full bloom (DAFB).....82

Figure 4.8. Daily total reference evapotranspiration (ET_0 , A), mean temperature (T_{mean} , B), mean relative humidity (RH_{mean} , C) and mean vapour pressure deficit (VPD_{mean} , D) along the considered four stages of fruit growth in days after full bloom (DAFB). Missing data from 106 to 110 DAFB.83

Figure 4.9. Fraction of absorbed photosynthetically active radiation (f_{APAR}) in control irrigated trees during a clear sky day at fruit growth stage I (57 DAFB). Error bars represent standard errors of means ($n = 36$).84

Figure 4.10. Effective area of shade (EAS) at fruit growth stages I, II, IIIa and IIIb of 'September Bright' nectarine. Error bars represent standard errors of means ($n = 36$) and different letters indicate significant differences within each stage determined with analysis of variance and Tukey's pairwise comparison ($P < 0.05$).....85

Figure 4.11. Fruit diameter at stage I (A), II (B), IIIa (C) and IIIb (D) of 'September Bright' nectarine fruit growth. Timeline expressed in days after full bloom (DAFB). Error bars represent standard errors of means ($n = 36$). Significant differences determined with analysis of variance and Tukey's Honest Significant Difference (HSD, $P < 0.05$).85

Figure 4.12. Daily curves of stem water potential (Ψ_{stem}) at stages I (A), II (B), IIIa (C) and IIIb (D) of 'September Bright' nectarine fruit growth. Error bars represent standard errors of means ($n = 6$). Significant differences determined with analysis of variance and Tukey's Honest Significant Difference (HSD, $P < 0.05$).86

Figure 4.13. Midday stem water potential (Ψ_{stem}) at fruit growth stages I (A), II (B), IIIa (C) and IIIb (D) in 'September Bright' nectarines. Timeline expressed in days after full bloom (DAFB). Error bars represent standard errors of means ($n = 6$). Significant differences determined with analysis of variance and Tukey's Honest Significant Difference (HSD, $P < 0.05$).87

Figure 4.14. Daily curves of leaf water potential (Ψ_{leaf}) at stages IIIa (A) and IIIb (B) of 'September Bright' nectarine fruit growth. Error bars represent standard errors of means ($n = 6$). Significant differences determined with analysis of variance and Tukey's Honest Significant Difference (HSD, $P < 0.05$).87

Figure 4.15. Daily curves of leaf relative water content (RWC) at stages I (A), II (B), IIIa (C) and IIIb (D) of 'September Bright' nectarine fruit growth. Error bars represent

standard errors of means (n = 6). Significant differences determined with analysis of variance and Tukey's Honest Significant Difference (HSD, P < 0.05).....	88
Figure 4.16. Daily curves of leaf hydraulic conductance (g_l) in control, DI-40, DI-20 and DI-0 trees at stages II (A), IIIa (C) and IIIb (E) of 'September Bright' nectarine fruit growth, and in West- and East-oriented trees (Stage II = B, IIIa = D, IIIb = F). Bars in panels B, D and F show means of photosynthetic photon flux density (PPFD) for West and East trees. Bars represent standard errors of means (irrigation treatment n = 6; canopy orientation n = 12). Significant differences determined with analysis of variance and Tukey's Honest Significant Difference (HSD, P < 0.05). The HSD bar in panel B highlights only differences in g_l , and not in PPFD.	90
Figure 4.17. Mid-morning leaf hydraulic conductance (g_l) at stages II (A), IIIa (C) and IIIb (D) of 'September Bright' nectarine fruit growth. Error bars represent standard errors of means (n = 6). Significant differences determined with analysis of variance and Tukey's Honest Significant Difference (HSD, P < 0.05).....	91
Figure 4.18. Efficiency of PSII (Φ_{PSII}) at the end of fruit growth stages I, IIIa and IIIb of 'September Bright' nectarine. Error bars represent standard errors of means (n = 36). When present, different letters indicate significant differences within each stage determined with analysis of variance and Tukey's pairwise comparison (P < 0.01).....	92
Figure 4.19. Diel trends of fruit diameter (FD, n = 3) and fruit relative growth rate (RGR, n = 3) (A), attenuated pressure of leaf patches (p_p) and leaf relative pressure change rate (RPCR) (B) in control irrigated trees at stage I (51 DAFB) of 'September Bright' nectarine fruit growth.....	93
Figure 4.20. Scatter plots of diel leaf relative pressure change rate (RPCR) and fruit relative growth rate (RGR) in control, DI-40, DI-20 and DI-0 at stages I (A), II (B), IIIa (C) and IIIb (D) of 'September Bright' nectarine fruit growth. Midday Ψ_{stem} for each of the days considered is reported in its relative panel. Axis scales are equal in all panels and consequently omitted.	95
Figure 4.21. Maximum nocturnal fruit relative growth rate (MAX_{RGR}) vs midday Ψ_{stem} (A) and minimum diel leaf relative pressure change rate (MIN_{RPCR}) vs midday Ψ_{stem} (B). Nonlinear regression in panel A: $MAX_{RGR} = 0.04 / \{1 + [(\Psi_{stem} + 1.56) / 0.57]^2\}$, $R^2 = 0.597$, $P < 0.001$. Linear regression in panel B: $MIN_{RPCR} = -0.70 + 0.55 \times \Psi_{stem}$, $R^2 = 0.369$, $P < 0.001$. Data from all fruit growth stages included in the models.	96
Figure 4.22. Diel (A), diurnal (B) and nocturnal ratios (C) of relative standard deviations of fruit relative growth rate (RSD_{RGR}) and leaf relative pressure change rate (RSD_{RPCR}) vs midday Ψ_{stem} . Expo-linear model in panel C: $RSD_{RGR}/RSD_{RPCR} = -0.07 + 2.88E-07 \times \exp(-3.89 \times \Psi_{stem}) - 0.12 \times \Psi_{stem}$, $R^2 = 0.650$, $P < 0.001$. Data from all fruit growth stages included in the model.....	98

TABLE OF CONTENTS

1. GENERAL INTRODUCTION.....	1
2. LITERATURE REVIEW.....	2
ABSTRACT.....	2
INTRODUCTION.....	3
LEAF-MOUNTED SENSORS	5
Leaf thickness sensors.....	6
Leaf pressure probes	6
Leaf thermal sensing.....	9
STEM-MOUNTED SENSORS	10
Stem dendrometers.....	10
Sap flow probes	12
Additional sensors.....	13
FRUIT-MOUNTED SENSORS	14
CONCLUSIONS	17
LIST OF REFERENCES.....	17
3. OLIVE TREE WATER RELATIONS	25
Genotype-dependent strategies to cope with drought - A case study: “Transpiration rates and hydraulic conductance of two olive genotypes with different sensitivity to drought”	25
ABSTRACT.....	25
INTRODUCTION	25
MATERIALS AND METHODS	26
Transpiration.....	27
Hydraulic conductance	27
Leaf area and dry matter content	28
Statistical procedures	28
RESULTS AND DISCUSSION.....	28
Weather conditions.....	28
Transpiration.....	29
Dry matter content, leaf area and root/leaf ratio	30
Hydraulic conductance	31
CONCLUSIONS	32
LIST OF REFERENCES.....	33
The combined use of leaf turgor pressure probes and fruit diameter sensors as an indicator of tree water status	36
ABSTRACT.....	36
INTRODUCTION	36
MATERIALS AND METHODS	39
Experimental design	39
Fruit characteristics	40
Plant water status.....	40
Fruit- and leaf-based sensing	41
Statistical analysis.....	43
RESULTS AND DISCUSSION.....	43

Weather conditions and irrigation	43
Fruit characteristics	45
Plant water status	46
Fruit- and leaf-based sensing.....	50
CONCLUSIONS	58
LIST OF REFERENCES	59
4. NECTARINE TREE WATER RELATIONS	63
Preliminary test of fruit- and leaf-based sensors in high-density nectarine orchards. A caste study: “Continuous detection of new plant water status indicators in stage I of nectarine fruit growth”	63
ABSTRACT	63
INTRODUCTION.....	63
MATERIALS AND METHODS	65
RESULTS AND DISCUSSION	66
Tree size, fruit bearing habit and leaf chlorophyll concentration	66
Plant water status	67
Fruit and vegetative growth.....	68
Continuous measurements of fruit size and leaf turgor pressure	69
CONCLUSIONS	71
LIST OF REFERENCES	71
The combined use of leaf turgor pressure probes and fruit diameter sensors as an indicator of tree water status	74
ABSTRACT	74
INTRODUCTION.....	74
MATERIALS AND METHODS	78
Experimental design.....	78
Light interception and fruit size.....	79
Tree water relations and leaf fluorescence	79
<i>Water potential</i>	79
<i>Leaf relative water content</i>	79
<i>Leaf hydraulic conductance</i>	80
<i>Leaf fluorescence</i>	80
Fruit diameter and leaf turgor pressure continuous sensing	80
Statistical analysis	81
RESULTS AND DISCUSSION	81
Fruit developmental stages, weather conditions and crop water supply	81
Light interception and fruit size	84
Tree water relations and leaf fluorescence	86
<i>Water potential</i>	86
<i>Leaf relative water content</i>	88
<i>Leaf hydraulic conductance and fluorescence</i>	89
<i>The interdependency of plant water status indicators</i>	92
<i>Fruit diameter and leaf turgor pressure continuous sensing</i>	93
CONCLUSIONS	99
ACKNOWLEDGEMENTS	100
LIST OF REFERENCES	100
5. GENERAL CONCLUSIONS	105

1. GENERAL INTRODUCTION

In recent years, climate changes are influencing global agricultural production strategies and the trade of agri-food commodities. The general rise of temperature and the increase in the world's population are leading to an overuse of natural resources, of which water definitely represent the most essential for life. Although worldwide many cultivated areas still depend on rain water, the largest part of freshwater used by Man's activity is destined to crop irrigation. Most of the irrigated crops are fruit and vegetables, as some species could not be grown and/or produce fruit in semi-dry or dry areas without an additional use of water. Horticulturists are dealing with the increasing drought and the necessity to comply with environmentally-sustainable practices by using genetics, plant breeding and precision irrigation management. Scientists constantly attempt to develop new genotypes with higher drought resistance. Innovative orchard systems tend to optimise the use of resources, with irrigation being one of the farm's operations that has captured lot of attention in order to save water and increase profitability. Regulated deficit irrigation (RDI) has recently taken hold as it allows growers to reduce water use in specific phenological stages to avoid overuse of water and concurrently not affecting production. However, farmers need real-time continuous determination of plant water needs in order to automate irrigation and maximise their system efficiency. This is even more evident in modern high-density orchard systems, where the high competition for water among nearby trees requires an optimisation of water resources and a precision management of irrigation. The determination of plant water status can therefore represent an interesting approach to determine tree water needs in fruit crops. Luckily, plants are naturally made of bio-sensors that continuously respond to environmental and soil conditions. The use of sensing technologies on plant organs such as leaves, fruit, branches, trunk and roots provide complex but highly informative tools to understand when plants enter water deficit.

This work reviews the use of plant-based sensors in fruit trees to determine plant water status and then tests the use of fruit- and leaf-mounted probes for continuous plant water status assessment in high-density olive and nectarine orchards. We considered leaves and fruit as they are the two bio-sensors that directly exchange water with the environment by transpiration. The main goal of this dissertation is to reveal insights on fruit and leaf physiological mechanisms in response to drought, and to identify new multi-organ models that can be used for irrigation management in future systems.

2. LITERATURE REVIEW

Based on the published review paper:

Scalisi A., Bresilla K., Simões Grilo F. (2017). Continuous determination of fruit tree water-status by plant-based sensors. *Italus Hortus* 24 (2), 39-50. <https://doi.org/10.26353/j.itahort/2017.2.3950>

ABSTRACT

Recently, climate change has caused shortages of water worldwide, especially in semi-arid and arid regions. Several irrigation strategies have been studied with the aim of saving water overuse in agriculture. In the past most of the attention was directed towards soil water content, but recently the focus has moved to plant responses to water deficit. In recent years, crop evapotranspiration (ET_c) obtained from reference evapotranspiration (ET_0) and crop coefficients (K_c), has become common for irrigation scheduling in several crops, but it does not provide precise insights on the tree water status. Today an increasing focus is being given to plant-based sensors for the continuous monitoring of plant water status to provide support to irrigation management strategies with a precision approach. In this work several plant-based (leaf, stem and fruit) devices used for plant water status sensing and for irrigation scheduling, are reviewed. Scientists have managed to create and test a variety of small leaf-adapted sensors with the aim of collecting valuable information on water dynamics. Non-destructive continuous water status detection in leaves is difficult due to the intrinsic fragility of these organs. Yet, the data collected can provide insights on the actual status of one leaf, within a multitude of other leaves that might have a slightly different behaviour because of factors such as age, sun exposure, canopy position and others. Leaf thickness sensors, leaf pressure and leaf thermal probes are discussed in this review. Stems and shoots establish the connection between climatic conditions and water availability in the soil. Continuous measurements of stem water status by non-destructive sensors provide information not only on the variations of soil water availability but also on the reserves of plant tissues. The use of stem dendrometers, sap flow probes, stem hygrometers and stem microtensiometers for continuous determination of plant water status and irrigation management is discussed. Moreover, it has been demonstrated that fruit water relations have key implication on horticultural production and quality. Measurements of fruit water status and fruit growth dynamics under different irrigation strategies might be crucial in order to reduce water use, maintain yield and/or improve fruit quality. Advantages and disadvantages of different sensors ranging from linear variable displacement transducers (LVDTs), strain gauges,

potentiometers and/or optoelectric sensors, are discussed. However, a unique methodology for continuous plant water status determination in fruit trees has yet to be found. An integrated approach, which considers contemporary use of sensors on different plant organs, is proposed as effective strategy to collect exhaustive information on tree water status.

Keywords: fruit, irrigation management, leaf, probes, stem.

INTRODUCTION

In recent years, climate change has led to shortages of water worldwide, especially in semi-arid and arid regions (Ward and Pulido-Velazquez, 2008; Schewe et al., 2014; Chartzoulakis and Bertaki, 2015; Gosling and Arnell, 2016). As a consequence, water availability for horticultural crops has become a limiting factor (Costa et al., 2007; Stöckle et al., 2011; Snyder, 2017), leading to an increase in management costs and an overall increased number of technologies for increasing water use efficiency. Conventionally, optimal yields are obtained when irrigation allows soil water content to reach levels close to field capacity (FC) (Jones, 2004a), with optimal readily available water (RAW) levels. However, this approach does not match with the global requirement for water saving. Rainfed agriculture partly limits water wastes but it is not always applicable due to climate or horticultural crop limitations, although some temperate C3 crop species such as olive and almond show adaptive drought tolerance mechanisms (Connor, 2005; Rahemi and Yadollahi, 2005). Nevertheless, the use of mulching has been found to positively influence fruit production and water use efficiency in rainfed areas (Lal Bhardwaj, 2013; Wang et al., 2015) and is considered a sustainable practice in those areas in which irrigation is not feasible. Most fruit crops, though, need irrigation supply in order to produce a profitable yield when rain does not satisfy crop water requirement. However, deficit irrigation is a sustainable approach, which may limit water overuse and improve water productivity (Costa et al., 2007; Du et al., 2015; Chai et al., 2016). The two most adopted deficit irrigation strategies are RDI (regulated deficit irrigation), whose name was firstly introduced by Chalmers et al. (1986), and partial root-zone drying (PRD), which consists of an alternation of irrigated root sides (Dry et al., 1995; Dry and Loveys, 1998). While RDI was successfully used in several fruit crops, PRD results in some fruit species are controversial and still subject to debate because conflicting results have been found in previous studies, as reported by Mossad et al. (2017). Recently, for instance, PRD application in orange

trees has been either found to negatively affect fruit size and yield (Faber and Lovatt, 2014) or to maintain similar results when compared to full irrigation (Consoli et al., 2017).

Although rainfed and deficit-irrigated fruit production are extremely helpful strategies to save water worldwide, the use of the latter is not always rational and consistent with the real plant water status. As mentioned above, in the recent years most of the irrigation methods were based on soil water content, but recently the focus has moved to plant responses to water deficit (Jones, 1990; 2004a). Indeed, the main plant physiological indicators of water deficit respond primarily to changes in tissue water content rather than to soil water dynamics (McCutchan and Shackel, 1992; Jones, 2004a; Steppe et al., 2008). Determination of stem water status is a reliable indicator of plant response to water deficit (Kramer 1988; Boyer 1989), while instead root water status provides only partial insights on the whole plant, due to heterogeneous water content in drying soils particularly when localized irrigation method is adopted (Jones, 1990). Today, one of the most widely accepted indicators of plant water status is stem water potential (Ψ_{stem}) (Shackel et al., 1997). Nevertheless, the determination of stem water potential is commonly done with a pressure chamber (Scholander et al., 1965), a destructive, time- and labour-consuming method (Zimmermann et al., 2008; Zia et al., 2011) which cannot provide real-time and continuous information on plant water status, thus not allowing the supply of the right amount of water when mostly needed. Measurements of leaf water potential (Ψ_{leaf}) have proven ineffective for irrigation scheduling, due to stomatal control on leaf water status (Bates and Hall, 1981; Jones 1984; Jones 1990). Leaf relative water content (RWC) may be effectively used as a water deficit indicator (Scalisi et al., 2016; Lo Bianco and Scalisi, 2017; Mossad et al., 2017) but it does not provide information on the actual energy status of water in plants (Jones, 2007), as delivered by water potential readings. In addition, the use of RWC in highly isohydric species (e.g. cowpea, maize, poplar, etc.) may provide misleading information for irrigation scheduling (Jones, 2004a), because few changes in water status occur due to adaptive stomatal closure under drought.

Alternative approaches might be used for irrigation management. The use of crop evapotranspiration (ET_c), obtained from reference evapotranspiration (ET_0) and crop coefficients (K_c), has become common for irrigation scheduling in several crops (Paço et al., 2006). The ET_c can be easily assessed using the FAO-56 method described by Allen et al. (1998). Recently there has been growing interest in two quite different

approaches to irrigation management. One relies on broad-scale image analysis of large areas (e.g. satellite, UAVs), while the other allows a more precision-management approach with plant-based sensors. If we accept that the pressure chamber method is not suitable for automated irrigation scheduling (Steppe et al., 2008), other plant-based sensors may be more appropriate for providing the reliable, real-time and continuous plant water status data needed for accurate scheduling of automated, micro-irrigation in fruit crops. Methods that can provide this type of data are very important for efficiently managing modern irrigation systems. Modern drip irrigation systems can be very accurate, precise and efficient at delivering the optimum amount of water to the root-zone of fruit trees to achieve the desired crop production requirements. However, the full potential of drip irrigation can only be achieved with good management decisions that can be made only with good plant water status data. The use of continuous sensing systems allows to determine irrigation requirement at pre-determined intervals and/or in real-time with remote data retrieval. Jones (1990, 2004a) has repeatedly emphasized that greater precision in irrigation management is possible with plant stress-sensing methods than with soil-based methods. In this work, the main plant-based methods used for plant water status sensing and for irrigation scheduling are discussed. We reviewed leaf, stem and fruit-mounted sensors, whereas roots were not considered as they are less sensitive indicators of water deficit, as reported by Jones (1990). Most of the attention has been directed towards systems which are either already real-time, continuous and remotely controlled, or have the potential to be easily automated. Indeed, today, continuous sensors may be connected straightforwardly to simple and cheap I/O boards (e.g. the open-source single-board microcontrollers ©Arduino), which in turn may be programmed to regulate irrigation levels and timing in response to given water deficit thresholds. However, we should acknowledge the inevitable constraints of plant-based methods that are related to their commonly accepted inability to provide information on the quantity of water to be supplied, when certain thresholds are reached.

LEAF-MOUNTED SENSORS

Non-destructive and continuous measurement of water status in leaves is difficult due to the intrinsic fragility of these organs. Measurements of RWC and Ψ_{leaf} are relatively easy, but they are destructive and done at set time intervals. Yet, although the data collected can provide insights on the actual status of one leaf, within a multitude of other leaves, that leaves might not be a good representation the entire canopy due to

factors such as age, sun exposure, canopy position and others. Nevertheless, scientists have managed to create and test a variety of small leaf-adapted sensors with the aim of collecting valuable information on water dynamics.

LEAF THICKNESS SENSORS

Variations of leaf thickness over time have long been studied as indicators of water deficit (Bachmann, 1922; Meidner, 1952). Syversten and Levy (1982) measured leaf thickness variations by linear variable displacement transducers (LVDTs) on grapefruit, aiming to find some significant relationships with leaf water potential (Ψ_{leaf}). In their experiment, the authors found a significant correlation between the two indicators over a three-day period ($r^2=0.69$). Other authors have attempted to determine thickness variations in relation to leaf water status by using LVDTs (Fensom and Donald, 1982; Malone, 1993) or capacitive displacement sensors (McBurney, 1992). Bùrquez (1987) used a gear-wheel type micrometer to measure thickness micro-changes in leaves of rapeseed, bean, impatiens and four o'clock flowers. Leaf thickness had a highly significant correlation with RWC in the four species under study (r^2 between 0.98 and 0.99), in agreement with the results from Meidner (1952). Therefore, thickness changes appear to be best connected with water loss from cells and probably with leaf turgor pressure (Ψ_p), rather than with Ψ_{leaf} . In 1996, Sharon and Bravdo attempted to manage irrigation in citrus through the measurement of leaf thickness by a linear-displacement sensing device.

Despite leaf thickness sensors offering a useful approach for continuous monitoring of leaf water content, and possibly leaf water status, most of the available probes cannot be kept on the same leaf for a long time, because they typically damage the leaf's surface after a short time (Zimmermann et al., 2008). In addition, in young leaves a part of cell shrinkage/enlargement goes in the direction of the leaf axis, while the sensor measures only leaf cross-sectional distance (Jones, 1973). More recently, further displacement sensors were tested for measurements of leaf thickness, although their appropriateness for assessing plant water status is yet to be investigated (Jinwen et al., 2009; Hu et al., 2013).

LEAF PRESSURE PROBES

Green and Stanton (1967) first devised a technique to measure plant cell-pressure directly by inserting a microscopic capillary, fused at one end and filled with water, into a *Nitella* internodal cell. Cell pressure led to the compression of a bubble in the

capillary, which allowed the authors to determine cell turgor with exceptional precision, after small adjustments due to capillarity. Green (1968) used the same instrument to determine turgor pressure for a subsequent derivation of cell extensibility. This method inspired further research papers that adopted similar pressure probes. In 1969, Zimmermann et al. developed a pressure probe that was firstly tested in giant algal cells and used afterwards in bladder cells of higher plants (Steudle et al., 1975). Hüsken et al. (1978) were able to miniaturize the same sensor and use it in *Capsicum annuum* for the determination of Ψ_p , hydraulic conductivity, and volumetric elastic modulus. Later, in 1990, Balling and Zimmermann used the pressure probe to measure xylem pressure in tobacco plants, and suggested that both turgor and osmotic pressure in subsidiary cells found along the xylem play a key role in maintaining xylem tension at a constant level. A similar type of pressure probe was used by Wei et al. (1999) to test the hydraulic architecture model of maize plants. However, despite its wide use in science, the pressure probe technique is not suitable for automation (Zimmermann et al., 2008). In 1979, Heathcote et al. used portable instruments to estimate leaf turgor potential from voltage outputs. However, Turner and Sobrado (1983), found no correlation between the output of the instrument and turgor pressure on two *Eliaanthus spp.*, arguing that the obtained data might be influenced by leaf thickness and large veins. Another non-destructive method to measure cell turgor pressure is the ball tonometer, well described by Lintilhac et al. (2000). The authors found a good correlation between this method and the pressure probe mentioned above. However, also this type of sensor is very difficult to automate in field studies due to its complex and sensitive assembly.

In 2008, Zimmermann et al. used a leaf patch clamp pressure (LPCP) probe for the continuous monitoring of leaf water status. This relatively new sensor has caught the attention of many scientists worldwide, for its non-invasive nature and real-time data retrieval through an online platform. The sensor was composed of a piezoresistive Wheatstone bridge mounted on a circular metal pad of a spring clamp. LPCP sensors were tested on chestnut vines (*Tetrastigma voinierianum*) with output readings ranging from 0 to 100 kPa. Sensors were firstly calibrated using a pressure chamber, and subsequently they were attached to leaves and connected to radio transmitters via wires. Data were afterwards sent to a receiving base station and transmitted to an internet server through a GPRS network. Output of LPCP probes with oil-filled capillaries inserted in the abaxial leaf surface were compared with results obtained from the turgor pressure probe and the results were found to be consistent (Zimmermann et al., 1969).

Westhoff et al. (2009) mounted the pressure sensor chip on a metal pad with a toric magnet, and built a counter pad with a second toric magnet moving along a threaded rod. Data obtained by LPCP probes represent the attenuated pressure of leaf patches (P_p) as a reaction to clamp pressure (P_{clamp}). P_p values might be influenced by temperature (i.e. effects on cell elasticity) or leaf height within the tree canopy. Zimmermann et al. (2008) eventually concluded that P_p values are inversely related to cell turgor pressure (P_c), although a certain delay occurs in P_p morning changes compared to P_c , based on leaf height in the canopy. The authors found a delay of 1, 1.5 and 2.5 hours for leaves from 10, 6 and 0.2 m height, respectively, most likely due to different transpiration influences. Ehrenberger et al. (2012) found an inverse relationship between P_p and P_c in well turgid olive leaves, whereas the same P_p response was not observed at low or near-to-zero P_c values. They also noticed that a reversal of P_p curves occurred towards low turgor pressure values in both laboratory and field conditions (Fig. 2.1).

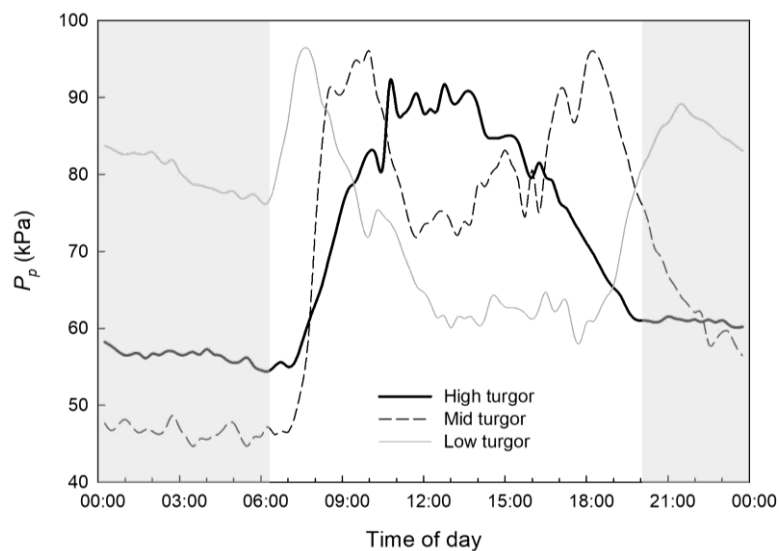


Figure 2.1. Diel curves of attenuated pressure (P_p) of leaf patch clamp pressure probes in olive leaves at high, mid (half-inverted curve) and low turgor (fully inverted) states.

According to the authors, this is likely to be due to a higher volume of air residing within the leaf's spongy mesophyll in leaves experiencing low P_c , compared to turgid leaves. Therefore, P_c contribution to P_p values is nearly negligible and values mostly reflect the changes in air volume in leaves, although a part of the turgor pressure is restored by nocturnal water uptake. After re-watering, reversed P_p responses are easily resettable and leaf turgor returns to its previous state. Also other authors (Fernández et al., 2011a; Rodriguez-Dominguez et al., 2012; Padilla-Díaz et al., 2016; Marino et al., 2016) found similar reversed responses of P_p to drought in olive trees. So far, LPCP probes have been successfully used to monitor leaf water status in fruit crops

such as banana (Zimmermann et al., 2010), grapevine (Rüger et al., 2010), clementine (Ballester et al., 2015) and persimmon (Ballester et al., 2015; Martínez-Gimeno et al., 2017). Nevertheless, the practical application of the LPCP probe for use with irrigation scheduling is still controversial because, unless many sensors are placed in different parts of the canopy, it can provide only partial insights on total plant water status. In this case, the use of a sensor system (Yara International ASA, Oslo, Norway) necessary for accurate monitoring of orchards would most likely be too costly for most smallholder farm-managers. In addition, most of the studies have been conducted in a tough-leaved species such as olive, suggesting prolonged use of sensors on fruit crops with soft leaves might damage leaf tissue and alter P_p readings (Fig. 2.2).

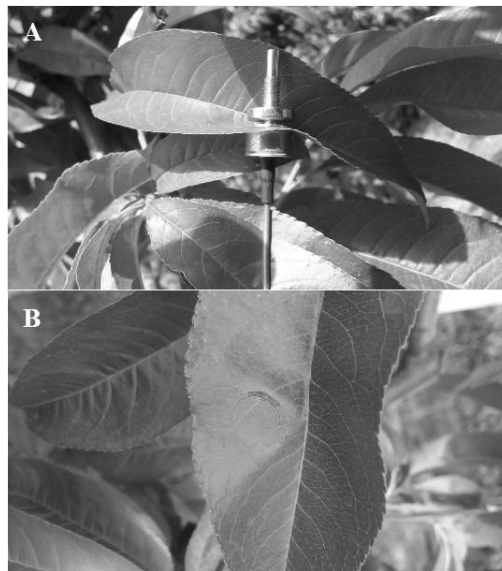


Figure 2.2. Leaf patch clamp pressure probe mounted on a ‘September Bright’ nectarine leaf (A) and mark left on the leaf after a three-day measurement period (B).

LEAF THERMAL SENSING

Measurements of canopy temperature (T_c) as an index of water stress can be carried out by thermal imaging both at ground level and from above the crop (e.g. towers, unmanned aerial vehicles (UAVs), planes, satellites, etc.) (Fernández et al., 2017). The application of thermography or infrared thermometry and the resulting T_c have been related to leaf stomatal aperture (Jones, 2004b; Jones and Schofield, 2008; Lima et al., 2016; Park et al., 2017) and to Ψ_{stem} (Park et al., 2017). However, continuous measurements of plant water status by UAVs or planes are not currently achievable and satellite images often have low resolution. In order to get data that are more accurate on the response of each plant to water stress, leaf thermal sensors might represent a better solution. In 2012, Atherton et al. developed a microfabricated thermal

sensor for the assessment of water content in leaves. This device is composed of a thin-film resistive heater and two thin-film thermocouple temperature sensors patterned on a 10 μ m thick polyimide substrate. The thermal sensor was clamped to pak choi and lettuce leaves, and provided results about the overall thermal resistance of the leaf. When the device's output (ΔT) was compared to RWC, a positive, linear correlation was found. Despite the device being suitable for automation and for continuous data collection, it has not been tested on smaller leaves of fruit trees. In addition, as highlighted in the introductory section, RWC is not the most appropriate indicator for irrigation scheduling.

STEM-MOUNTED SENSORS

Water status in fruit plants is a complex response to climatic conditions and water availability in the soil (Reicosky et al., 1975). Stems and shoots are the bridges that establish the driving force between these two factors. Thus, continuous measurements of stem water status by non-destructive sensors provide insights not only on the variations of soil water availability but also on the reserves of plant tissues.

STEM DENDROMETERS

Diel changes in stem diameter are indirectly determined by the aperture/closure mechanism of stomata, which respond to both air temperatures and vapour pressure deficit (VPD), and soil water availability. While seasonal changes in stem and shoot diameter are a result of plant growth and changes in tissue reserves (Kozłowski and Winget, 1964), diurnal changes are caused by plant tissue hydration (Simonneau et al., 1993). Trees with a C3 photosynthetic metabolism usually shrink during the day and swell at night (Fig. 2.3). However, CAM plants show an inverse behaviour due to their nocturnal stomatal opening (Scalisi et al., 2016) (Fig. 2.3). During the day, as xylem water potential becomes more negative, a radial diffusion of water from bark tissues into the xylem occurs (Parlange et al., 1975). In the late afternoon, plant water uptake exceeds water loss by transpiration and there is a recovery in xylem water potential. This leads to a reversal in the radial flow of water from the xylem back to the phloem. Thus, xylem water potential is the driving force for diurnal stem/trunk diameter variations (Klepper et al., 1971; Whitehead and Jarvis, 1981; Sevanto et al., 2011). The magnitude of stem shrinkage is dependent on the elastic modulus (Génard et al. 2001) and diffusive water properties of phloem tissues (Parlange et al., 1975). The magnitude

of stem diameter changes is also affected by differences in osmotic pressure between bark and xylem (Cochard et al., 2001), by the reflection coefficient to solutes (Génard et al., 2001) and by stem growth rates (McBurney and Costigan 1982). Stem diameter variations provide several water stress indicators for irrigation management, such as maximum and minimum daily stem diameters, maximum daily shrinkage, daily recovery, daily growth, stem growth rate, cumulative growth and early daily shrinkage, as summarized by Fernández (2017). As for other continuous methods, good data interpretation is crucial to allow the sensors to be used for accurate irrigation scheduling (Fernández and Cuevas, 2010; Fernández et al., 2014). Stem diameter variations have been effectively related to plant water content in peach (Simonneau et al., 1992). Fereres and Goldhamer (2015) found a weak relationship between changes in stem diameter and Ψ_{stem} , whereas Intrigliolo and Castel proposed a phenology-dependent relationship between Ψ_{stem} and maximum daily stem shrinkage in plum (2004) and grapevine (2007).

Fernández and Cuevas (2010) published an exhaustive review on the analysis of stem diameter variations for irrigation management in fruit crops. Measuring stem/shoot diameter variations is relatively easy and the use of reliable and cheap dendrometers makes this method easily accessible for fruit growers as an irrigation management tool (Goldhamer and Fereres 2001). Nevertheless, stem diameter variations often do not reveal useful information on fruit and leaf status and their use is not extremely reliable in young plants, as the effect of organ growth might cause misleading results.

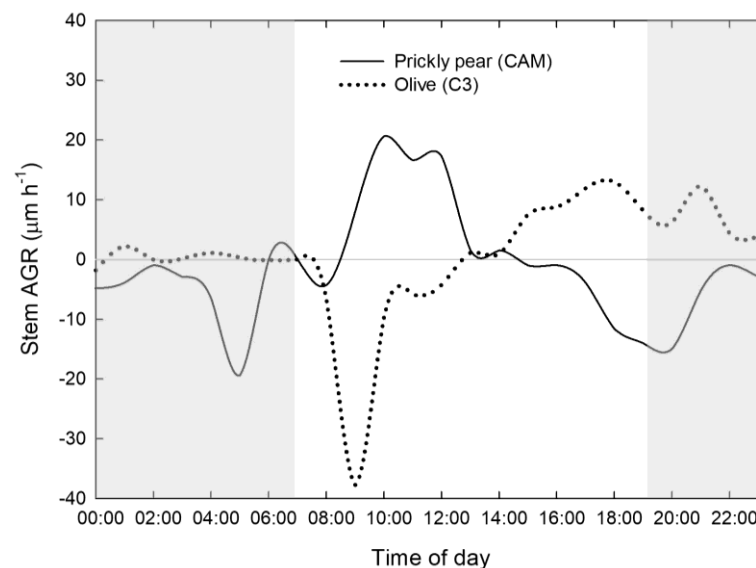


Figure 2.3. Diel stem absolute growth rate (AGR) in 1-year-old prickly pear (CAM metabolism) and olive (C3 metabolism) plants.

SAP FLOW PROBES

Sap flow probes have been widely used for the determination of transpired water in fruit trees, and several methods can be applied for the quantification of sap flow related indexes. All the available methods use heat as the main component of water flow determinations. The methods include stem heat balance (SHB), trunk sector heat balance, heat dissipation, heat field deformation, Cohen's heat-pulse, Green's heat pulse velocity (HPV), heat radio, SapFlow+ and transient thermal dissipation. These technologies are exhaustively described on the website of the Working Group on Sap Flow of the International Society for Horticultural Science, in the paper of main methods (http://www.ishs.org/sites/default/files/documents/methods_0.pdf).

Field data based on diurnal patterns of transpiration through continuous stem flow measurements were reported by Sakuratani (1987), using the SHB method described by Sakuratani (1981). Today, one of the most used methods takes into account the use of thermal dissipation probes (Granier, 1985), whose efficacy depends on some factors such as xylem thermal dissipation and tree size, as described in the review paper published by Lu et al. (2004). Yet, Forester (2017) recently reviewed heat-pulse velocity methods.

The compensation heat pulse (CHP) method (Swanson, 1962) has been successfully tested on species such as olives and pistachios, providing more accurate results than other sap-flow methods even with limitation under reduced transpiration rates (i.e. night, high humidity and cloudy conditions) (Swanson and Whitfield, 1981; Green et al., 2003; Steppe et al., 2010). Testi and Villalobos (2009) built a new calibration that not only allow measurements at low transpiration rates but also assesses the sensor performance along usage. Additional errors may arise during the installation of the probes. Lopez-Bernal et al. (2017) developed a single-probe heat pulse method for estimating sap velocity. These probes were tested on several plant species and generated similar results to CHP method, with the advantage of being simpler and causing less damage to plants. Furthermore, in 2017 Miner et al. developed affordable and simple probes based on the heat pulse theory. The latter can be fabricated by a 3D printer and connected to an ©Arduino board for data acquisition. Despite these probes showing some limitations for low or very high sap flow rate determination, they are a good option when a large number of probes is needed.

In 1999, Nadezhdina associated apple plant water status with sap flow measurements, by matching Ψ_{leaf} with HPV and sap flow index (SFI). Sap flow

measurements were also associated with other Ψ_{stem} in lemon (Ortuno et al., 2006) and olive (Fernández et al., 2011b), among others.

The changes in sap flow indicators are highly affected by stomatal aperture; however, transpiration responses are driven by other factors such as air VPD (Fig. 2.4). Despite sap flow measurements being highly suitable for irrigation automation (Jones, 2004a), the appropriateness of the probes for estimating the correct threshold of plant water status is questionable. The use of sap flow probes is therefore suggested in combination with other sensors on the plant, in order to obtain enough information on tree water status.

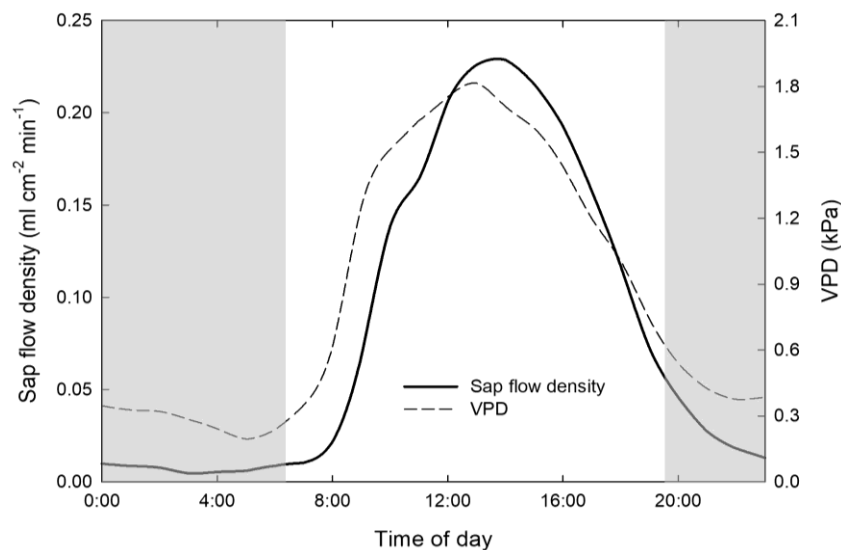


Figure 2.4. Sap flow density fluctuations in 25-year-old orange trees and vapour pressure deficit (VPD) variations over 24 hours in spring.

ADDITIONAL SENSORS

A number of other interesting stem-mounted sensors have been studied for their appropriateness for continuous plant water status determination. McBurney and Costigan (1982), and Dixon and Tyree (1984) obtained continuous Ψ_{stem} data by using a stem-mounted hygrometer, which yielded results concordant with those obtained with a pressure chamber. However, these devices are known to be unreliable (Jones, 2004a). Meron et al. (2015) recently tested an osmometric stem water potential sensor on tangerine and peach stems. The sensor is based on the fluid-to-fluid contact osmometer principle, rather than well-known psychrometry of the vapour phase. Sensor outputs were found to be highly related with pressure chamber Ψ_{stem} results, although delayed in time. Finally, Stroock et al. (2014) have released a recent patent of a stem-embedded microtensiometer that is non-destructive and relatively easy to install, despite this

method being still in the development phase.

FRUIT-MOUNTED SENSORS

Optimum water supply is extremely important for horticultural commercial yield, and water makes up around 90% of the harvest weight of most fruit crops (Schroeder and Wieland, 1956). In different studies, it was demonstrated that fruit water relations have key implication on production and quality (Cuartero and Fernandez-Munoz, 1999; Johnson et al., 1992; Mitchell et al., 1991). Fruit volume is the overall balance of water inflows and outflows from phloem and xylem, as well as from atmosphere through skin exchanges. The latter is a highly complex system and depends on many factors (Lang, 1989).

Whilst presenting a very intuitive way to measure fruit growth patterns, the different sensors ranging from LVDTs, strain-gauges, potentiometers and/or optoelectric sensors, still have many constraints due to the nature of the fruit and to its relation to overall tree water content.

In 1996, Génard and Huguet developed a model to calculate the fruit water content during the monocarp development stage on peach. Based on earlier research on in-out fluid flow of fruit, the model assumed that the flow into the fruit increases with fruit weight and diameter and decreases with maximum daily shrinkage of the trunk, which was used as an indicator of water stress. Fruit transpiration plays a huge role in increasing fruit size as does radiation and other environmental factors (Lang and Thorpe, 1989). Almost all the work in literature links fruit relative water content to volume/size changes. Due to the nature of fruit and their sensitivity, it is very difficult to estimate the plant water content based solely on fruit water content (Lang and Thorpe, 1989). However, different studies have shown how custom-built fruit growth sensors can be used for the overall plant water status determination (Jones and Higgs, 1982; Ho et al., 1987; Berger and Selles, 1993; Morandi et al., 2007a; Thalheimer, 2016). In 1989, using Archimedes' principle, Lang and Thorpe studied the water balance between xylem and phloem in berry fruits. The procedure was easy to perform and needed only common laboratory equipment and a modern electronic scale. They measured the volume increases of fruit by immersing it completely in water. Although air movement and winds influenced the data, output responded largely to other influences like air temperature, water content, evaporation and fruit surface tension. Changes in fruit diameter have been commonly studied with non-destructive equipment such as

callipers, although they require intensive work and they are non-continuous (Higgs and Jones 1984). Klepper et al. (1971) started using LVDTs to continuously measure stem diameters, while Beedlow et al. (1986) designed a strain gauge (dendrometer) to detect changes in stem size through deformation of an attached metal. LVDTs were developed for precision and continuous measurement of stem diameter and they are commonly composed of the sensing part, a frame and data logging unit.

Lang (1989) used LVDTs to measure apple fruit growth. In order to be less sensitive to air and wind movement, hot glue was applied on two sides of the apple where the sensor touched the fruit. In addition, the whole system was covered with aluminium foil to obtain a thermal equilibrium, and to protect the fruit from rain as osmotic water uptake through the skin of the fruit would modify results that assume only xylem, phloem and transpiration exchanges have taken place. The sensor then interfaced to data logging equipment to record data at specific intervals. Subsequently, signals in millivolts can be converted to micrometres (Link et al. 1998). LVDTs and/or strain-gauges have a $<10\mu\text{m}$ accuracy to estimate diameter changes. Volume change (volume growth) can be calculated using the elliptical equation (Yuan and Sun 1994) or an easier perfect sphere equation of the fruit (Hamilton 1929). Different supporting frames have been tested. Primarily, LVDTs or strain-gauges (dendrometers) were used. Although very accurate, these sensors are relatively expensive, taking into consideration that a large number of sensors is needed, both for research or orchard management (Morandi et al., 2007b). Morandi et al. (2007b) worked on a low-cost frame to be built around the LVDT. It was composed of a light-stainless steel frame that reinforces the sensor (a 50 kOhm linear potentiometer) and attaches it to the fruit and to the tree (Fig. 2.5). Sensors' mV outputs can be easily converted to fruit diameter, absolute growth rate (AGR) and relative growth rate (RGR) (Fig. 2.6). The fruit gauges were used to study vascular flows in peach (Morandi et al., 2007b), kiwifruit (Morandi et al., 2010) and pear (Morandi et al., 2014). In 2016, Thalheimer described another method for monitoring radial fruit growth, based on low-cost optoelectronic sensors. The reflective sensor detects the movement of flexible tape with black and white bars that correspond to logic state, and the microcontroller assigns the values to upper or lower thresholds. Despite having a relatively low cost, this technique is not suitable for water status detection, as the sensor is only able to detect fruit enlargement and not shrinkage.



Figure 2.5. Fruit gauge mounted on an olive drupe at its growth stage III (A) and on a nectarine fruit at its growth stage I (B).

Despite the fact that the measurement of fruit water status and fruit growth dynamics under different irrigation strategies might be crucial in order to increase water use efficiency, maintain yield and/or improve fruit quality, assessing stem water potential through fruit attached sensors is usually not practical. Therefore, continuous fruit diameter sensors can be a powerful tool if their output is supported by other continuous data on leaves and/or on stem water status indicators.

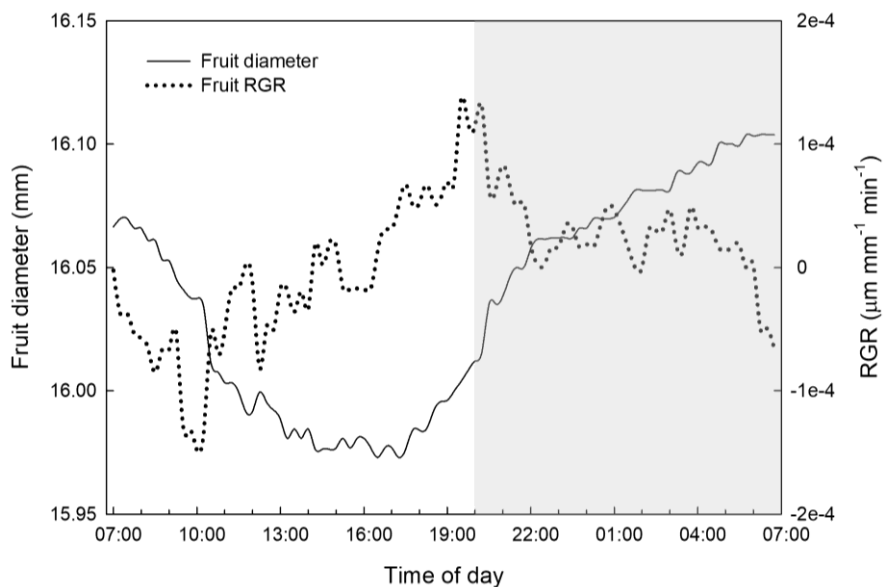


Figure 2.6. Diel fruit diameter and relative growth rate (RGR) variations in an olive drupe at its growth stage III.

CONCLUSIONS

One of the biggest challenges for scientists and farmers to increase water use efficiency worldwide is to develop and understand better sensors and methods for measuring plant water status to use for irrigation scheduling. Indeed, there is not a single best method for plant water status determination that can be universally applied (Jones, 2007). This paper presents a subjective classification of the relevance or usefulness of the different sensors that are available (Table 2.1).

A more integrated approach, which takes into consideration the contemporary use of sensors mounted on several plant organs is suggested in future studies in order to collect integrative information on plant water status. The development of a plant water model that provides real-time information on water indicators based on continuous sensors outputs is certainly a future challenge for scientists, farmers and entrepreneurs who aim to an efficient total automation of irrigation in horticulture.

Table 2.1. Authors' subjective relevance of sensors discussed in this paper for each plant water indicator. Scale from 1 to 5, where 1= poor relevance, and 5= high relevance.

Ψ_{stem} = stem water potential; Ψ_{leaf} = leaf water potential; Ψ_{fruit} = fruit water potential; Ψ_p = leaf turgor pressure; RWC = relative water content; g_s = leaf stomatal conductance; E = transpiration.

Sensor type	Plant water indicators							
	Ψ_{stem}	Ψ_{leaf}	Ψ_{fruit}	Ψ_p	Leaf RWC	Fruit RWC	g_s	E
Leaf thickness sensors	1	2	1	4	5	1	2	2
Leaf pressure probes	2	3	1	5	4	1	2	1
Leaf thermal probes	1	2	1	3	5	1	2	2
Stem dendrometers	3	1	1	1	1	1	4	4
Sap flow probes	2	1	2	2	1	1	4	5
Stem hygrometers	4	1	1	1	1	1	2	2
Stem microtensiometers	5	1	1	1	1	1	2	2
Fruit diameter sensors	2	1	3	1	1	5	1	1

LIST OF REFERENCES

- Allen, R.G., Pereira, L.S., Raes, D., Smith, M., 1998. Crop evapotranspiration. Guidelines for computing crop water requirements. FAO Irrigation and Drainage Paper No. 56. FAO, Rome, Italy.
- Atherton, J.J., Rosamond, M.C., Zeze, D.A., 2012. A leaf-mounted thermal sensor for the measurement of water content. *Sensor Actuat A-Phys*, 187:67-72.
- Bachmann, F., 1922. Studien uber Dickenanderungen von Laubblättern. *Jb. Wiss. Bot*, 61:372-429.
- Ballester, C., Castiella, M., Zimmermann, U., Rüger, S., Martínez Gimeno, M.A., Intrigliolo, D.S., 2015. Usefulness of the ZIM-probe technology for detecting

- water stress in clementine and persimmon trees. Proc. 8th Int. Symp. on Irrigation of Horticultural Crops, Lleida (Spain) 1150:105-112.
- Balling, A., Zimmermann, U., 1990. Comparative measurements of the xylem pressure of *Nicotiana* plants by means of the pressure bomb and pressure probe. *Planta*, 182:325-338.
- Bates, L.M., Hall, A.E., 1981. Stomatal closure with soil water depletion not associated with changes in bulk leaf water status. *Oecologia*, 50:62-65.
- Beedlow, P.A., Daly, D.S., Thiede, M.E., 1986. A new device for measuring fluctuations in plant stem diameter: implications for monitoring plant responses. *Environ Monit Assess*, 6(3):277-282.
- Berger, A., Selles, G., 1993. Diurnal fruit shrinkage: a model. In: Borghetti, Grace, and Raschi (eds.) *Water transport in plants under climatic stress*. Cambridge Univ. Press, Cambridge: 261–267.
- Boyer, J.S., 1989. Water potential and plant metabolism: comments on Dr PJ Kramer's article 'Changing concepts regarding plant water relations', Volume 11, Number 7, pp. 565–568, and Dr JB Passioura's Response, pp. 569–571. *Plant Cell Environ*, 12(2):213-216.
- Bürquez, A., 1987. Leaf thickness and water deficit in plants: a tool for field studies. *J Exp Bot*, 38(1):109-114.
- Chai, Q., Gan, Y., Zhao, C., Xu, H.L., Waskom, R.M., Niu, Y., Siddique, K.H., 2016. Regulated deficit irrigation for crop production under drought stress. A review. *Agron Sustain Dev*, 36(1):3.
- Chalmers, D.J., Burge, G., Jerie, P. H., Mitchell, P. D., 1986. The mechanism of regulation of Bartlett pear fruit and vegetative growth by irrigation withholding and regulated deficit irrigation. *J Am Soc Hortic Sci*, 111(6):904-907.
- Chartzoulakis, K., Bertaki, M., 2015. Sustainable water management in agriculture under climate change. *Agriculture and Agricultural Science Procedia*, 4, 88-98.
- Cochard, H., Forestier, S., Améglio, T., 2001. A new validation of the Scholander pressure chamber technique based on stem diameter variations. *J Exp Bot*, 52(359):1361-1365.
- Connor, D.J., 2005. Adaptation of olive (*Olea europaea* L.) to water-limited environments. *Aus J Agr Res*, 56(11):1181-1189.
- Consoli, S., Stagno, F., Vanella, D., Boaga, J., Cassiani, G., Roccuzzo, G., 2017. Partial root-zone drying irrigation in orange orchards: Effects on water use and crop production characteristics. *Eur J Agron*, 82:190-202.
- Costa, J.M., Ortuño, M.F., Chaves, M.M., 2007. Deficit irrigation as a strategy to save water: physiology and potential application to horticulture. *J Integr Plant Biol*, 49(10):1421-1434.
- Cuartero, J., Fernandez-Munoz, R., 1999. Tomato and salinity. *Sci Hort* 78:83-125.
- Dixon, M.A. Tyree, M.T., 1984. A new stem hygrometer, corrected for temperature gradients and calibrated against the pressure bomb. *Plant Cell Environ*, 7(9):693-697.
- Dry, P.R., Loveys, B.R., 1998. Factors influencing grapevine vigour and the potential for control with partial rootzone drying. *Aus J Grape Wine R*, 4(3):140-148.
- Dry, P.R., Loveys, B.R., Botting, D., During, H., 1995. Effects of partial root-zone drying on grapevine vigour, yield, composition of fruit and use of water. Proc. 9th Aus. wine industry technical conference, Adelaide (Australia), 126-131.
- Du, T., Kang, S., Zhang, J., Davies, W.J., 2015. Deficit irrigation and sustainable water-resource strategies in agriculture for China's food security. *J Exp Bot*, 66(8):2253-2269.

- Ehrenberger, W., Rüger, S., Rodríguez-Domínguez, C.M., Díaz-Espejo, A., Fernández, J.E., Moreno, J., Zimmermann, D., Sukhorukov, V.L., Zimmermann, U., 2012. Leaf patch clamp pressure probe measurements on olive leaves in a nearly turgorless state. *Plant Biol*, 14(4):666-674.
- Faber, B.A., Lovatt, C.J., 2014. Effects of applying less water by partial root zone drying versus conventional irrigation on navel orange yield. *Acta Horti*, 1038:523-530.
- Fensom, D.S., Donald, R.G., 1982. Thickness fluctuations in veins of corn and sunflower detected by a linear transducer. *J Exp Bot*, 33(6):1176-1184.
- Fernández, J.E., 2014. Plant-based sensing to monitor water stress: Applicability to commercial orchards. *Agr Water Manage*, 142:99-109.
- Fernández, J.E., 2017. Plant-Based Methods for Irrigation Scheduling of Woody Crops. *Horticulturae*, 3(2):35.
- Fernández, J.E., Cuevas, M.V., 2010. Irrigation scheduling from stem diameter variations: a review. *Agr Forest Meteorol*, 150(2):135-151.
- Fernández, J.E., Rodríguez-Domínguez, C.M., Pérez-Martin, A., Zimmermann, U., Rüger, S., Martín-Palomo, M.J., Torres-Ruiz, J.M., Cuevas, M.V., Sann, C., Ehrenberger, W., Díaz-Espejo, A., 2011a. Online-monitoring of tree water stress in a hedgerow olive orchard using the leaf patch clamp pressure probe. *Agr Water Manage*, 100(1):25-35.
- Fernández, J.E., Moreno, F., Martín-Palomo, M.J., Cuevas, M.V., Torres-Ruiz, J.M., Moriana, A., 2011b. Combining sap flow and trunk diameter measurements to assess water needs in mature olive orchards. *Environ Exp Bot*, 72(2):330-338.
- Génard M., Huguet J.G., 1996. Modeling the response of peach fruit growth to water stress. *Tree Physiol*, 16(4):407-415.
- Génard, M., Fishman, S., Vercambre, G., Huguet, J.G., Bussi, C., Besset, J., Habib, R., 2001. A biophysical analysis of stem and root diameter variations in woody plants. *Plant Physiol*, 126(1):188-202.
- Goldhamer, D.A., Fereres, E., 2001. Irrigation scheduling protocols using continuously recorded trunk diameter measurements. *Irrigation Sci*, 20(3):115-125.
- Gosling, S.N., Arnell, N.W., 2016. A global assessment of the impact of climate change on water scarcity. *Climatic Change*, 134(3):371-385.
- Granier, A., 1985. Une nouvelle méthode pour la mesure du flux de sève brute dans le tronc des arbres. In "Annales des Sciences forestières", EDP Sciences, 42(2):193-200.
- Green, P.B., 1968. Growth physics in *Nitella*: a method for continuous in vivo analysis of extensibility based on a micro-manometer technique for turgor pressure. *Plant Physiol*, 43(8):1169-1184.
- Green, P.B., Stanton, F.W., 1967. Turgor pressure: direct manometric measurement in single cells of *Nitella*. *Science*, 155(3770):1675-1676.
- Green, S., Clothier, B., Jardine, B., 2003. Theory and practical application of heat pulse to measure sap flow. *Agron J*, 95(6):1371-1379.
- Hamilton, C.C., 1929. The growth of the foliage and fruit of the apple in relation to the maintenance of a spray coating. *J Econ Entomol*, 22(2):387-396.
- Heathcote, D.G., Etherington, J.R., Woodward, F.I., 1979. An instrument for non-destructive measurement of the pressure potential (turgor) of leaf cells. *J Exp Bot*, 30(4):811-816.
- Higgs, K.H., Jones, H.G., 1984. A microcomputer-based system for continuous measurement and recording fruit diameter in relation to environmental factors. *J Exp Bot* 35:1646-1655.

- Ho, L.C., Grange, R.I., Picken, A.J., 1987. An analysis of the accumulation of water and dry matter in tomato fruit. *Plant Cell Environ*, 10(2):157-162.
- HU, J.C., CHENG, Y., WANG, M.B., SONG, X., LI, D.S., 2013. Development of Precision Plant Leaf Thickness Measuring Instrument. *Automat Ins*, 12:6.
- Hüsken, D., Steudle, E., Zimmermann, U., 1978. Pressure probe technique for measuring water relations of cells in higher plants. *Plant Physiol*, 61(2):158-163.
- Intrigliolo, D.S., Castel, J.R., 2004. Continuous measurement of plant and soil water status for irrigation scheduling in plum. *Irrigation Sci*, 23(2):93-102.
- Intrigliolo, D.S., Castel, J.R., 2007. Evaluation of grapevine water status from trunk diameter variations. *Irrigation Sci*, 26(1):49-59.
- Jinwen, L., Jingping, Y., Pinpin, F., Junlan, S., Dongsheng, L., Changshui, G., Wenyue, C., 2009. Responses of rice leaf thickness, SPAD readings and chlorophyll a/b ratios to different nitrogen supply rates in paddy field. *Field Crop Res*, 114(3):426-432.
- Johnson R.W., Dixon M.A., Lee D.R., 1992. Water relations of the tomato during fruit growth. *Plant Cell Environ*, 15:947-953.
- Jones, H.G., 1973. Estimation of plant water status with the beta-gauge. *Agr Meteorol*, 11:345-355.
- Jones, H.G., 1984. Physiological mechanisms involved in the control of leaf water status: implications for the estimation of tree water status. *Proc. 1st Int. Sym. on Water Relations in Fruit Crops, Pisa (Italy)* 171:291-296.
- Jones, H.G., 1990. Plant water relations and implications for irrigation scheduling. *Acta Hortic*, 278:67-76.
- Jones, H.G., 2004a. Irrigation scheduling: advantages and pitfalls of plant-based methods. *J Exp Bot*, 55(407):2427-2436.
- Jones, H.G., 2004b. Application of thermal imaging and infrared sensing in plant physiology and ecophysiology. *Adv Bot Res*, 41:107-163.
- Jones, H. G., 2007. Monitoring plant and soil water status: established and novel methods revisited and their relevance to studies of drought tolerance. *J Exp Bot*, 58(2):119-130.
- Jones, H.G., Higgs, K.H., 1982. Surface conductance and water balance of developing apple (*Malus pumila* Mill) fruits. *J Exp Bot* 132:67-77.
- Jones, H.G., Schofield, P., 2008. Thermal and other remote sensing of plant stress. *Gen App Plant Physiol*, 34(1-2):19-32.
- Klepper, B., Browning, V.D. Taylor, H.M., 1971. Stem diameter in relation to plant water status. *Plant Physiol*, 48(6):683-685.
- Kozlowski, T.T., Winget, C.H., 1964. Diurnal and seasonal variation in radii of tree stems. *Ecology*, 45(1):149-155.
- Kramer, P.J., 1988. Changing concepts regarding plant water relations. *Plant Cell Environ*, 11(7):565-568.
- Lal Bhardwaj, R., 2013. Effect of mulching on crop production under rainfed condition- a review. *Agr Rev*, 34(3): 188-197.
- Lang A., 1989. Xylem, Phloem and Transpiration flow in developing apple fruits. *J Exp Bot*, 41(227):645-651.
- Lang A., Thorpe M., 1989. Xylem, Phloem and Transpiration flow in a grape: Application of a technique for measuring the volume of attached fruits to high resolution using Archimedes' principle. *J Exp Bot*, 40(219):1069-1078.
- Lima, R.S.N., García-Tejero, I., Lopes, T.S., Costa, J.M., Vaz, M., Durán-Zuazo, V.H., Chaves, M., Glenn, D.M., Campostrini, E., 2016. Linking thermal imaging to physiological indicators in *Carica papaya* L. under different watering regimes. *Agr*

- Water Manage, 164:148-157.
- Link, S.O., Thiede, M.E., Van Bavel, M.G., 1998. An improved strain gauge device for continuous field measurement of stem and fruit diameter. *J Exp Bot* 49:1583-1587.
- Lintilhac, P.M., Wei, C., Tanguay, J.J., Outwater, J.O., 2000. Ball tonometry: a rapid, nondestructive method for measuring cell turgor pressure in thin-walled plant cells. *J Plant Growth Regul*, 19(1):90-97.
- Lo Bianco, R., Scalisi, A., 2017. Water relations and carbohydrate partitioning of four greenhouse-grown olive genotypes under long-term drought. *Trees*, 31(2):717-727.
- López-Bernal, Á., Testi, L., Villalobos, F.J., 2017. A single-probe heat pulse method for estimating sap velocity in trees. *New Phytolog*, 216(1):321-329.
- Lu, P., Urban, L., Zhao, P., 2004. Granier's thermal dissipation probe (TDP) method for measuring sap flow in trees: theory and practice. *Acta Bot Sin*, 46(6):631-646.
- Malone, M., 1993. Rapid inhibition of leaf growth by root cooling in wheat: kinetics and mechanism. *J Exp Bot*, 44(11):1663-1670.
- Marino, G., Pernice, F., Marra, F.P., Caruso, T., 2016. Validation of an online system for the continuous monitoring of tree water status for sustainable irrigation managements in olive (*Olea europaea* L.). *Agr Water Manage*, 177:298-307.
- Martínez-Gimeno, M.A., Castiella, M., Rüger, S., Intrigliolo, D.S., Ballester, C., 2017. Evaluating the usefulness of continuous leaf turgor pressure measurements for the assessment of Persimmon tree water status. *Irrigation Sci*, 35(2):159-167.
- McBurney, T., 1992. The relationship between leaf thickness and plant water potential. *J Exp Bot*, 43(3):327-335.
- McBurney, T., Costigan, P.A., 1982. Measurement of stem water potential of young plants using a hygrometer attached to the stem. *J Exp Bot*, 33(3):426-431.
- McCutchan, H., Shackel, K.A., 1992. Stem-water potential as a sensitive indicator of water stress in prune trees (*Prunus domestica* L. cv. French). *J Am Soc Hortic Sci*, 117(4):607-611.
- Meidner, H., 1952. An instrument for the continuous determination of leaf thickness changes in the field. *J Exp Bot*, 3(3):319-325.
- Meron, M., Goldberg, S.Y., Solomon-Halgor, A., Ramon, G., 2015. Embedded stem water potential sensor. In: Stafford (ed.), *Precision agriculture '15*, Wageningen Academic Publishers, Wageningen: 527-532.
- Miner, G.L., Ham, J.M., Kluitenberg, G.J., 2017. A heat-pulse method for measuring sap flow in corn and sunflower using 3D-printed sensor bodies and low-cost electronics. *Agric Forest Meteorol*, 246:86-97.
- Mitchell, J.P., Shennan, C., Grattan, S.R., 1991. Developmental changes in tomato fruit composition in response to water deficit and salinity. *Physiol Plant*, 83:177-185.
- Morandi B., Manfrini, L., Zibordi, M., Noferini, M., Fiori, G., Corelli Grappadelli, L., 2007a. A Low-cost device for accurate and continuous measurement of fruit diameter. *HortScience*, 42(6):1380-1382.
- Morandi, B., Rieger, M., Corelli Grappadelli, L. 2007b. Vascular flows and transpiration affect peach (*Prunus persica* Batsch.) fruit daily growth. *Journal of Experimental Botany*, 58(14):3941-3947.
- Morandi, B., Manfrini, L., Losciale, P., Zibordi, M., Corelli Grappadelli, L., 2010. Changes in vascular and transpiration flows affect the seasonal and daily growth of kiwifruit (*Actinidia deliciosa*) berry. *Ann Bot-London*, 105(6):913-923.
- Morandi, B., Losciale, P., Manfrini, L., Zibordi, M., Anconelli, S., Pierpaoli, E., Corelli Grappadelli, L., 2014. Leaf gas exchanges and water relations affect the daily

- patterns of fruit growth and vascular flows in Abbé Fétel pear (*Pyrus communis* L.) trees. *Sci Hortic-Amsterdam*, 178:106-113.
- Mossad, A., Scalisi, A., Lo Bianco, R., 2017. Growth and water relations of field-grown 'Valencia' orange trees under long-term partial rootzone drying. *Irrigation Sci*, 1-16.
- Nadezhkina, N., 1999. Sap flow index as an indicator of plant water status. *Tree physiol*, 19(13):885-891.
- Ortuno, M.F., García-Orellana, Y., Conejero, W., Ruiz-Sánchez, M.C., Alarcón, J.J., Torrecillas, A., 2006. Stem and leaf water potentials, gas exchange, sap flow, and trunk diameter fluctuations for detecting water stress in lemon trees. *Trees*, 20(1):1-8.
- Paço, T. A., Ferreira, M. I., Conceição, N., 2006. Peach orchard evapotranspiration in a sandy soil: Comparison between eddy covariance measurements and estimates by the FAO 56 approach. *Agr Water Manage*, 85(3):305-313.
- Padilla-Díaz, C.M., Rodríguez-Dominguez, C.M., Hernandez-Santana, V., Perez-Martin, A., Fernández, J.E., 2016. Scheduling regulated deficit irrigation in a hedgerow olive orchard from leaf turgor pressure related measurements. *Agr Water Manage*, 164:28-37.
- Park, S., Ryu, D., Fuentes, S., Chung, H., Hernández-Montes, E., O'Connell, M., 2017. Adaptive estimation of crop water stress in nectarine and peach orchards using high-resolution imagery from an unmanned aerial vehicle (UAV). *Remote Sens-Basel*, 9(8):828.
- Parlange, J.Y., Turner, N.C., Waggoner, P.E., 1975. Water uptake, diameter change, and nonlinear diffusion in tree stems. *Plant Physiol*, 55(2):247-250.
- Rahemi, A., Yadollahi, A., 2005. Rainfed almond orchards in Iran, ancient and new methods and the value of water harvesting techniques. *Proc. 4th Int. Sym. on Pistachios and Almonds, Teheran (Iran)* 726:449-454.
- Reicosky, D.C., Campbell, R.B., Doty, C.W., 1975. Diurnal fluctuation of leaf-water potential of corn as influenced by soil matric potential and microclimate. *Agron J*, 67(3):380-385.
- Rodríguez-Dominguez, C.M., Ehrenberger, W., Sann, C., Rüger, S., Sukhorukov, V., Martín-Palomo, M.J., Diaz-Espejo, A., Cuevas, M.V., Torres-Ruiz, J.M., Perez-Martin, A., Zimmermann, U., 2012. Concomitant measurements of stem sap flow and leaf turgor pressure in olive trees using the leaf patch clamp pressure probe. *Agr water manage*, 114:50-58.
- Rüger, S., Netzer, Y., Westhoff, M., Zimmermann, D., Reuss, R., Ovadiya, S., Gessner, P., Zimmermann, G., Schwartz, A., Zimmermann, U., 2010. Remote monitoring of leaf turgor pressure of grapevines subjected to different irrigation treatments using the leaf patch clamp pressure probe. *Aus J Grape Wine R*, 16(3):405-412.
- Sakuratani, T., 1981. A heat balance method for measuring water flux in the stem of intact plants. *J Agr Meteorol*, 37(1):9-17.
- Sakuratani, T., 1987. Studies on Evapotranspiration from Crops. *J Agr Meteorol*, 42(4):309-317.
- Scalisi, A., Morandi, B., Inglese, P., Lo Bianco, R., 2016. Cladode growth dynamics in *Opuntia ficus-indica* under drought. *Env Exp Bot*, 122:158-167.
- Schewe, J., Heinke, J., Gerten, D., Haddeland, I., Arnell, N.W., Clark, D.B., ..., Gosling, S.N., 2014. Multimodel assessment of water scarcity under climate change. *P Natl Acad Sci*, 111(9):3245-3250.
- Scholander, P.F., Hammel, H.T., Bradstreet, E.D., Hemmingsen, E.A., 1965. Sap pressure in vascular plants. *Science*, 148(3668):339-346.

- Schroeder C.A., Wieland P.A., 1956. Diurnal fluctuation in size in various parts of the avocado tree and fruit. *P Am Soc Hortic Sci*, 68:253-258
- Sevanto, S., Hölttä, T. and Holbrook, N.M., 2011. Effects of the hydraulic coupling between xylem and phloem on diurnal phloem diameter variation. *Plant Cell Environ*, 34(4):690-703.
- Shackel, K.A., Ahmadi, H., Biasi, W., Buchner, R., Goldhamer, D., Gurusinghe, S., Hasey, J., Kester, D., Krueger, B., Lampinen, B., McGourty, G., 1997. Plant water status as an index of irrigation need in deciduous fruit trees. *HortTechnology*, 7(1):23-29.
- Sharon, Y. and Bravdo, B.A., 1996. Irrigation control for citrus according to the diurnal cycling of leaf thickness. *Proc. Int. Con. on Water & Irrigation, Tel Aviv (Israel)* 273-283.
- Simonneau, T., Habib, R., Goutouly, J.P., Huguet, J.G., 1993. Diurnal changes in stem diameter depend upon variations in water content: direct evidence in peach trees. *J Exp Bot*, 44(3):615-621.
- Snyder, R.L., 2017. Climate Change Impacts on Water Use in Horticulture. *Horticulturae*, 3(2):27.
- Steppe, K., De Pauw, D.J., Lemeur, R., 2008. A step towards new irrigation scheduling strategies using plant-based measurements and mathematical modelling. *Irrigation Sci*, 26(6):505.
- Steppe, K., De Pauw, D.J., Doody, T. M., Teskey, R.O., 2010. A comparison of sap flux density using thermal dissipation, heat pulse velocity and heat field deformation methods. *Agric and Forest Meteorol*, 150(7): 1046-1056.
- Stedle, E., Lüttge, U., Zimmermann, U., 1975. Water relations of the epidermal bladder cells of the halophytic species *Mesembryanthemum crystallinum*: direct measurements of hydrostatic pressure and hydraulic conductivity. *Planta*, 126(3):229-246.
- Stöckle, C.O., Marsal, J., Villar, J.M., 2011. Impact of climate change on irrigated tree fruit production. *Acta Hort*, 889:41-52.
- Stroock, A.D., Lakso, A.N., Pagay, V., Ilic, B., Metzler, M., Cornell University, 2014. Microtensiometer sensor, probe and method of use. U.S. Patent 8,695,407.
- Swanson, R.H., 1962. An instrument for detecting sap movement in woody plants. Paper 68, USDA Forest Service, Fort Collins, CO.
- Swanson, R.H., Whitfield, W.A. 1981. A numerical analysis of heat pulse velocity theory and practice. *J Exp Bot*, 32(126): 221-239.
- Syversten, J.P. Levy, Y., 1982. Diurnal changes in citrus leaf thickness, leaf water potential and leaf to air temperature difference. *J Exp Bot*, 33(4):783-789.
- Testi, L., Villalobos, F.J., 2009. New approach for measuring low sap velocities in trees. *Agr Forest Meteorol*, 149(3):730-734.
- Thalheimer, M., 2016. A new optoelectronic sensor for monitoring fruit or stem radial growth. *Comput Electron Agric*, 123:149-153.
- Turner, N.C., Sobrado, M.A., 1983. Evaluation of a non-destructive method for measuring turgor pressure in *Helianthus*. *J Exp Bot*, 34(11):1562-1568.
- Wang, H., Wang, C., Zhao, X., Wang, F., 2015. Mulching increases water-use efficiency of peach production on the rainfed semiarid Loess Plateau of China. *Agr Water Manage*, 154:20-28.
- Ward, F.A., Pulido-Velazquez, M., 2008. Water conservation in irrigation can increase water use. *P Natl A Sci*, 105(47):18215-18220.
- Wei, C., Tyree, M.T., Stedle, E., 1999. Direct measurement of xylem pressure in leaves of intact maize plants. A test of the cohesion-tension theory taking hydraulic

- architecture into consideration. *Plant Physiol*, 121(4):1191-1205.
- Westhoff, M., Reuss, R., Zimmermann, D., Netzer, Y., Gessner, A., Geßner, P., Zimmermann, G., Wegner, L.H., Bamberg, E., Schwartz, A., Zimmermann, U., 2009. A non-invasive probe for online-monitoring of turgor pressure changes under field conditions. *Plant Biol*, 11(5):701-712.
- Whitehead, D., Jarvis, P.G., 1981. Coniferous forests and plantations. In: Kozlowski (ed.) *Water deficits and plant growth*, VI, Academic Press Ltd., New York, 49-152.
- Yuan, K., Sun, R., 1995. A New Method for Measuring and Calculating Volume of Apple Fruit. *Acta Horti Sin*, 22:386-388.
- Zia, S., Spohrer, K., Wenyong, D., Spreer, W., Romano, G., Xiongkui, H., 2011. Monitoring physiological responses to water stress in two maize varieties by infrared thermography. *Int J Agr Biol Eng*, 4(3):7-15.
- Zimmermann, D., Reuss, R., Westhoff, M., Geßner, P., Bauer, W., Bamberg, E., ..., Zimmermann, U. 2008. A novel, non-invasive, online-monitoring, versatile and easy plant-based probe for measuring leaf water status. *J Exp Bot*, 59(11):3157-3167.
- Zimmermann, U., Råde, H., Steudle, E., 1969. Kontinuierliche druckmessung in pflanzenzellen. *Naturwissenschaften*, 56(12):634-634.
- Zimmermann, U., Rüger, S., Shapira, O., Westhoff, M., Wegner, L.H., Reuss, R., Gessner, P., Zimmermann, G., Israeli, Y., Zhou, A., Schwartz, A., 2010. Effects of environmental parameters and irrigation on the turgor pressure of banana plants measured using the non-invasive, online monitoring leaf patch clamp pressure probe. *Plant Biol*, 12(3), 424-436.

3. OLIVE TREE WATER RELATIONS

Genotype-dependent strategies to cope with drought - A case study: “Transpiration rates and hydraulic conductance of two olive genotypes with different sensitivity to drought”

Based on the paper:

Scalisi A., Marra F.P., Caruso T., Illuminati C., Costa F., Lo Bianco R. Transpiration rates and hydraulic conductance of two olive genotypes with different sensitivity to drought. Accepted by Acta Horti (August 2018, presented at the symposium “Water and Nutrient Relations and Management of Horticultural Crops”, IHC 2018, Istanbul, Turkey).

ABSTRACT

Although some mechanisms of leaf dehydration tolerance are known in olive (*Olea europaea* L.), insights on adjustments in stem and root hydraulic conductance (K) in response to drought are yet to be explored. This work investigated transpiration mechanisms and K regulations in two olive genotypes showing different sensitivity to drought stress. In 2017, one-year-old potted 'Nocellara del Belice' (NB) and 'Cerasuola' (CE) plants were set in a greenhouse and double-bagged to avoid evaporation from soil surface. Half of the plants were drought-stressed (DS, no irrigation) for more than 30 days and the remaining plants were well-watered (WW). At the end of the drought period, stem and root portions were separated and used to determine hydraulic conductance (K). Results were then normalized using stem cross-sectional area and expressed as sapwood specific conductance (K_s). NB plants were able to keep a normalized transpiration rate (T_N) stable until a lower transpirable soil water fraction (W_{fraction}) than CE plants, indicating lower tolerance to sudden drought events in the former. Dry matter content sensibly increased after drought in NB, not in CE. In addition, drought increased root/leaf ratio in NB, not in CE. Regardless of genotype, stem K_s was double in DS when compared to WW plants. Conversely, root K_s was not affected by drought, suggesting that xylem modifications in response to water deficit occur mainly in aboveground organs. Overall, these results show that the two olive genotypes use different mechanisms to cope with drought and confirm that the CE genotype tolerates quick tissue dehydration better than NB.

Keywords: dry matter, leaf area, root, stem, stomatal regulation, water deficit.

INTRODUCTION

Olive (*O. europaea* L.) genotypes have developed various strategies to cope with

drought stress (Bacelar et al., 2007; Boussadia et al., 2008; Bacelar et al., 2009; Faraloni et al., 2011). Among them, osmotic adjustments and water potential lowering seem to have pivotal importance in olive responses to water deficit (Xiloyannis et al., 1999; Dichio et al., 2003; Lo Bianco and Scalisi, 2017). Although some mechanisms of genotype-dependent leaf dehydration tolerance, leaf morphological and structural adaptations are known (Bacelar et al., 2004; Ennajeh et al., 2010), insights on transpiration patterns and stem and root hydraulic conductance (K) adjustments after prolonged drought are yet to be explored.

Plant transpiration patterns in response to soil drying follow a two-segment trend with a first section characterised by no responses to reduction of available water, and a second section of linear decrease (Sinclair et al., 2005). The threshold of soil available water at which transpiration begins its linear decrease may change depending on stomatal sensitivity to water deficit; indeed, early stomatal closure may be a convenient strategy to cope with sudden drought events (Sinclair and Muchow, 2001). Yet, environmental conditions seem to have no influence at all on the two-segment transpiration response to soil drying (Sadras and Milroy, 1996). Hence, the study of transpiration mechanisms may provide useful information on strategies adopted by olive genotypes to withstand water deficit.

The high-pressure flow meter (HPFM), firstly described by Tyree et al. (1993), allows for a relatively quick assessment of K in roots, stems and leaves (Tyree et al., 1994; Tyree et al., 1998; Tyree et al., 1999). Severe long-term drought may cause embolism and cavitation in xylem conduits of woody plants (Tyree and Dixon, 1986), although species adapted to drought are less susceptible to these phenomena (Delzon and Cochard, 2014). Cavitation events cause a reduction of K (Cochard et al., 1996), which instead, in drought-adapted plants, may be incremented by aquaporin activity (Afzal et al., 2016).

The Sicilian olive germplasm is characterised by high genetic diversity (La Mantia et al., 2005; Caruso et al., 2007; Lo Bianco et al., 2013; Lo Bianco and Avellone, 2014; Marra et al., 2013), and a pool of genotypes with different responses to water deficit is available. This work aimed to investigate K regulations and transpiration pattern in two Sicilian olive genotypes characterised by different sensitivity to drought.

MATERIALS AND METHODS

The experiment was conducted in summer 2017 in a greenhouse at the

Department of Agricultural, Food and Forest Sciences of the University of Palermo. A total of twelve one-year-old self-rooted 'Nocellara del Belice' (NB) and 'Cerasuola' (CE) plants were used in the experiment, as the two genotypes are known for their different degree of sensitivity to drought and high temperatures (Grisafi et al., 2004). Three months before the beginning of the experiment, plants were transplanted into 10-L pots with sandy loam soil. In the first two months, potted plants received full irrigation, calculated on the basis of total plant evapotranspiration (ET). Pots were weighed at three-day intervals, before and after each irrigation event. The difference between the weight of each pot before and after irrigation represented total ET. Hourly climate parameters were recorded with a μ Metos weather station (Pessl Instruments, Weiz, AT). After the two months at full irrigation, a pressure chamber (PMS 600, Instrument Company, Albany, US) was used to determine midday stem water potential (Ψ_{stem}).

TRANSPIRATION

The day after Ψ_{stem} measurements, pots were enclosed in two white plastic bags to avoid evaporation from soil surface and then equally divided in two treatments: drought-stressed (DS, no water until no further weight loss by means of transpiration occurred) and well-watered (WW) at full ET. Potted plants were weighed each day with a precision Gibertini 45/N bench scale (Gibertini Elettronica, Milano, IT) to determine transpired water, and WW plants were watered daily with the amount of water lost during the previous 24 hours. Transpiration was plotted against the fraction of total transpirable water (W_{fraction}), a concept introduced by Sinclair and Ludlow (1986). In this study, we used an upper limit W_{fraction} equal to 1.0, corresponding to the weight of pots at field capacity, and a lower limit of 0.1, equivalent to the threshold at which transpiration decreased to 10% of field capacity (Sinclair et al., 2005). A normalized transpiration rate (T_N) was then estimated using the method described by Sinclair et al. (2005).

HYDRAULIC CONDUCTANCE

At the end of the drought period (from July 4 to August 5, 2017), plants were removed from pots and above- and below-ground portions were sampled separately. The excision was carried out under water to avoid embolism, but samples were not rehydrated before measurements. A HPFM (Gen-2, Dynamax Inc., Houston, TX, USA) was used to determine K by the transient analysis method (Tyree et al., 1994) (i.e. flow is measured across an increasing water pressure gradient) in stem and root sections. A

pressure range between 0 and 500 kPa was used for all the transient measurements, with the yellow valve open. The yellow valve pressure range was selected in accordance with the ‘correct flow range’ procedure described in the HPFM manual, with the working range for the differential pressure between the two pressure transducers (PT1 and PT2) set to 20-120 kPa. K was equal to the slope of the increasing flow and pressure. Values were then normalized using the stem cross-sectional area, which is a good estimate of sapwood area in young plants, and sapwood-specific conductance (K_s) was obtained for stem and root sections.

LEAF AREA AND DRY MATTER CONTENT

Leaf area and leaf size were measured using a LI3000A leaf area meter equipped with a LI3050 Belt Conveyer (LICOR Inc., Lincoln, NE), and leaf fresh (FW) and dry weight (DW) were subsequently determined. Root FW and DW were also obtained after roots were gently washed off the soil in pots. Leaf and root DW were determined after drying samples in an oven at 60°C until constant weight. Dry matter content (DMC) was calculated as g of DW in g of FW (Shipley and Vu, 2002).

STATISTICAL PROCEDURES

Data were analysed with analysis of variance followed by Tukey’s Honestly Significant Differences test and linear regression analysis using SYSTAT 13.1 (Systat software Inc., Chicago, Illinois, USA) procedures and results were plotted using SigmaPlot 12.5 (Systat software Inc., Chicago, Illinois, USA). The two genotype-dependent slopes of the linear T_N decrease in drying soils were compared with a t-test.

RESULTS AND DISCUSSION

As expected, before the beginning of the drought experiment (July 3, 2017), plants were experiencing optimal water status. Indeed, midday Ψ_{stem} in NB and CE was -1.19 MPa (S.E. = 0.07, N = 6) and -1.00 MPa (S.E. = 0.09, N = 6), respectively. Lower values of Ψ_{stem} in NB are in accordance with unpublished data, in which CE has been found to keep higher Ψ_{stem} than NB at a wide range of drought levels.

WEATHER CONDITIONS

Drought in DS plants lasted 33 days (from July 4 to August 5, 2017), reaching an almost zero-transpiration, right before death of plants because of tissue dehydration. During drought, the average daily maximum temperature was 40.2° C and the average

daily maximum vapour pressure deficit (VPD) was 5.52 kPa, with peaks of 44.1° C and 7.23 kPa, respectively, on the very last day of experiment (Fig. 3.1).

TRANSPIRATION

Normalized transpiration rate (T_N) of NB and CE followed the expected two-segment pattern during soil drying (Fig. 3.2), in accordance with results from Sinclair et al. (2005). In NB plants, T_N remained at its maximum until W_{fraction} reached 0.45 (Fig. 3.2A), whereas T_N of CE plants began its decrease at $W_{\text{fraction}} = 0.55$ (Fig. 3.2B). As the T_N in NB started to decrease at lower W_{fraction} levels than CE, the slope of its linear decline was found to be significantly higher in NB than in CE ($p < 0.001$). This difference indicates a higher sensitivity of the NB genotype to sudden drought. Indeed, CE plants may close their stomata earlier than NB to avoid excessive water loss, a mechanism that occurs in maize and sorghum (Sinclair and Muchov, 2001), and to reduce risks of xylem cavitation. Decreases in T_N are the logical consequence of stomatal closure. Grisafi et al. (2004) previously found a higher sensitivity to water deficit in NB, when compared to CE. Our results also agree with findings of Lo Bianco and Scalisi (2017), who suggested that NB is relatively intolerant to leaf dehydration, as there is a steep drop in transpiration rates that might lead to plant desiccation.

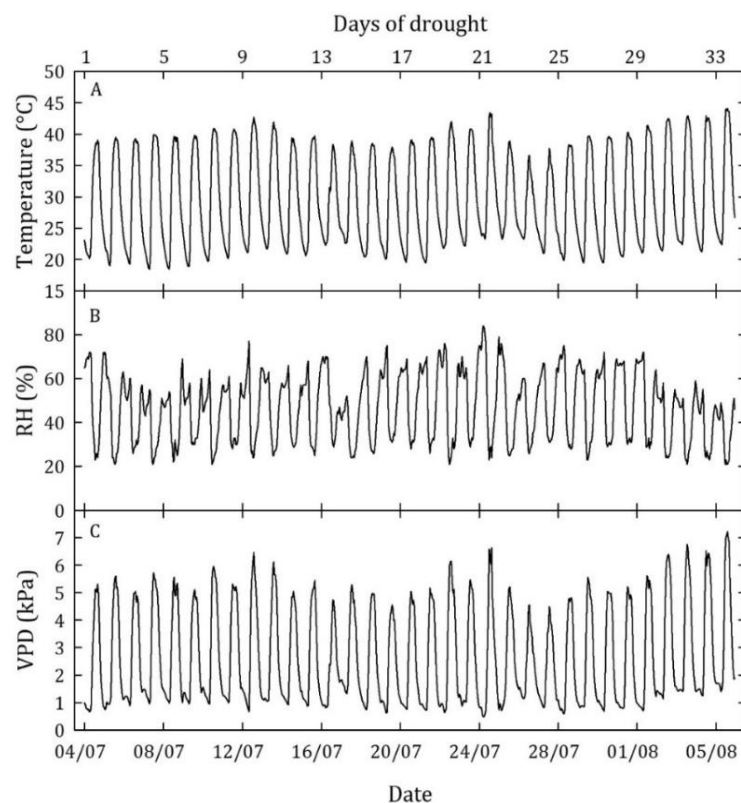


Figure 3.1. Temperature (A), relative humidity (RH, B) and vapour pressure deficit (VPD, C) inside the greenhouse during the drought period.

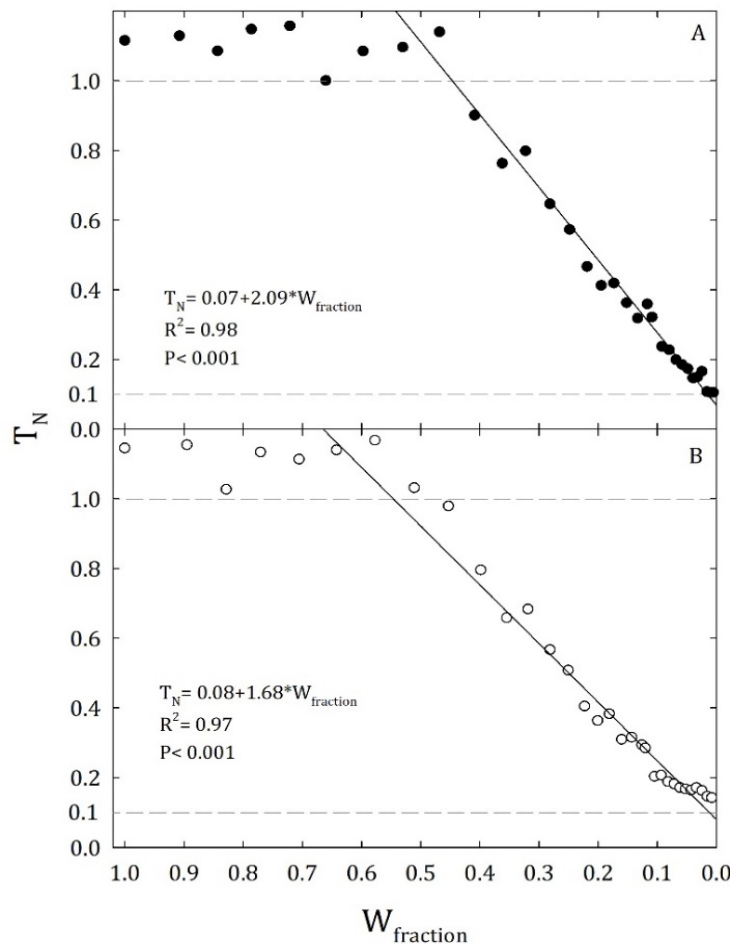


Figure 3.2. Normalized transpiration rate (T_N) of ‘Nocellara del Belice’ (A) and ‘Cerasuola’ (B) olive genotypes under different fractions of total transpirable water (W_{fraction}). Dashed lines (— —) indicate T_N upper and lower limits.

DRY MATTER CONTENT, LEAF AREA AND ROOT/LEAF RATIO

Analysis of variance on leaf DMC showed a significant interaction between genotypes and drought treatments ($P < 0.01$). Indeed, leaf DMC sensibly increased after drought in NB but did not significantly change in CE (Fig. 3.3A). This was likely to be due to the low resistance of NB against leaf dehydration suggested by Lo Bianco and Scalisi (2017). On the other hand, when roots were considered, no significant differences were found between genotypes and the interaction between genotypes and irrigation treatments was not significant. Nevertheless, the overall root DMC increased in DS plants (Fig. 3.3B). This increase of DMC is expected and most likely to be due to a reduction of water in plant organs.

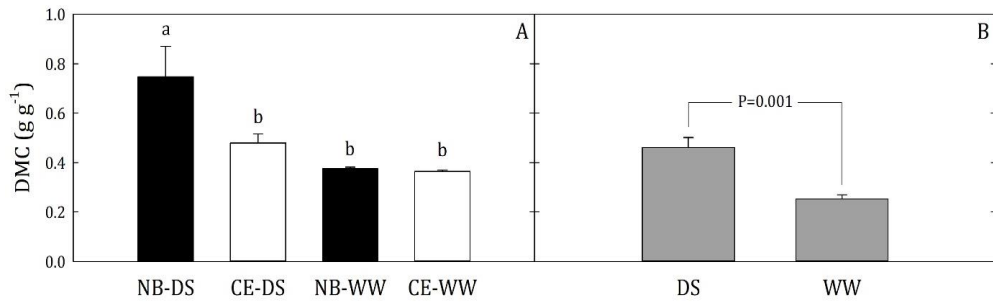


Figure 3.3. Dry matter content (DMC) in leaves (A) of ‘Nocellara del Belice’ and ‘Cerasuola’ olive under well-watered (WW) and drought-stressed (DS) conditions, and in roots (B) of WW and DS plants. Error bars indicate standard errors of the means. Different letters in panel A indicate significant differences determined with Tukey’s multiple range test ($P \leq 0.05$). P value in panel B from analysis of variance.

Regardless of drought, NB plants yielded a significantly higher leaf area, and leaves were significantly larger than CE plants ($P < 0.05$, Tab. 3.1). Nevertheless, drought led to a significant similar reduction of leaf size in both genotypes ($P < 0.05$, Tab. 3.1). When root fresh weight (FW_{root}) was related to leaf fresh weight (FW_{leaf}) to determine a change in balance between below- and above-ground mass, NB showed a generally higher (non-significant) root/leaf ratio than CE and also a tendency to allocate more biomass to roots than leaves under drought (Tab. 3.1). Modification of root/leaf ratios have been often documented in response to abiotic stress (Landsberg and Jones, 1981), and increased root growth under severe water deficit may positively affect drought tolerance (McCully, 1999). Increased partitioning to roots in response to mild water deficit was also observed in young cherry (*Prunus avium* L.) trees (Flore and Layne, 1999). A similar tendency was not observed in CE plants under drought.

Table 3.1. Leaf area, leaf size and root fresh weight to leaf fresh weight ratio ($FW_{\text{root}}/FW_{\text{leaf}}$) in well-watered (WW) and drought-stressed (DS) ‘Nocellara del Belice’ (NB) and ‘Cerasuola’ (CE) olive genotypes. Means \pm standard errors are shown. Different letters indicate significant differences by Tukey’s multiple range test ($P \leq 0.05$).

Genotype	Irrigation treatment	Leaf area (cm ²)	Leaf size (cm ²)	$FW_{\text{root}}/FW_{\text{leaf}}$
NB	WW	1,765 \pm 198	5.55 \pm 0.13	0.81 \pm 0.06 ab
	DS	1,103 \pm 153	4.28 \pm 0.40	1.27 \pm 0.09 a
CE	WW	530 \pm 44	3.73 \pm 0.46	0.95 \pm 0.15 b
	DS	860 \pm 137	3.32 \pm 0.22	0.62 \pm 0.04 b

HYDRAULIC CONDUCTANCE

When K_s data were analysed using genotype, drought and plant sections (stem/root) as main factors, no significant differences were found between NB and CE (genotype $P = 0.20$). This means that, conduits of the two genotypes were similarly

affected by drought. However, the analysis of variance highlighted a significant interaction ($P < 0.05$) between drought and plant sections (stem/root) (Fig. 3.4), showing that drought caused a significant rise in stem K_s but did not affect root K_s . Surprisingly, there was a 100% increase of stem K_s after the severe drought period, when compared to WW plants. This might be explained by a drought-induced aquaporin regulation mediated by abscisic acid (ABA), although most studies found in literature have linked ABA to changes in root K (Parent, et al. 2009). Our results suggested a total absence of embolism or cavitation in vessels and tracheids of our drought stressed plants, as the occurrence of cavitation would have decreased K_s at high water deficit levels. This is also valid for the NB genotype, which is less tolerant to tissue dehydration and drought stress.

The average root K_s was more than 3-fold lower than stem K_s . Oppositely to what seen in stems, root K_s was not affected by drought (Fig. 3.4), suggesting that drought-induced modifications of the conducting network only happen in above-ground parts of the plant.

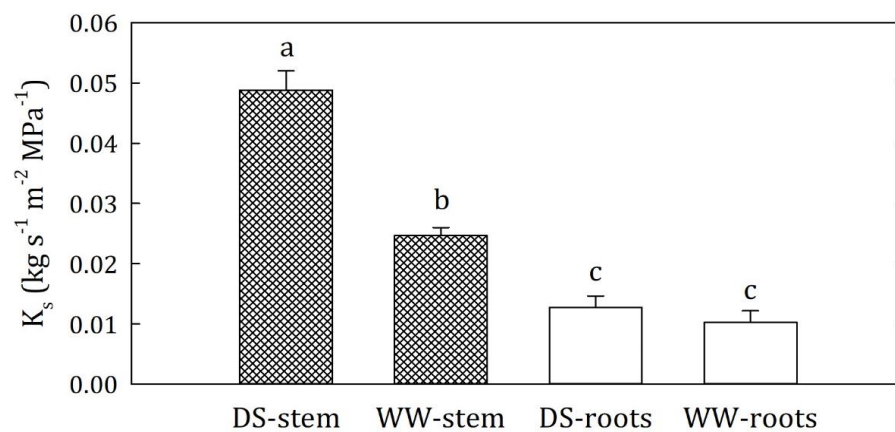


Figure 3.4. Sapwood-specific hydraulic conductance (K_s) of well-watered (WW) and drought-stressed (DS) stem (cross-patterned bars) and root sections (white bars). Bar graphs represent mean values of pooled data from ‘Nocellara del Belice’ and ‘Cerasuola’ olive genotypes. Error bars represent standard errors of the means and different letters indicate significant differences determined with Tukey’s multiple range test ($P \leq 0.05$).

CONCLUSIONS

In conclusion, CE plants appear to be more prone to tolerate quick tissue dehydration than NB, probably due to stomatal regulation and osmotic adjustment, rather than genotype-dependent modifications to xylem conductance. Therefore, the use of CE olive trees in areas where irrigation water is a limiting factor might allow growers to obtain better productive performances than NB. Water deficit caused an increase of

the root/leaf biomass ratio in NB, as reducing transpiring surface or increasing root system size might be specific strategies adopted by this genotype to cope with drought. Ultimately, the drought-induced increase of stem K_s found in both olive genotypes needs to be further investigated in future experiments, perhaps considering older plants and a higher number of genotypes.

LIST OF REFERENCES

- Afzal, Z., Howton, T.C., Sun, Y., and Mukhtar, M.S. (2016). The roles of aquaporins in plant stress responses. *J. Dev. Bio.*, 4(1), 9. <https://dx.doi.org/10.1186%2Fs40659-018-0152-0>
- Bacelar, E.A., Correia, C.M., Moutinho-Pereira, J.M., Gonçalves, B.C., Lopes, J.I., and Torres-Pereira, J.M. (2004). Sclerophylly and leaf anatomical traits of five field-grown olive cultivars growing under drought conditions. *Tree physiology*, 24(2), 233-239. <https://doi.org/10.1093/treephys/24.2.233>
- Bacelar, E.A., Moutinho-Pereira, J.M., Gonçalves, B.C., Ferreira, H.F., and Correia, C.M. (2007). Changes in growth, gas exchange, xylem hydraulic properties and water use efficiency of three olive cultivars under contrasting water availability regimes. *Environmental and Experimental Botany*, 60(2), 183-192. <https://doi.org/10.1016/j.envexpbot.2006.10.003>
- Bacelar, E.A., Moutinho-Pereira, J.M., Gonçalves, B.C., Lopes, J.I., and Correia, C.M. (2009). Physiological responses of different olive genotypes to drought conditions. *Acta Physiologiae Plantarum*, 31(3), 611-621. <https://doi.org/10.1007/s11738-009-0272-9>
- Boussadia, O., Mariem, F.B., Mechri, B., Boussetta, W., Braham, M., and El Hadj, S.B. (2008). Response to drought of two olive tree cultivars (cv Koroneki and Meski). *Sci. Hortic.*, 116(4), 388-393. <https://doi.org/10.1016/j.scienta.2008.02.016>
- Caruso, T., Marra, F.P., Costa, F., Campisi, G., Macaluso, L., and Marchese, A. (2014). Genetic diversity and clonal variation within the main Sicilian olive cultivars based on morphological traits and microsatellite markers. *Scientia Horticulturae*, 180, 130-138.
- Cochard, H., Bréda, N., and Granier, A. (1996). Whole tree hydraulic conductance and water loss regulation in *Quercus* during drought: evidence for stomatal control of embolism? *Annals of Forest Sci.* 53, 197-206. <https://doi.org/10.1051/forest:19960203>
- Delzon, S., and Cochard, H. (2014). Recent advances in tree hydraulics highlight the ecological significance of the hydraulic safety margin. *New Phytologist*, 203(2), 355-358. <https://doi.org/10.1111/nph.12798>
- Dichio, B., Xiloyannis, C., Angelopoulos, K., Nuzzo, V., Bufo, S.A., and Celano, G. (2003). Drought-induced variations of water relations parameters in *Olea europaea*. *Plant and Soil*, 257(2), 381-389. <https://doi.org/10.1023/A:1027392831483>
- Ennajeh, M., Vadel, A. M., Cochard, H., and Khemira, H. (2010). Comparative impacts of water stress on the leaf anatomy of a drought-resistant and a drought-sensitive olive cultivar. *J. Hortic. Sci. Biotech.*, 85(4), 289-294. <https://doi.org/10.1080/14620316.2010.11512670>
- Faraloni, C., Cutino, I., Petruccelli, R., Leva, A.R., Lazzeri, S., and Torzillo, G. (2011). Chlorophyll fluorescence technique as a rapid tool for in vitro screening of olive

- cultivars (*Olea europaea* L.) tolerant to drought stress. *Environmental and Experimental Botany*, 73, 49-56. <https://doi.org/10.1016/j.envexpbot.2010.10.011>
- Flore, J.A. and Layne, D.R. (1999). Photoassimilate production and distribution in cherry. *HortScience* 34, 1015-1019.
- Grisafi, F., Bonafede, E., Vecchia, F.D., and Rascio, N. (2004). Some morphological, anatomical, physiological responses of different olive cultivars to high temperatures and drought stress. *Acta botanica gallica*, 151(3), 241-253. <https://doi.org/10.1080/12538078.2004.10515427>
- La Mantia, M., Lain, T., Caruso, T., and Testolin, R. (2005). SSR-based DNA fingerprints reveal the genetic diversity of Sicilian olive (*Olea europaea* L.) germplasm. *The Journal of Horticultural Science and Biotechnology*, 80(5), 628-632. <https://doi.org/10.1080/14620316.2005.11511989>
- Landsberg, J.J. and Jones, H.G. (1981). Apple orchards. In *Water deficits and plant growth*. Vol 6, *Woody Plant Communities*. T.T. Kozlowski ed. (New York, NY, USA: Academic Press) p. 419-469.
- Lo Bianco, R., and Avellone, G. (2014). Diurnal regulation of leaf water status in high- and low-mannitol olive cultivars. *Plants* 3, 196-208. <https://doi:10.3390/plants3020196>
- Lo Bianco, R., Panno, G., and Avellone, G. (2013). Characterization of Sicilian olive genotypes by multivariate analysis of leaf and fruit chemical and morphological properties. *Journal of Agricultural Science*, 5(11), 229-245. <http://dx.doi.org/10.5539/jas.v5n11p229>
- Lo Bianco, R., and Scalisi, A. (2017). Water relations and carbohydrate partitioning of four greenhouse-grown olive genotypes under long-term drought. *Trees*, 31(2), 717-727. <https://doi.org/10.1007/s00468-016-1502-6>
- Marra, F.P., Caruso, T., Costa, F., Di Vaio, C., Mafra, R., and Marchese, A. (2013). Genetic relationships, structure and parentage simulation among the olive tree (*Olea europaea* L. subsp. *europaea*) cultivated in Southern Italy revealed by SSR markers. *Tree genetics & genomes*, 9(4), 961-973. <https://doi.org/10.1007/s11295-013-0609-9>
- McCully, M. (1999). Roots in soil: Unearthing the complexities of roots and their rhizospheres. *Annu. Rev. Plant Physiol. Plant Mol. Biol.* 50, 695-718.
- Parent, B., Hachez, C., Redondo, E., Simonneau, T., Chaumont, F., and Tardieu, F. (2009). Drought and abscisic acid effects on aquaporin content translate into changes in hydraulic conductivity and leaf growth rate: a trans-scale approach. *Plant physiology*, 149(4), 2000-2012.
- Sadras, V.O., and Milroy, S.P. (1996). Soil-water thresholds for the responses of leaf expansion and gas exchange: a review. *Field Crops Research*, 47(2-3), 253-266.
- Shipley, B., and Vu, T.T. (2002). Dry matter content as a measure of dry matter concentration in plants and their parts. *New Phytologist*, 153(2), 359-364. <https://doi.org/10.1046/j.0028-646X.2001.00320.x>
- Sinclair, T.R., and Ludlow, M.M. (1986). Influence of soil water supply on the plant water balance of four tropical grain legumes. *Functional Plant Biology*, 13(3), 329-341. <https://doi.org/10.1071/PP9860329>
- Sinclair, T.R., and Muchow, R.C. (2001). System analysis of plant traits to increase grain yield on limited water supplies. *Agronomy Journal*, 93(2), 263-270. <https://doi.org/doi:10.2134/agronj2001.932263x>
- Sinclair, T.R., Holbrook, N.M., and Zwieniecki, M.A. (2005). Daily transpiration rates of woody species on drying soil. *Tree physiology*, 25(11), 1469-1472. <https://doi.org/10.1093/treephys/25.11.1469>

- Tyree, M.T., and Dixon, M.A. (1986). Water stress induced cavitation and embolism in some woody plants. *Physiologia Plantarum*, 66(3), 397-405. <https://doi.org/10.1111/j.1399-3054.1986.tb05941.x>
- Tyree, M.T., Sinclair, B., Lu, P., and Granier, A. (1993). Whole shoot hydraulic resistance in *Quercus* species measured with a new high-pressure flowmeter. *Annals of Forest Sci.* 50, 417-423. <https://doi.org/10.1051/forest:19930501>
- Tyree, M.T., Yang, S., Cruiziat, P., and Sinclair, B. (1994). Novel methods of measuring hydraulic conductivity of tree root systems and interpretation using AMAIZED (a maize-root dynamic model for water and solute transport). *Plant Physiology*, 104(1), 189-199. <https://doi.org/10.1104/pp.104.1.189>
- Tyree, M.T., Velez, V., and Dalling, J. W. (1998). Growth dynamics of root and shoot hydraulic conductance in seedlings of five neotropical tree species: scaling to show possible adaptation to differing light regimes. *Oecologia*, 114(3), 293-298. <https://doi.org/10.1007/s004420050450>
- Tyree, M.T., Sobrado, M.A., Stratton, L.J., and Becker, P. (1999). Diversity of hydraulic conductance in leaves of temperate and tropical species: possible causes and consequences. *Journal of Tropical Forest Science*, 11(1), 47-60.
- Xiloyannis, C., Dichio, B., Nuzzo, V., and Celano, G. (1999). Defence strategies of olive against water stress. *Acta Horti*, 474, 423-426. <https://doi.org/10.17660/ActaHortic.1999.474.86>

The combined use of leaf turgor pressure probes and fruit diameter sensors as an indicator of tree water status

Based on the paper:

Scalisi A., Marra F.P., Marino G., Caruso T., Lo Bianco R. “A genotype-sensitive approach for the continuous monitoring of olive tree water status by fruit and leaf sensing”, ready for submission to Agricultural Water Management.

ABSTRACT

Today, precision irrigation is crucial to reduce water use and management costs in modern orchard systems. Plant-based sensing is an innovative approach for the continuous monitoring of plant water status. Olive (*Olea europaea* L.) genotypes can respond to drought using different mechanisms of leaf and fruit dehydration tolerance and morphological adaptations. This study aimed to identify whether olive fruit and leaf water dynamics of two different genotypes are affected by water deficit and how they respond to changes of midday stem water potential (Ψ_{stem}), the most common indicator of plant water status. Plant water status indicators such as leaf stomatal conductance (g_s) and Ψ_{stem} were measured in the olive cultivars Nocellara del Belice (NB) and Olivo di Mandanici (MN), in stage II and III of fruit development. Fruit gauges and leaf patch clamp pressure probes were mounted on trees and their raw data were converted in fruit relative growth rate (RGR) and leaf pressure change rate (RPCR), sensitive indicators of tissue water exchanges. The analysis of diel, diurnal and nocturnal fluctuations of RGR and RPCR highlighted differences, at times opposite, between the two genotypes under water deficit. A combination of statistical parameters extrapolated from RGR and RPCR diurnal and nocturnal curves were successfully used to obtain significant multiple linear models for the prediction of midday Ψ_{stem} . Fruit and leaf water exchanges suggest that olive genotypes can privilege fruit or leaf water status, with MN likely preserving leaf water status by osmotic adjustments and NB increasing fruit cell wall elasticity under severe water deficit. In conclusion, this work highlights the advantages of the integration of fruit and leaf water dynamics as predictor of plant water status and the need for genotype-specific models.

Keywords: fruit diameter, *Olea europaea* L., precision irrigation, turgor pressure, water potential.

INTRODUCTION

In recent years, precision irrigation has become a crucial aspect of orchard

management to reduce inputs in agricultural systems. Both environmentally and economically oriented reasons provide the basis for this water saving approach, which is today of fundamental importance in irrigated orchards. Automated irrigation management becomes even more important in high-density systems in which growers tend to mechanize agricultural practices. Although in the past, most of the irrigation management was based upon soil water or environmental indices, plants represent the intermediate component of the soil-plant-atmosphere continuum (SPAC) and their tissue water status is likely to provide the most precise tool to predict drought stress. This implies an advantage of plant-based over soil-based methods for precision irrigation scheduling (Fernández, 2017).

Plant water requirements differ among species and even cultivars, making irrigation scheduling and management a complex task for growers. Indeed, the physiological responses of plants to decreasing water availability are various and depend on evolutionary adaptation and acclimation to new climatic conditions. Within C3 species, two main groups (i.e. isohydric and anisohydric plants) are distinguished based on stomatal behaviour in response to drought (Stocker, 1956). Isohydric plants tend to close stomata in cases of drought to avoid dehydration and drops in leaf water potential (Ψ_{leaf}), although this behaviour has negative consequences on gas exchanges and reduces photosynthesis (Tardieu and Simonneau, 1998). On the other hand, anisohydric plants keep their leaf stomata open at decreasing soil water availability to maximize transpiration and photoassimilation, allowing a decrease in Ψ_{leaf} (Tardieu and Simonneau, 1998). In these plants, other mechanisms such as osmotic adjustments and reduced cell-wall elasticity can avoid cavitation or tissue desiccation. Sade et al. (2012) suggested that isohydric plants close stomata to maintain leaf relative water content (RWC) constant rather than Ψ_{leaf} . Isohydric plants are generally classified as drought avoidant, and anisohydric plants as drought tolerant (Skelton et al., 2015). However, there is not a distinct separation between these two categories (Klein, 2014; Sade and Moshelion, 2014) and even genotypes within the same group can have very different levels of stomatal regulation, as found in grapevine by Schultz (2003).

The most widely adopted indicator for irrigation scheduling in anisohydric plants is midday stem water potential (Ψ_{stem}) (McCutchan and Shackel, 1992; Shackel et al., 1997; Naor, 1999). However, the same parameter is not a precise indicator of water deficit in isohydric plants, as when stomata close, midday Ψ_{stem} mostly respond to soil water potential fluctuations. In case of isohydry, leaf stomatal conductance (g_s) (Jones,

2007) and pre-dawn Ψ_{leaf} (Blanco-Cipollone et al., 2017) were found to provide more sensitive information for irrigation scheduling.

Olive (*Olea europaea* L.) is considered an anisohydric species (Naor et al., 2013) with a very wide genetic pool where genotypes can respond to drought using different mechanisms of leaf dehydration tolerance and leaf morphological and structural adaptations (Bacelar et al., 2004; Bacelar et al., 2006; Ennajeh et al., 2010; Lo Bianco and Scalisi, 2017). Gucci et al. (2000) and Lo Bianco and Scalisi (2017) found different leaf stomatal regulation in different cultivars. Hence, olive genotypes are likely to work along a gradient from highest to lowest anisohydry. In olive, midday Ψ_{stem} is considered a very sensitive parameter of plant water status (PWS) for irrigation management (Moriana and Fereres, 2002; Fernández, et al., 2006; Moriana et al., 2012; Marino et al., 2018). However, Ψ_{stem} is mostly measured by the Scholander pressure chamber, which does not allow for continuous monitoring and precision automated irrigation.

Recently, plant-based sensing technologies are taking hold for the continuous PWS monitoring in fruit trees. In most of cases, sensors are mounted on aboveground organs such as stem, fruit and leaves (Fernández, 2014; Fernández, 2017; Scalisi et al., 2017). In olive, trunk dendrometers have been associated with correct determination of tree water status and irrigation thresholds due to their relatively easy installation and stability across the season (Moreno et al., 2006; Cuevas et al., 2010; Fernández et al., 2011a).

In the last few years, particular emphasis has been given to leaf patch clamp pressure (LPCP) probes for the continuous assessment of olive leaf turgor pressure (Fernández et al., 2011b; Ehrenberger et al., 2012; Rodriguez-Dominguez et al., 2012; Padilla-Díaz et al., 2016; Marino et al., 2016; Fernandes et al., 2017). The output of LPCP probes is expressed in attenuated pressure of leaf patches (p_p), which is inversely related to cell turgor pressure (p_c) (Zimmermann et al., 2008). Therefore, the highest values of p_p occur around solar noon, as that is the moment in which leaf cell turgor is the lowest. Ben-Gal et al. (2010) first found an inversion of the p_p curve in olive subjected to deficit irrigation, and water deficit states were then classified by Fernández et al. (2011) based on the degree of inversion. State I represented no drought stress and leaves with a non-inverted curve, state II grouped leaves experiencing partial inversion of the curve and mild water deficit, and state III enclosed all leaves experiencing severe water deficit and full inversion of the curve.

Fruit-based probes based on linear variable displacement transducers (LVDTs) can

provide good information on fruit growth, which on a diel scale is mostly dominated by water in- and out-flows, rather than carbon gain; thus, fruit diameter (FD) variations respond to water deficit (Scalisi et al., 2017). Fernandes et al. (2018) studied olive FD dynamics in response to water deficit, suggesting the appropriateness of fruit gauges for continuous PWS monitoring. Although p_p and FD are strictly related to soil water availability and PWS, they are also influenced by environmental variables and phenology. The derived values of p_p and FD (namely leaf relative pressure change rate, RPCR, and fruit relative growth rate, RGR) can represent very good indicators of the rate at which water enters and exits leaf or fruit, respectively. Plants are likely to modulate water movements to and from the two main transpiring organs (i.e. leaf and fruit) using several strategies such as osmotic adjustments, stomatal closure or cell-wall elasticity regulation. As a result, we hypothesised that the water status of leaf or fruit might be privileged in case of severe water deficit and water exchanges can be affected, with different evidences among olive genotypes.

This work aimed to identify whether olive fruit and leaf water dynamics are strictly related to tree water status and water deficit levels and if the combined monitoring of RGR and RPCR can provide an even more accurate identification of PWS, rather than considering them independently. In addition, this study tried to identify genotype-specific RGR-to-RPCR ratios to better understand differences in physiological mechanisms and fruit/leaf water prioritisation at increasing water deficit.

MATERIALS AND METHODS

EXPERIMENTAL DESIGN

The experiment was carried out in summer 2016 in a high-density (6×3 spacing, ≈ 555 trees/ha) olive orchard located near Sciacca, in South-western Sicily ($37^{\circ}29'56.8''$ N $13^{\circ}12'13.4''$ E, 138 m a.s.l.). Three-year-old self-rooted trees from different Sicilian cultivars were trained to free palmette for the formation of a hedgerow along North-to-South rows. In this trial, two cultivars, Nocellara del Belice (NB) and Olivo di Mandanici (MN), were selected for their different vigour and fruit characteristics (Marino et al., 2016). Trees belonging to NB have a weeping habit and yield large fruit, whereas MN trees show a more vigorous habit and yield smaller fruit. The soil was a sandy clay loam (60% sand, 18% silt, and 22% clay) with pH of 7.7 and < 5 % of active carbonates. Trees were regularly fertilised in accordance with conventional practices and regularly pruned in winter.

Meteorological data were retrieved from the meteorological station of Sciacca (Servizio Informativo Agrometeorologico Siciliano). Reference evapotranspiration (ET_0) and vapour pressure deficit (VPD) were calculated using the methods described by Allen et al. (1998). Crop evapotranspiration (ET_c) was estimated by weighing ET_0 with an average K_c of 0.50 ± 0.05 (Allen et al., 1998).

Four irrigation treatments were imposed to the trees based on ET_c fractions: full irrigation (FI, 100 % of ET_c), two thirds of FI (TTI), one third of FI (OTI) and rainfed (RF). Trees were irrigated at weekly intervals using self-compensating in-line drippers delivering 16 L/h. Six, four, two and no drippers per plant were used for FI, TTI, OTI and RF treatments, respectively. Trees were arranged according to a completely randomised experimental design, with twelve replications for cultivar, and three for each irrigation level. Measurements were carried out at stages II and III of fruit development, as some of the measurement equipment was unavailable during stage I.

FRUIT CHARACTERISTICS

Fruit diameter was measured in FI trees at weekly intervals, from the pit hardening (stage II) to the cell expansion (stage III) phases of fruit development. The date of beginning of stage III was estimated based on fruit rapid growth after the period of steady size, typical of stage II. From the beginning of stage II to harvest, sixty fruits from twelve trees were sampled and collected at weekly intervals, brought to the laboratory and their diameter and weight were measured to characterise differences between the two genotypes under study.

PLANT WATER STATUS

Leaf stomatal conductance (g_s) was measured using a Delta-T AP4 dynamic porometer (Delta-T Devices LTD, Cambridge, UK) on three sun-exposed leaves in one tree per irrigation treatment. Daily measurements of g_s were undertaken at two-hour intervals (from 8.00 to 20.00 h) in a day at stage II (day of the year, DOY = 209) and a day at stage III (DOY = 287).

A pressure chamber (PMS Instrument Co., Corvallis – Oregon) was used for the determination of Ψ_{stem} , on twigs covered by plastic and aluminium foil one hour before measurement, as described by Turner (1988). Daily measurements of Ψ_{stem} were carried out on three twigs per tree, on the same trees and DOY of g_s measurements, at two-hour intervals and from pre-dawn (4.30 h) to 20.00 h at DOY 209, and to 18.00 h at DOY 287. Midday Ψ_{stem} was measured at around 14.00 h, at weekly intervals from 196 to 287

DOY, and using three twigs per tree.

FRUIT- AND LEAF-BASED SENSING

The fruit gauges based on LVDT sensors described by Morandi et al. (2007) were installed on olive drupes to determine FD continuously. Gauges were wired to four CR-1000 data loggers (Campbell scientific, Inc., Logan, US) and data were downloaded manually. A total of 16 gauges (eight on each genotype, two on a tree per irrigation treatment) were mounted on sun exposed fruit at medium canopy height. In addition, early in the morning, LPCP probes (Yara International, Oslo, NO) were clamped on sun exposed, mature leaves for continuous measurement of p_p . LPCP clamping was done a day after irrigation to ensure optimal leaf turgescence, carefully avoiding central leaf nerves and placing the piezoresistive sensor on the abaxial side of leaves. The initial LPCP clamping pressure ranged from 15 to 25 kPa. Data of p_p were recorded continuously and sent to a server online through a system equipped with radio transmitters and a main GPRS/radio controller. LPCP probes were mounted on leaves nearby the fruit monitored with fruit gauges, using the same number of sensors (i.e. 16). Both fruit gauges and LPCP probes were mounted on the same trees used for g_s and Ψ_{stem} measurements

Fruit gauges and LPCP probes were set to record FD and p_p at 15-min intervals for 8 days at fruit growth stages II and III. A buffer period corresponding to the first three days after sensor mounting was discarded, to allow adjustments and/or re-clamping in fruit and leaves. Raw FD and p_p data were processed using a 15-point convoluted spline function (Savitzky and Golay, 1964) to smooth sensors' signal and erase noise. Following data filtering, FD and p_p values were standardized by using z-scores (i.e. $z = (x - \text{mean}) / \text{standard deviation}$) to allow comparison among fruits or leaves with initial fruit diameter or leaf turgor pressure when sensors were mounted, respectively. The use of z-scores allowed to average FD and p_p obtained from different sensors on the same tree and to compare trees under different irrigation regimes. Second derivatives of FD and p_p were calculated to determine RGR and RPCR as shown in Eqs. 3.1 and 3.2, respectively. A standardisation of RGR and RPCR was not carried out as they are based on standardised FD and p_p , allowing possible comparisons among outputs from different sensors.

$$\text{RGR} = (\ln \text{FD}_2 - \ln \text{FD}_1) / t_2 - t_1 \quad (\text{Eq. 3.1}),$$

$$\text{RPCR} = (\ln p_{p2} - \ln p_{p1}) / t_2 - t_1 \quad (\text{Eq. 3.2}),$$

where, FD_2 and FD_1 are FD at time 2 (t_2) and 1 (t_1), and p_{p2} and p_{p1} are p_p at time 2 (t_2) and 1 (t_1), respectively.

Diel data were subdivided in diurnal (6.00 to 20.00 h) and nocturnal (20.15 to 5.45 h) intervals. Subsequently, diel, diurnal and nocturnal statistical parameters were calculated from data series for RGR and RPCR in order to find the best predictor of midday Ψ_{stem} . The parameters considered for each (i.e. 24h, night or day) were: a) the minimum value (MIN), b) the maximum value (MAX), c) the summation of values at 15-min intervals (SUM), and d) the difference between MAX and MIN (RANGE). An additional parameter was used to express the variance of diel, diurnal and nocturnal RGR and RPCR in terms of relative standard deviation (standard deviation divided by the mean, RSD) to allow comparison among variances expressed in different units. An example of all RGR statistical parameters calculated on diel basis is shown in Figure 3.5. Similarly, all parameters were calculated on diurnal and nocturnal timeframes. Raw data obtained from sensors that either caused damage to the organs or that were displaced by strong wind were discarded.

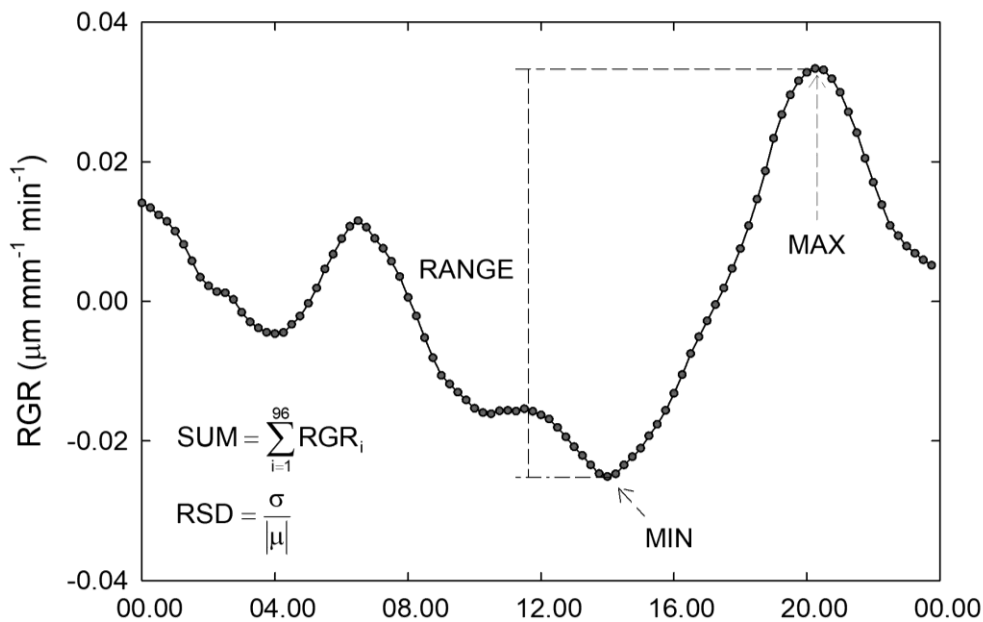


Figure 3.5. Schematisation of statistical parameters calculated on diel basis on a fruit relative growth rate (RGR) curve. MIN = minimum value of RGR, MAX = maximum value of RGR, RANGE = MAX-MIN, SUM = summation of RGR values taken at 15-min intervals from 1 (00.00 h) to 96 (23.45 h), RSD = relative standard deviation, where σ is the standard deviation and $|\mu|$ is the absolute value of the mean.

STATISTICAL ANALYSIS

Statistical data analysis was carried out using SPSS Statistics (IBM Corp. v 21.0., Armonk, NY, US). Analysis of variance (ANOVA) or t-tests was performed to test the effects of irrigation, genotype time and their interactions, and, when appropriate, means were compared by Tukey's multiple range test or Tukey's honestly significant difference (HSD). Multivariate analysis of variance (MANOVA) was used to determine the effect of irrigation, genotype and irrigation \times genotype on RGR, RPCR and RGR/RPCR statistical parameters. Sigmaplot procedures (Systat software Inc., Chicago, US) were used for linear and multiple linear regression analyses to test association of RGR and RPCR statistical parameters with Ψ_{stem} .

RESULTS AND DISCUSSION

WEATHER CONDITIONS AND IRRIGATION

Temperature (T) and vapour pressure deficit (VPD) were expectedly higher from 190 to 252 DOY (fruit development stage II), as the measured fraction of stage II occurred in full summer (Jul 8 to Sep 8) (Fig. 3.6A). Relatively low T and VPD were recorded in stage III from 280 to 290 DOY (Fig. 3.6A), due to high precipitations. In stage II, only limited rainfall occurred and irrigation was approximately constant, ranging from a weekly irrigation water supply of 19 to 26 mm to FI trees. Lower weekly volumes of water were supplied in stage III, as concomitant precipitations occurred from 252 to 289 DOY (Fig. 3.6B). The precipitation in the last 10 days of the measured timeframe corresponded to the general lowering of T and VPD observed in the same period (Fig. 3.6A). An overall higher average weekly crop water supply (CWS, irrigation + rainfall) was found to be higher in stage III than stage II (Fig. 3.6B), suggesting a low likelihood of tree water deficit in the latter. In stage II, the total CWS was mainly made up of irrigation water (Tab. 3.2). By contrast, precipitations at stage III were abundant and contributed to the 63, 72, 83 and 100 % of the CWS in FI, TTI, OTI and RF trees, respectively.

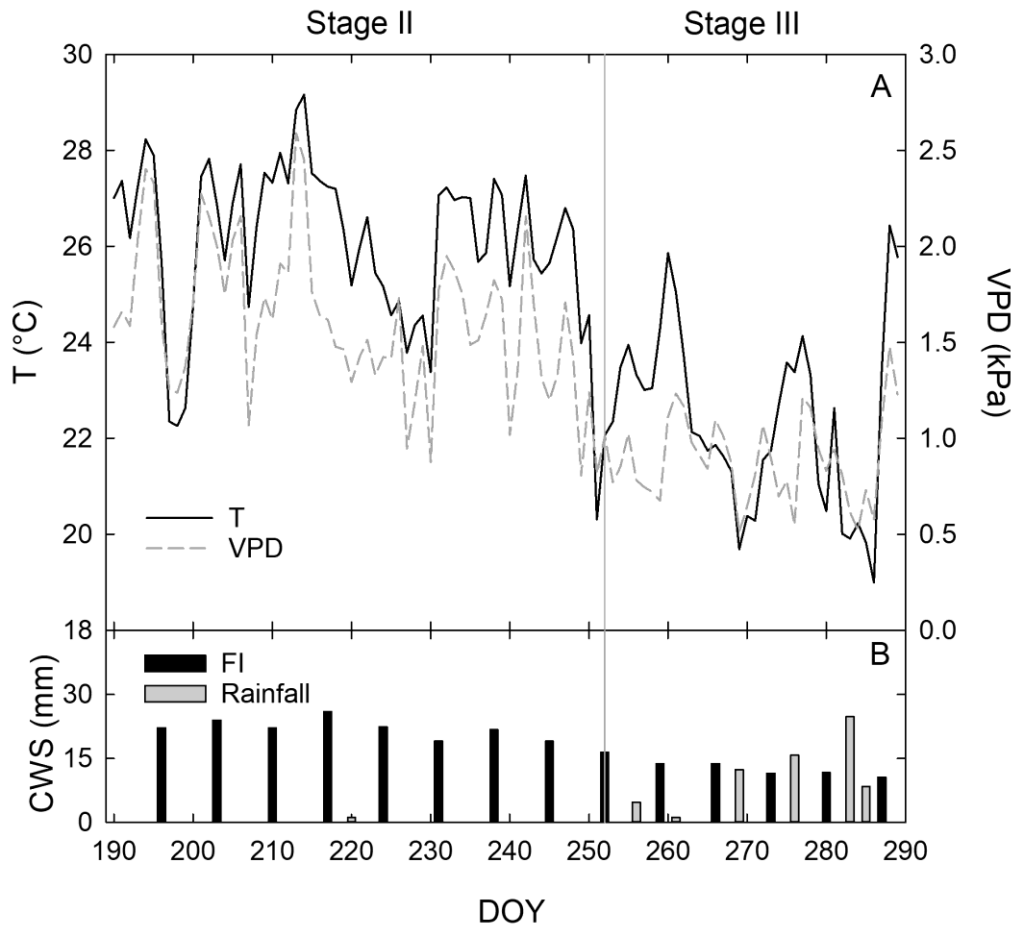


Figure 3.6. Daily mean temperature (T) and vapour pressure deficit (VPD) (A), and daily crop water supply (CWS = full irrigation (FI) + rainfall) (B) at fruit growth stages II and III.

Table 3.2. Crop water supply (CWS) in FI (full irrigated, 100 % of crop evapotranspiration), TTI (2/3 of FI), OTI (1/3 of FI) and RF (rainfed) trees at fruit growth stage II and III. Data represent means between 'Nocellara del Belice' and 'Cerasuola'.

Fruit growth stage	CWS	Volume of water (mm)			
		FI	TTI	OTI	RF
II	Irrigation	197	130	64	0
	Rainfall	1	1	1	1
	Sub-Total	198	131	65	1
III	Irrigation	112	74	38	0
	Rainfall	188	188	188	188
	Sub-Total	300	262	226	188
Total		438	393	291	189

FRUIT CHARACTERISTICS

The two genotypes showed different fruit morphological characteristics, (i.e. NB fruit were almost spherical whereas MN fruit were oblong in shape) from the beginning of fruit diameter measurements at stage II until harvest. Fruit size was also consistently greater in NB than in MN (Fig. 3.7), with nearly no fruit growth during stage II. Stage III was characterised by a steeper fruit diameter increment in MN compared to NB.

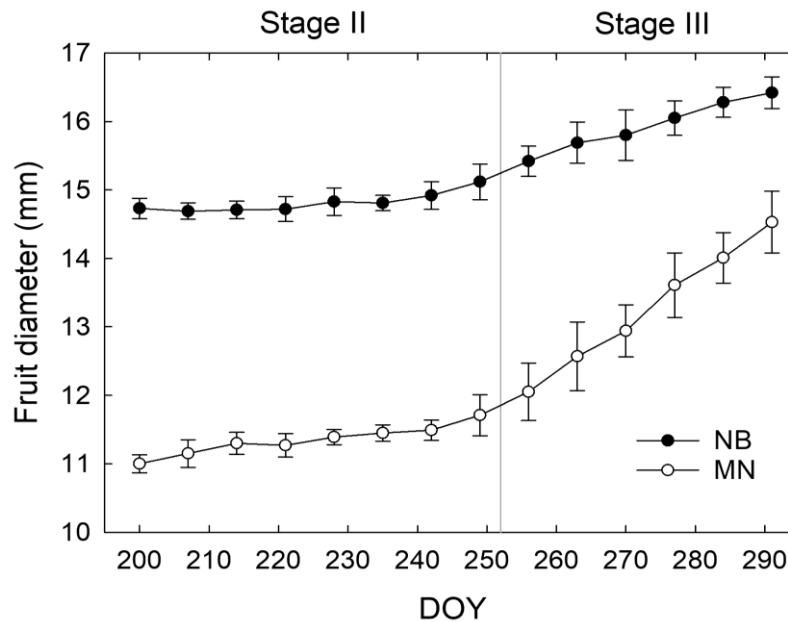


Figure 3.7. Weekly fruit diameter variations in 'Nocellara del Belice' (NB) and 'Olivo di Mandanici' (MN) olive genotypes from 200 to 291 days of the year (DOY). Error bars represent standard deviations of means ($n = 60$).

The steeper increase of fruit diameter in MN observed in Figure 3.7 is related to the first part of stage III (i.e. the part shown in Fig. 3.7), as when fruit were sampled until harvest average fruit size in MN reached a maximum of ≈ 16 mm. On the other hand, NB fruit diameter increased up to a maximum size of ≈ 23 mm at harvest, suggesting that they had a steeper growth after the end of the period considered in this study (i.e. after 290 DOY).

When a linear regression analysis between fruit diameter and weight was performed, also slopes from the linear associations were significantly different in NB and MN ($NB = 0.66 \pm 0.02$, $MN = 0.28 \pm 0.01$, $P < 0.001$ from t-test) (Fig. 3.8). These findings confirm once again the different fruit morphological characteristics of the two genotypes under study.

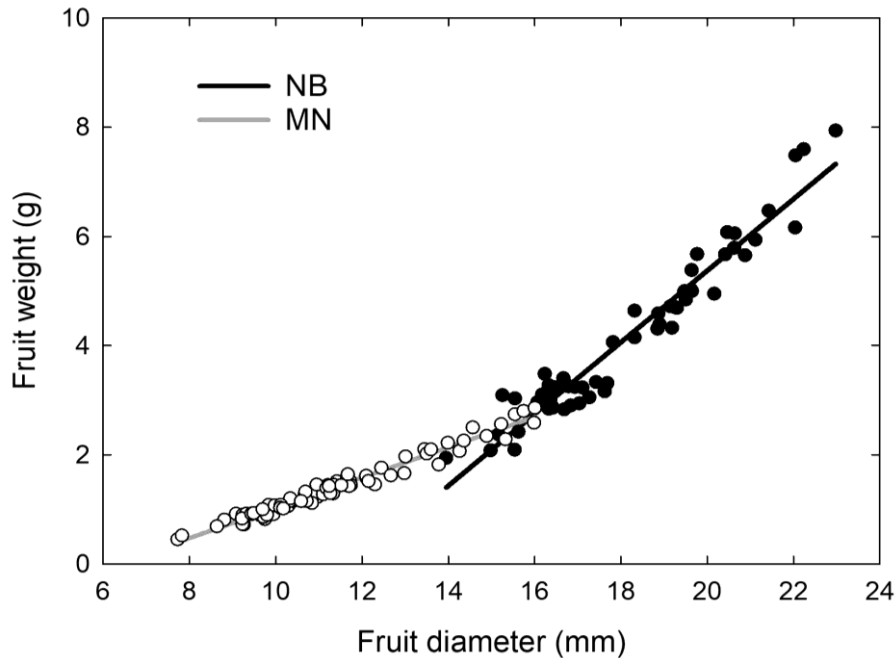


Figure 3.8. Association between weight and diameter in 'Nocellara del Belice' (NB) and 'Olivo di Mandanici' (MN) fruit sampled from the beginning of stage II to harvest. In NB, $FW = -7.75 + 0.66 \times FD$ ($P < 0.001$, $R^2 = 0.938$). In MN, $FW = -1.74 + 0.28 \times FD$ ($P < 0.001$, $R^2 = 0.968$).

PLANT WATER STATUS

Results from daily g_s measurements carried out at 209 and 287 DOY did not show significantly different patterns between the two days of measurements and among irrigation treatments. The daily curve at 209 DOY was plotted to represent the different g_s trends between NB and MN (Fig. 3.9). In MN, an overall peak of stomatal aperture occurred at mid-morning (10.00 h) with a subsequent sudden decrease at 12.00 h in response to increasing noon T and VPD. On the other hand, NB leaves did not show a peak in g_s in the morning and kept stomatal aperture stable from 8.00 h to 18.00 h, with a sudden drop at 20.00 h. MN leaves showed significantly higher g_s than NB at 10.00 h, implying a likely higher tree water consumption. This hypothesis is supported by dynamics of sup flux density measured with thermal dissipation probes in the previous year (unpublished data), where MN trees showed higher daily water consumption, especially because of greater flows in the first part of the morning. In the afternoon, NB leaves showed higher g_s than MN, with significant differences occurring at 18.00 h, suggesting a tendency to maintain higher photosynthetic activity late in the day, when T and VPD are lower, and a possible heat avoidance mechanism in NB that was not observed in MN (Fig. 3.9).

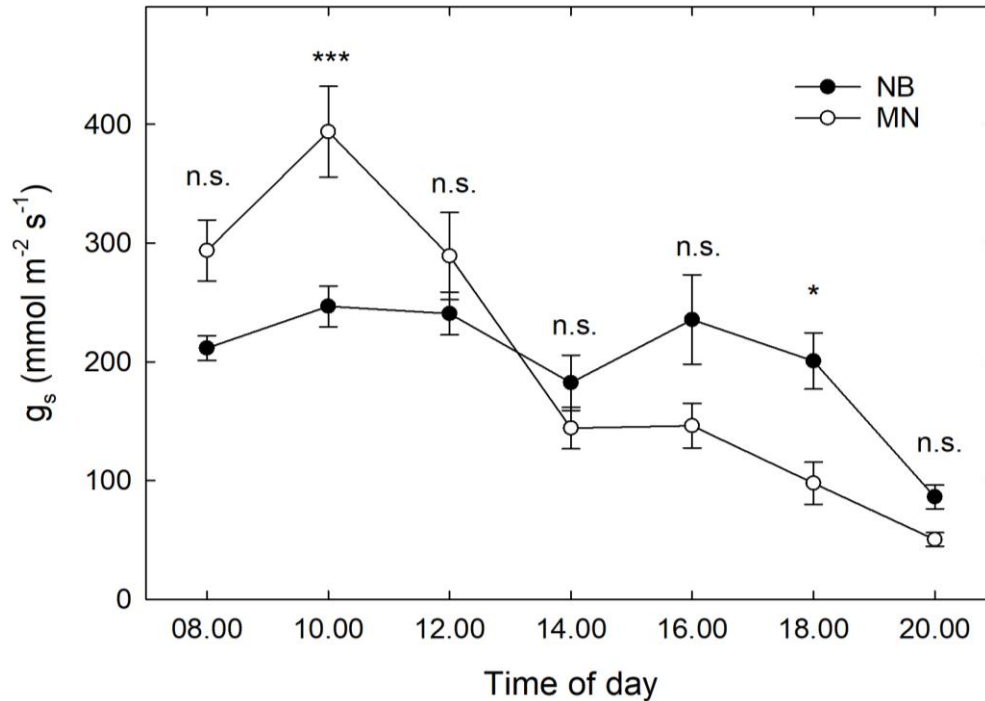


Figure 3.9. Daily curve of stomatal conductance (g_s) in 'Nocellara del Belice' (NB) and 'Olivo di Mandanici' (MN) leaves. Data averaged across different irrigation treatments at 209 days of the year. Error bars indicate standard errors of means. *, significantly different for $P < 0.05$; ***, significantly different for $P < 0.001$ by Tukey's test.

Daily curves of Ψ_{stem} at stage II (209 DOY) and III (287 DOY) showed the typical overall decreasing potential at solar noon in both genotypes, with a subsequent increase late in the afternoon (Fig. 3.10). When tested with ANOVA, only measurements in stage III showed significant differences among irrigation treatments with an interaction with time (i.e. HSD bars in Fig. 3.10B and D), with the lowest daily Ψ_{stem} always occurring between 14.00 and 16.00 h (Fig. 3.10B and D). The lowest Ψ_{stem} occurred in RF trees for both genotypes with significant differences when the two lowest Ψ_{stem} in NB and MN were compared (NB = $-2.53 \text{ MPa} \pm 0.03$, MN = $-2.33 \text{ MPa} \pm 0.03$, $P < 0.001$). Pre-dawn observations at stage III suggest a different behaviour in the two genotypes (Fig. 3.10B and D), with MN trees fully recovering to FI levels during the night in RF and OTI treatments. A rise of Ψ_{stem} was observed in NB and MN trees at 18.00 h, with non-irrigated MN trees recovering completely to FI levels (Fig. 3.10D).

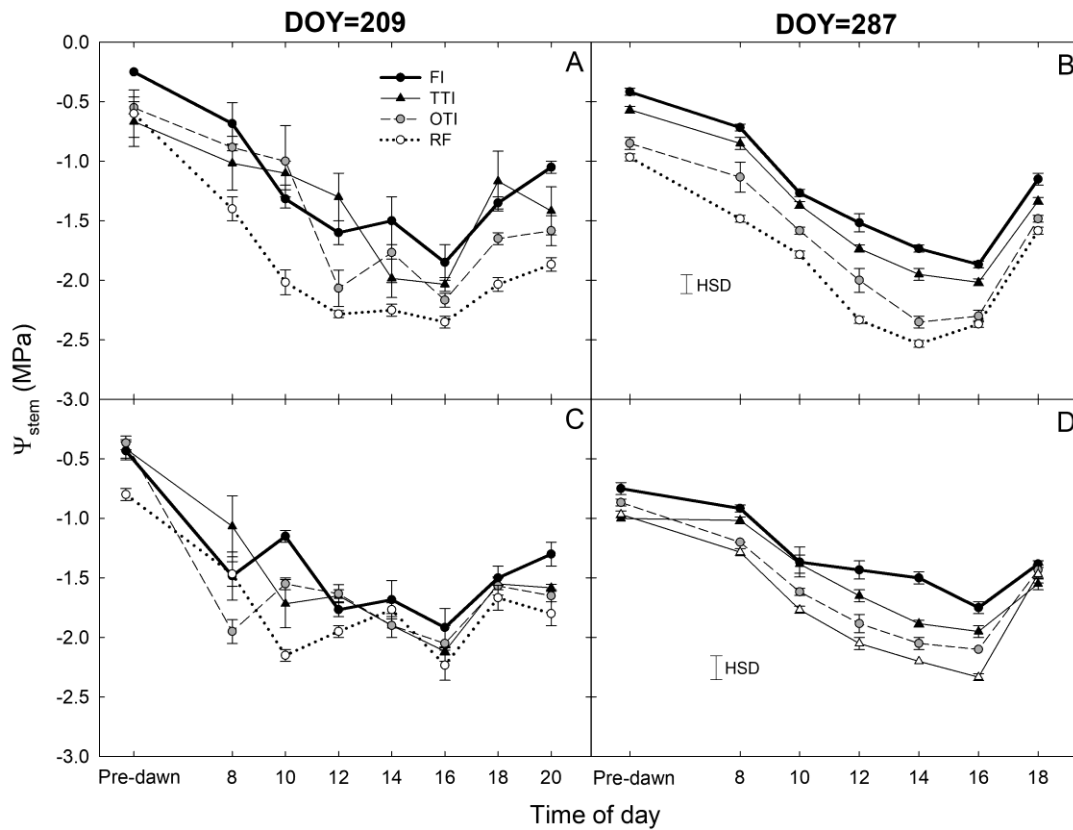


Figure 3.10. Daily curve of stem water potential (Ψ_{stem}) in 'Nocellara del Belice' (NB) (A and B) and 'Olivo di Mandanici' (MN) (C and D) at 209 and 287 days of the year (DOY). Trees subjected to full irrigation (FI), 2/3 of FI (TTI), 1/3 of FI (OTI) and no irrigation (RF). Error bars represent standard deviations of means ($n = 3$). Significant differences determined with analysis of variance and Tukey's Honest Significant Difference (HSD, $P < 0.05$).

Midday Ψ_{stem} measured weekly from 196 to 287 DOY exhibited different values according to the irrigation gradient (Fig. 3.11). Indeed, RF trees experienced the lowest midday Ψ_{stem} both in stages II and III. As expected, midday Ψ_{stem} was higher at stage II than at stage III, although T and VPD were generally higher in the former (Fig. 3.6). In this phenological phase, water deficit slows down the overall plant activity, inducing a reduction of vegetative growth and photosynthesis, which in turn might limit transpiration (Parent et al., 2000) and results in no fruit size changes. Consequently, as water loss by transpiration is likely to be reduced, plants under deficit irrigation at stage II do not reach as low Ψ_{stem} as when the same treatments are applied in stages I and III. The only exception occurred at 244 DOY, where RF trees experienced a very low Ψ_{stem} in both the genotypes, due to both particularly high T and VPD (Fig. 3.6A) and to the transition towards the beginning of stage III which was completed the following week. In stage III, the sudden steep increases of Ψ_{stem} at 287 DOY was determined by high precipitations (Fig. 3.6). Overall, genotypes showed a significantly different drop of

midday Ψ_{stem} in response to no-irrigation (t-test $P < 0.05$). Indeed, across the monitoring period, rainfed NB trees showed a lower average midday Ψ_{stem} (-2.75 ± 0.07 Mpa) than MN trees (-2.54 ± 0.08 MPa). These findings suggest that MN avoids excessive Ψ_{stem} lowering, not by stomatal control, as g_s is much higher in MN than in NB in the morning (Fig. 3.9), but by other mechanisms. Marino et al. (2016) suggested that osmotic adjustments might be responsible of a higher Ψ_{stem} in a clone of MN. Furthermore, changes in the leaf cell elastic modulus occur in other olive genotypes under drought (Karamanos, 1984; Dichio et al., 2003; Bacelar et al., 2006). Both osmotic adjustments and reduced cell wall elasticity contribute to turgor preservation (Patakas and Noitsakis, 1997) and might have led to the high Ψ_{stem} found in MN.

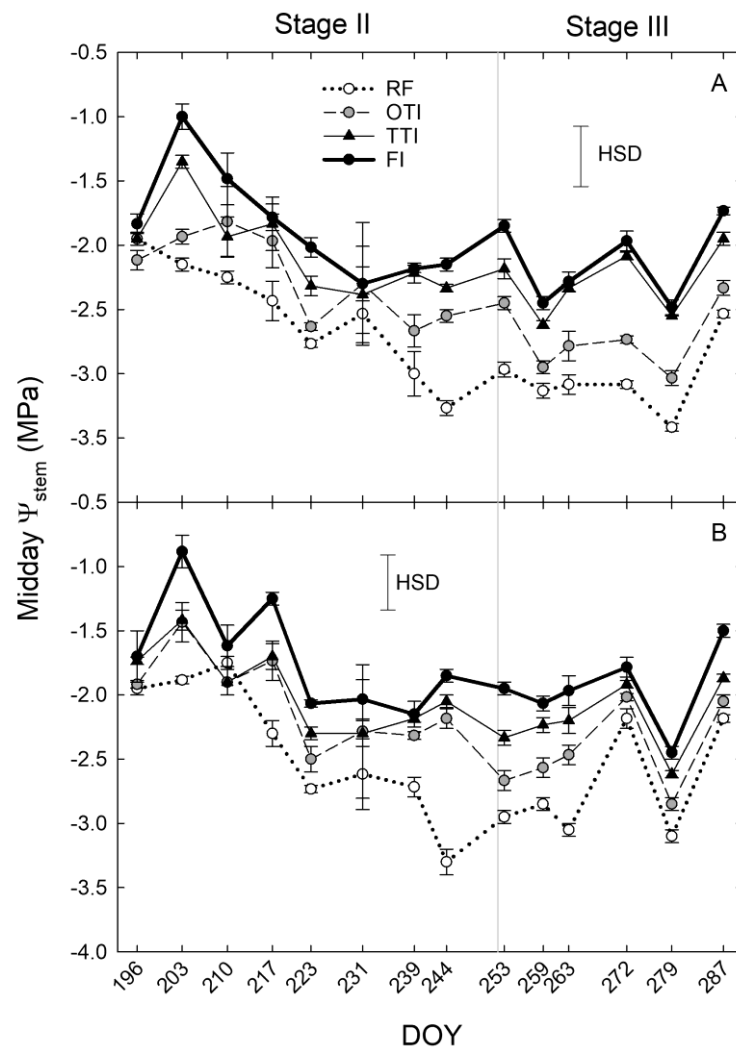


Figure 3.11. Midday stem water potential (Ψ_{stem}) in 'Nocellara del Belice' (NB) (A) and 'Olivo di Mandanici' (MN) trees (B) under full irrigation (FI), 2/3 of FI (TTI), 1/3 of FI (OTI) and no irrigation (RF) during stage II (from 196 to 252 DOY) and stage III (from 253 to 287 DOY) of fruit growth. Error bars represent standard deviations of means ($n = 3$). Significant differences determined with analysis of variance and Tukey's Honest Significant Difference (HSD, $P < 0.05$).

FRUIT- AND LEAF-BASED SENSING

After the buffer period of three days was removed from data of FD, p_p , RGR and RPCR, a five-day interval in stage II was obtained (Fig. 3.12). Dynamics of FD (Fig. 3.12A and E) did not highlight different fruit growth dynamics among irrigation treatments in stage II, for both NB and MN. Irrigation in FI trees only in some days induced a deeper shrinkage of fruit, especially at 222 and 223 DOY, as fruit transpiration in well-watered trees is higher, and fruit from these trees are likely to lose more water in the warmest hours of the day.

Dynamics of p_p highlighted the typical inversion phenomenon of the diel curve in olive leaves from trees under deficit irrigation (Fernández et al., 2011). In NB, TTI and OTI trees entered the half-inverted state (state II), whereas leaves from RF trees showed a total inversion of the curve (state III) (Fig. 3.12B). On the contrary, in MN trees, a tendency to enter state II was observed only at 219 DOY, with no apparent differences among irrigation treatments (Fig. 3.12F). This suggests that MN leaves are able to maintain high cell turgor, probably by reduced cell wall elasticity or osmotic adjustments, as found in drought-tolerant genotypes (Bacelar et al., 2009; Dichio et al., 2009; Lo Bianco and Scalisi, 2017).

The highest RGR always occurred early in the night as fruit quickly rehydrated their tissues (Fig. 3.12C and G). As expected, the most negative RGR rate (i.e. the highest fruit shrinkage rate) always occurred in the warmest hours of the day. RGR dynamics were also affected by deficit irrigation in NB, as the diel RANGE was higher in RF and OTI trees than in TTI and FI trees (Fig. 3.12C). A completely different behaviour was observed in MN fruit, which instead had the largest diel RANGE in FI treatments. In addition, the overall diel RANGE of fruit RGR in MN was almost double than in NB, implying larger water in- and out-flows per unit of fruit volume in the former, determined by high fruit sink power for water.

A general positive peak of RPCR was exhibited early in the morning (Fig. 3.12D and F), representing a quick leaf turgor loss (i.e. p_p is the inverse of p_c) after pre-dawn highest turgor in the 24-h timeframe. Even in this case, the two genotypes responded differently to water deficit, with NB RF trees exhibiting minimal diel fluctuations (i.e. RANGE) while MN RF trees showing the largest RANGE.

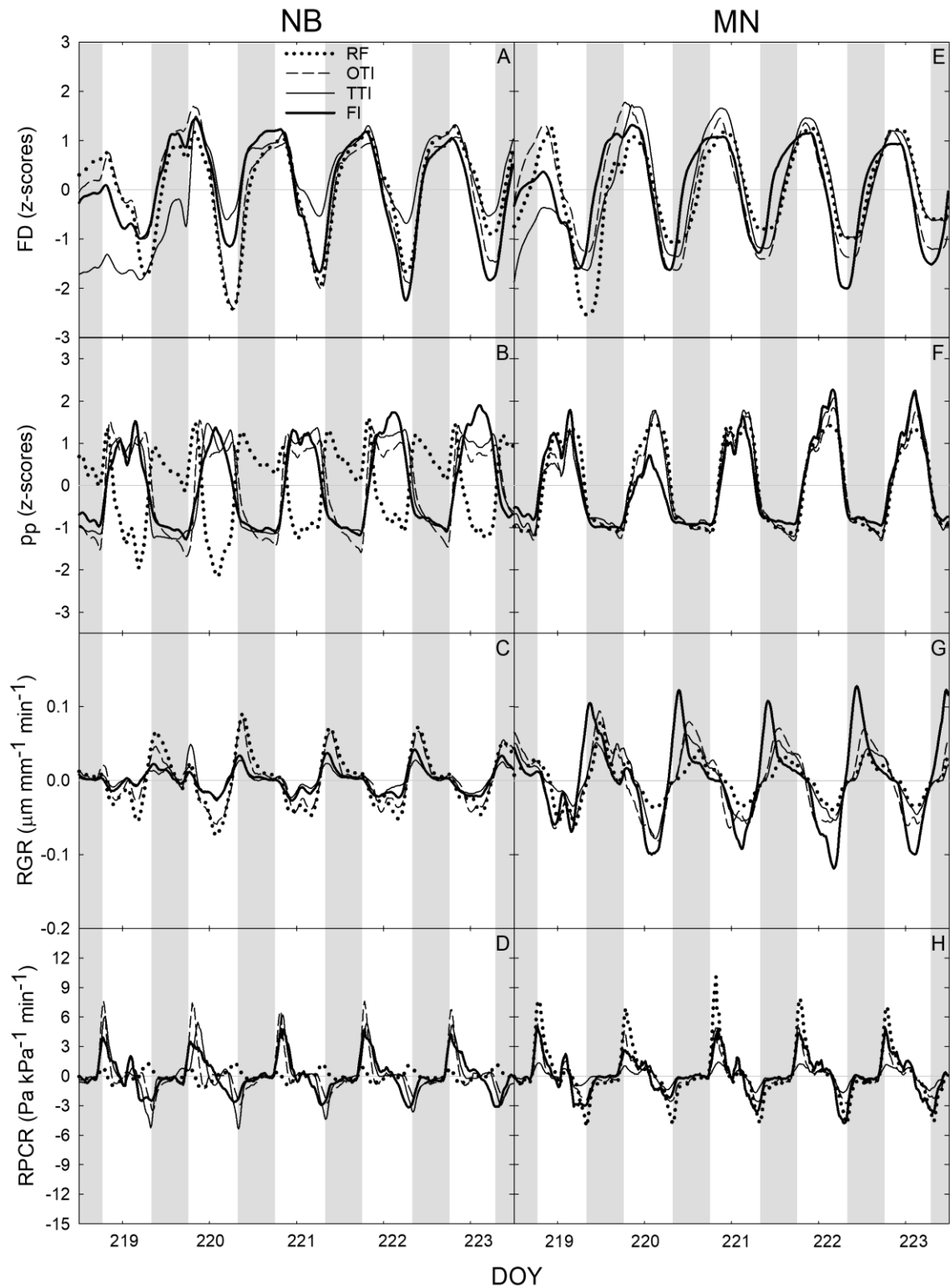


Figure 3.12. Fruit diameter (FD), leaf patch clamp pressure (p_p), fruit relative growth rate (RGR) and leaf relative pressure change rate (RPCR) recorded at 15-min intervals for five days during stage II of fruit growth in 'Nocellara del Belice' (NB) (A, B, C, D, respectively) and 'Olivo di Mandanici' (MN) trees (E, F, G, H) under full irrigation (FI), 2/3 of FI (TTI), 1/3 of FI (OTI) and no irrigation (RF). Grey and white areas show night and day time, respectively.

Another 5-day interval was considered at stage III of fruit development (Fig. 3.13). Differently from stage II (Fig. 3.12 A and E), FD responses were characterised by an evident diel diameter increase in both genotypes, as in stage III fruit are in full cell enlargement phase (Fig. 3.13A and E). Daily curves of p_p (Fig. 3.13B and F) did not show pronounced inversion phenomena, as this week was characterised by high rainfall (Fig. 3.6B) and general higher midday Ψ_{stem} (Fig. 3.11). Only RF NB trees showed a partially inverted p_p curve. Diel RANGE of RGR was found to be highly reduced at stage III (Fig. 3.13C and G) compared to stage II (Fig. 3.12C and G). In the former low VPD (Fig. 3.6A) and good soil water availability determined by abundant precipitations (Fig. 3.6B) led to an increase of water content in fruit and a consequent lower degree of fruit water exchanges. For similar reasons, the diel RANGE of RPCR was reduced in stage III (Fig. 3.13D and H), although NB and MN showed different trends in response to deficit irrigation gradients in agreement with results from stage II (Fig. 3.12D and H).

Considering the interesting findings from RGR and RPCR dynamics, these two indices were further related to each other regressing their diel data at 15-min intervals in a clear sky day at stage II (DOY = 223) and stage III (DOY = 287). Scatter plots in Figure 3.14 show anti-clockwise hysteretic relationships between RGR and RPCR, both for NB (Fig. 3.14A and B) and MN (Fig. 3.14C and D). Hystereses are common when relating outputs from different sensors of plant water status mounted on different organs (Tognetti et al., 1996; Fernández, 2017), as there is generally a lag in tissue water de- and re-hydration, and in our case, also a likely different pattern of the RPCR to RGR relationship between day and night. An overall decrease of the hysteretic loop area occurred from DOY 223 to 287 in both genotypes (i.e. for NB Fig. 3.14A and B, and for MN Fig. 3.14C and D), probably driven by the different fruit growth pattern at stages II and III which induced a reduction of the RGR diel range (Fig. 3.13C and G). In both DOY 223 and 287, the hysteretic loops in NB progressively flattened along the RGR axis with increasing water deficit (Fig. 3.14A and B), as a consequence of the change in the ratio between RGR and RPCR range. Oppositely, MN loops tended to flatten along the RPCR axis with increasing water deficit (Fig. 3.14C and D). This opposite trend suggests a completely different mechanism of leaf and fruit water exchanges along increasing water deficit in the two genotypes, which might be driven by different osmotic adjustments and cell-wall elasticity.

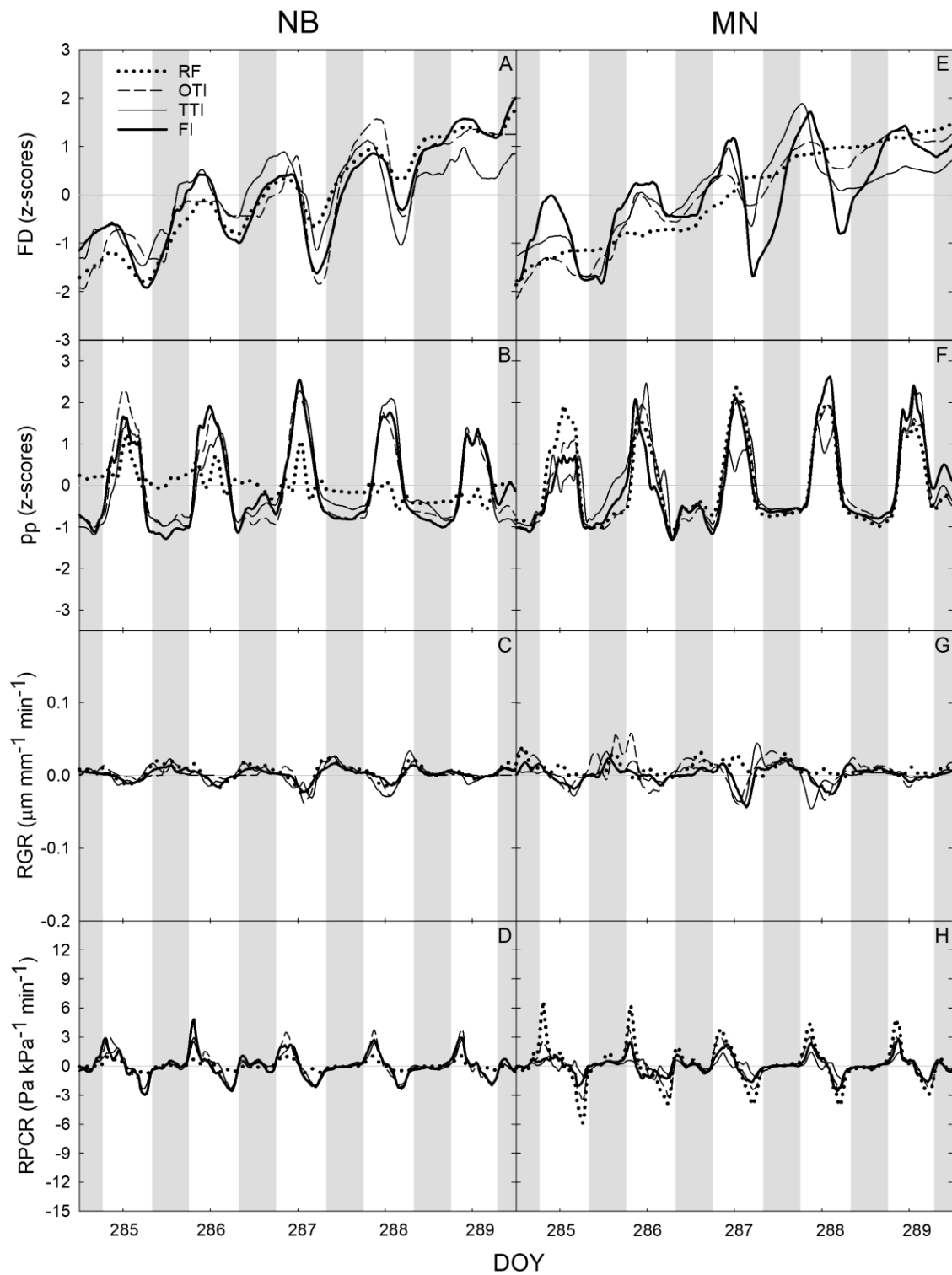


Figure 3.13. Fruit diameter (FD), leaf patch clamp pressure (p_p), fruit relative growth rate (RGR) and leaf relative pressure change rate (RPCR) recorded at 15-min intervals for five days during stage III of fruit growth in 'Nocellara del Belice' (NB) (A, B, C, D, respectively) and 'Olivo di Mandanici' (MN) trees (E, F, G, H) under full irrigation (FI), 2/3 of FI (TTI), 1/3 of FI (OTI) and no irrigation (RF). Grey and white areas show night and day time, respectively.

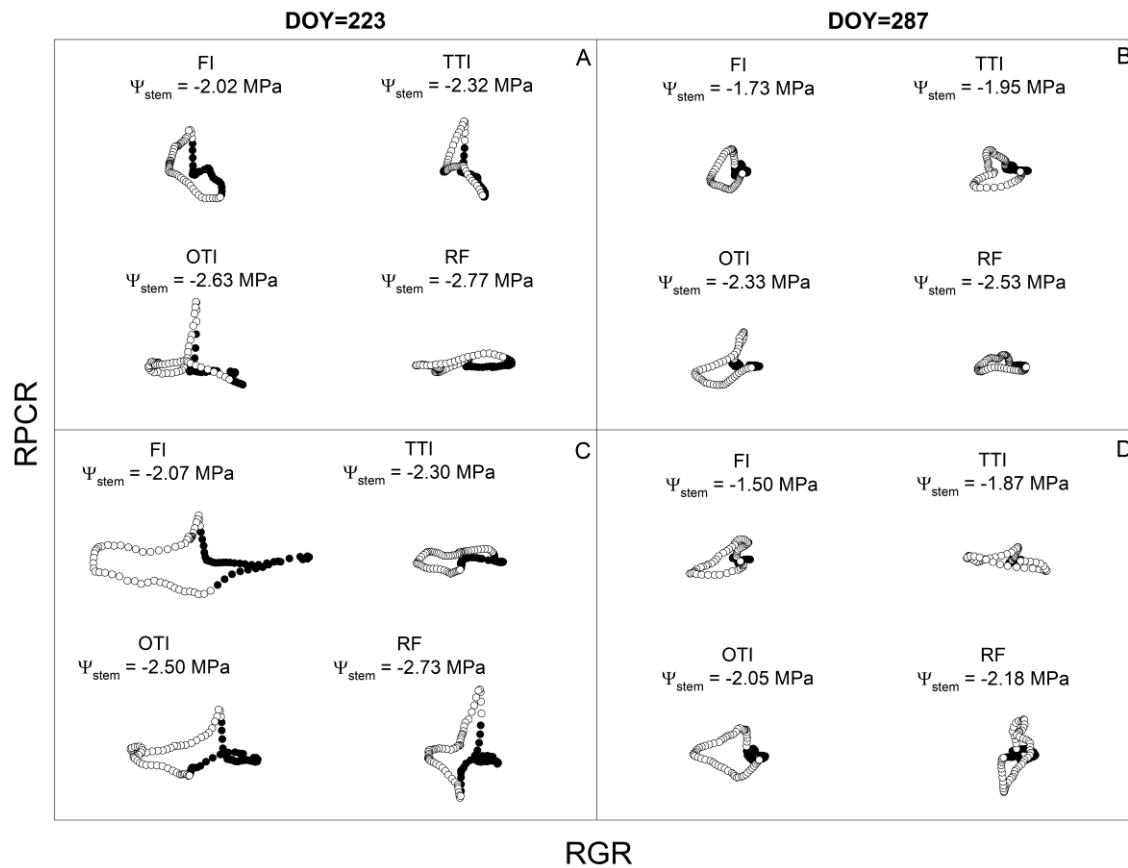


Figure 3.14. Scatter plots of diel leaf relative pressure change rate (RPCR) vs fruit relative growth rate (RGR) in 'Nocellara del Belice' (A and B) and 'Olivo di Mandanici' trees (C and D) under full irrigation (FI), 2/3 of FI (TTI), 1/3 of FI (OTI) and no irrigation (RF) at 223 and 287 days of the year (DOY). Midday stem water potential (Ψ_{stem}) reported for each genotype * DOY * irrigation treatment combination. White and black circles represent diurnal and nocturnal measurements, respectively. Axis scales are equal in all panels and consequently omitted.

The statistical diel, nocturnal and diurnal parameters of RGR (i.e. MIN, MAX, SUM, RANGE and RSD) were associated to the corresponding RPCR parameters in order to understand the importance of the RGR-to-RPCR relationships with water deficit. Subsequently, data were analysed by MANOVA to determine whether the combined response of parameters is affected by genotypes, irrigation levels, and the genotype \times irrigation interaction. The genotype did not influence significantly diel, diurnal and nocturnal RGR/RPCR when statistical parameters were considered together (Tab. 3.2). Diel and diurnal RGR/RPCR parameters changed significantly in response to irrigation levels, but the interaction between genotype and irrigation had the strongest effect (Tab. 3.2), indicating that RGR/RPCR statistical parameters can be used as genotype-dependent predictors of water deficit. Specifically, the highest F was found in the MANOVA that tested diurnal RGR/RPCR responses to genotype \times irrigation. These

results suggest that genotypic control of fruit to leaf water relations under increasing water deficit is predominant in day hours.

Table 3.3. Multivariate analyses of variance (MANOVAs) testing the effects of genotype, irrigation and the genotype \times irrigation interaction on the ratios of statistical parameters extrapolated from fruit relative growth rate (RGR) and leaf relative pressure change rate (RPCR) from diel, diurnal and nocturnal intervals. Ratios: minimum RGR / minimum RPCR (MIN), maximum RGR / maximum RPCR (MAX), summation of RGR values at 15-min intervals / summation of RPCR values at 15-min intervals (SUM), RGR difference between MAX and MIN / RPCR difference between MAX and MIN (RANGE), and RGR relative standard deviation (RSD) / RPCR relative standard deviation (RSD). Significance levels and F shown for each MANOVA.

FACTOR	TIMEFRAME	Significance level for Wilk's Lambda test					F
		MIN	MAX	SUM	RANGE	RSD	
Genotype	Diel			0.495			0.894
	Diurnal			0.260			1.365
	Nocturnal			0.104			1.991
Irrigation	Diel			0.025			1.965
	Diurnal			0.001			2.783
	Nocturnal			0.238			1.266
Genotype \times Irrigation	Diel			< 0.001			5.195
	Diurnal			< 0.001			6.515
	Nocturnal			0.031			1.907

Ratios between RGR and RPCR diel, diurnal and nocturnal parameters were often linearly related to midday Ψ_{stem} . Interestingly, linear regression models highlighted an inverse slope between the two genotypes in many of the several associations tested. Figure 3.15 shows the significant linear regressions with the highest R^2 for the diel (Fig. 3.15A and B), diurnal (Fig. 3.15C and D) and nocturnal (Fig. 3.15E and F) timeframes. In NB, the diel $\text{RGR}_{\text{RANGE}} / \text{RPCR}_{\text{RANGE}}$ ($\text{RANGE}_{\text{diel}}$) was higher at lower midday Ψ_{stem} , suggesting more marked water exchanges (e.g. in and out) in fruit rather than leaves at pronounced water deficit (Fig. 3.15A). An opposite trend was observed in MN, in which decreasing midday Ψ_{stem} lead to higher leaf water exchanges (Fig. 3.15B). This inverted trend agrees with RGR and RPCR fluctuations shown in Fig. 3.12C, D, G and H. In NB, during the day the $\text{RGR}_{\text{MIN}} / \text{RPCR}_{\text{MIN}}$ (MIN_{diur}) increased along increasing water deficit (Fig. 3.15C). This indicates that at increasing water deficit the highest diurnal speed of fruit water loss is higher compared to the peak of speed of leaf turgor gain. Even in this case, an opposite trend is found in MN, with the diurnal rate of fruit water loss being higher than leaf rehydration at low midday Ψ_{stem} . (Fig. 3.15D). At night, in

NB the $RGR_{SUM} / RPCR_{SUM}$ ratio (SUM_{noct}) decreased with increasing water deficit, with leaf rehydration being favoured over fruit water gain (Fig. 3.15E). Oppositely, in MN the SUM_{noct} ratio was inversely related to midday Ψ_{stem} (Fig. 3.15F), suggesting a stronger nocturnal sink power of fruit compared to leaves as water deficit increases.

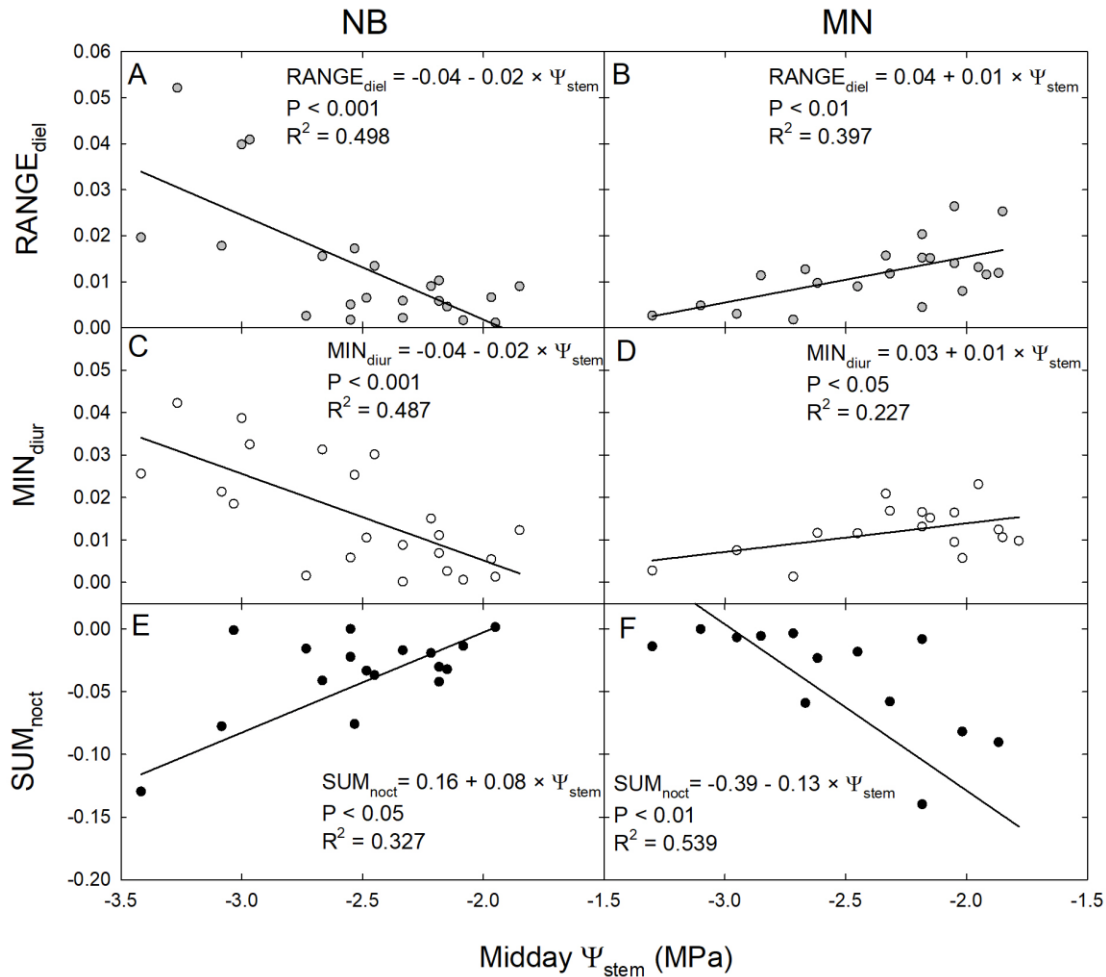


Figure 3.15. Linear relationships of diel $RGR_{RANGE} / RPCR_{RANGE}$ ($RANGE_{diel}$) (A and B), diurnal $RGR_{MIN} / RPCR_{MIN}$ (MIN_{diur}) (C and D) and nocturnal $RGR_{SUM} / RPCR_{SUM}$ (SUM_{noct}) (E and F) with midday stem water potential (Ψ_{stem}). Grey, white and black circles represent diel, diurnal and nocturnal data, respectively, for 'Nocellara del Belice' (NB) and 'Olivo di Mandanici' (MN).

All the insights obtained so far suggest that fruit to leaf relationships in terms of RGR and RPCR dynamics at different time of the day can be strictly related to midday Ψ_{stem} , thus to PWS. Data from each genotype were fitted into multiple regression models that considered all the statistical parameters from nocturnal and diurnal timeframes. The backward stepwise procedure was used to discard the non-significant parameters that do not contribute to a precise prediction of midday Ψ_{stem} . In NB, most of the parameters used in the model (Eq. 3.3) were significant ($P < 0.05$), and only diurnal $RGR_{MIN} / RPCR_{MIN}$ (MIN_{diur}), diurnal $RGR_{RSD} / RPCR_{RSD}$ (RSD_{diur}) and nocturnal

$RGR_{MIN} / RPCR_{MIN}$ (MIN_{noct}) were non-significant. The nocturnal $RGR_{RSD} / RPCR_{RSD}$ ratio (RSD_{noct}) provided the highest contribution to the model ($P < 0.001$, $F = 29.400$). In MN, only four parameters were found significant: diurnal $RGR_{RANGE} / RPCR_{RANGE}$ ($RANGE_{diur}$), RSD_{diur} , MIN_{diur} and RSD_{noct} . In the MN model (Eq. 3.4), similarly to what found in NB, RSD_{noct} was the parameter which more significantly contributed to the prediction of midday Ψ_{stem} ($P < 0.001$, $F = 24.569$).

$$NB \Psi_{stem} = -1.96 + (65.54 * MAX_{diur}^r) - (106.84 * RANGE_{diur}^s) - (21.27 * SUM_{diur}^t) - (3.20 * MAX_{noct}^u) + (89.56 * RANGE_{noct}^v) + (25.96 * SUM_{noct}^w) - (0.365 * RSD_{noct}^x) \\ (P < 0.001, R^2 = 0.924, S.E. = 0.14) \quad (Eq. 3.3),$$

$$MN \Psi_{stem} = -1.35 - (40.01 * RANGE_{diur}) - (0.11 * RSD_{diur}^y) - (21.649 * MIN_{diur}^z) - (0.280 * RSD_{noct}) \\ (P < 0.001, R^2 = 0.879, S.E. = 0.17) \quad (Eq. 3.4),$$

where, r = diurnal $RGR_{MAX} / RPCR_{MAX}$; s = diurnal $RGR_{RANGE} / RPCR_{RANGE}$; t = diurnal $RGR_{SUM} / RPCR_{SUM}$; u = nocturnal $RGR_{MAX} / RPCR_{MAX}$; v = nocturnal $RGR_{RANGE} / RPCR_{RANGE}$; w = nocturnal $RGR_{SUM} / RPCR_{SUM}$; x = nocturnal $RGR_{RSD} / RPCR_{RSD}$; y = diurnal $RGR_{RSD} / RPCR_{RSD}$; z = diurnal $RGR_{MIN} / RPCR_{MIN}$.

The results of this study suggest relevant differences in the mechanisms of fruit and leaf water exchanges in the two olive genotypes under increasing water deficit gradients. NB seems to favour fruit water exchanges over leaf's as water deficit increases (Fig. 3.15A) by increasing the fluctuations of fruit water in- and out-flows in trees under RF conditions (Fig. 3.12C). At the same time, RF leaves reduce their transpiration and water in-flow leading to minimum turgor gain to the (Fig. 3.12D). On the contrary, MN leaf water exchanges become predominant compared to fruit in water limiting conditions, whereas fluctuations of fruit water in- and out-flows are relatively much higher than leaf's in FI trees, (Figs. 3.12G and H and 2.15B). This differentiation in the response to drought is likely to be due to both fruit and leaf characteristics. Indeed, the water potential in NB leaves is likely to go negative, as suggested by the daily Ψ_{stem} curves (Fig. 3.10A and B) and considering that RF leaves do not particularly limit transpiration by stomatal closure, as indicated by g_s results. This leads to a loss of leaf cell turgor that happens at much higher midday Ψ_{stem} than MN, as suggested by the inversion of p_p curves in Figure 3.12C and D. A relatively low turgor leads to a

consequent decrease of diel fluctuation of RPCR. A more pronounced loss of turgor in NB leaves might also be driven by the lower leaf cell-wall elasticity in this genotype. Indeed, Bacelar et al. (2009) found higher cell elasticity in drought-tolerant genotypes. Concurrently, fruit instead increase their RGR fluctuations in RF conditions, perhaps driven by high cell-wall elasticity, acting as the main pump of water exchanges in NB under drought. The generally significantly higher midday Ψ_{stem} exhibited by MN can also be associated to a relatively higher water potential in the leaves compared to NB, as also in this case stomatal regulation did not differ among irrigation treatments (i.e. see g_s results). The hypothesised higher leaf osmotic adjustments and cell-wall elasticity in the MN genotypes under drought may justify the low tendency to an inversion of the p_p curve (Fig. 3.12F), and consequently explain why the diel RPCR range increases under drought (Fig. 3.12H). In addition, the positive relationship between $\text{RANGE}_{\text{diel}}$ and midday Ψ_{stem} in MN (Fig. 3.15B) is determined by the lower fruit water exchanges in RF treatments (Fig. 3.12G), which may be driven by lower fruit cell-wall elasticity in MN compared to NB.

The different mechanisms in the two genotypes may explain why Girón et al. (2015) found that fruit are the main water sinks during drought, whereas Dell'Amico et al. (2012) observed a higher leaf sink power. Changes in osmotic adjustments (Dichio et al., 1997; Dichio et al., 2009; Lo Bianco and Scalisi, 2017) and cell-wall elasticity (Xiloyannis et al., 1993; Bacelar et al., 2009) along water deficit gradients have been reported for leaves. However, to the best of our knowledge, no consideration has been previously given to concomitant changes of similar drought tolerance mechanisms in fruit. The analyses of both fruit and leaf water exchanges indicates that olive genotypes can privilege fruit or leaf water status preservation based on their evolutionary pathway.

CONCLUSIONS

The results of this work suggest that, overall, a lower amount of water can be used for irrigation in MN, as this cultivar tends to lose leaf cell turgor at lower Ψ_{stem} than NB and therefore can withstand drought for longer periods. However, our findings reveal opposite strategies of drought tolerance mechanisms between fruit and leaves, suggesting that olive genotypes can favour one organ over the other in conditions of water scarcity. The use of genotype-dependent models is therefore essential to determine how leaf and fruit water exchanges can be related to plant water status. These models can provide the basis for the automated modulation of irrigation in response to

pre-defined thresholds of water deficit. Genotype-specific stress thresholds of midday Ψ_{stem} for irrigation can be reasonably selected by analysing the inversion of the diel p_p curves, as schematised by Fernández et al. (2011b), as this represents a good indication of leaf turgor loss. The two models described in Eqs. 3 and 4 can be used for the highly precise day-by-day assessment of midday Ψ_{stem} in the two genotypes under study. These models were built based on data from stages II and III of fruit development, and in future studies responses from stage I should be integrated in the multiple regression analyses. Nevertheless, so far, the technologies that sense fruit and leaves water dynamics are still independent and need to be fit in a unique system for data to be processed with our method in real-time.

In conclusion, this work highlights the advantages of the integration of fruit and leaf water dynamics as predictor of plant water status, whose use is also recommended for other fruit species of horticultural interest.

LIST OF REFERENCES

- Allen, R. G., Pereira, L. S., Raes, D., & Smith, M. (1998). Crop evapotranspiration-Guidelines for computing crop water requirements-FAO Irrigation and drainage paper 56. FAO, Rome, 300(9), D05109.
- Bacelar, E. A., Correia, C. M., Moutinho-Pereira, J. M., Gonçalves, B. C., Lopes, J. I., & Torres-Pereira, J. M. (2004). Sclerophylly and leaf anatomical traits of five field-grown olive cultivars growing under drought conditions. *Tree physiology*, 24(2), 233-239.
- Bacelar, E. A., Santos, D. L., Moutinho-Pereira, J. M., Gonçalves, B. C., Ferreira, H. F., & Correia, C. M. (2006). Immediate responses and adaptative strategies of three olive cultivars under contrasting water availability regimes: changes on structure and chemical composition of foliage and oxidative damage. *Plant Science*, 170(3), 596-605.
- Bacelar, E. A., Moutinho-Pereira, J. M., Gonçalves, B. C., Lopes, J. I., & Correia, C. M. (2009). Physiological responses of different olive genotypes to drought conditions. *Acta Physiologiae Plantarum*, 31(3), 611-621.
- Ben-Gal, A., Kool, D., Agam, N., van Halsema, G. E., Yermiyahu, U., Yafe, A., ... & Segal, E. (2010). Whole-tree water balance and indicators for short-term drought stress in non-bearing 'Barnea' olives. *Agricultural Water Management*, 98(1), 124-133.
- Blanco-Cipollone, F., Lourenço, S., Silvestre, J., Conceição, N., Moñino, M. J., Vivas, A., & Ferreira, M. I. (2017). Plant Water Status Indicators for Irrigation Scheduling Associated with Iso- and Anisohydric Behavior: Vine and Plum Trees. *Horticulturae*, 3(3), 47.
- Cuevas, M. V., Torres-Ruiz, J. M., Álvarez, R., Jiménez, M. D., Cuerva, J., & Fernández, J. E. (2010). Assessment of trunk diameter variation derived indices as water stress indicators in mature olive trees. *Agricultural Water Management*, 97(9), 1293-1302.
- Dell'Amico, J., Moriana, A., Corell, M., Girón, I. F., Morales, D., Torrecillas, A., &

- Moreno, F. (2012). Low water stress conditions in table olive trees (*Olea europaea* L.) during pit hardening produced a different response of fruit and leaf water relations. *Agricultural water management*, 114, 11-17.
- Dichio, B., Nuzzo, V., Xiloyannis, C., Celano, G. and Angelopoulos, K. (1997). Drought stress-induced variation of pressure-volume relationships in *Olea europaea* L. Cv. "Coratina". *Acta Hort.* 449, 401-410. DOI: 10.17660/ActaHortic.1997.449.56
- Dichio, B., Xiloyannis, C., Angelopoulos, K., Nuzzo, V., Bufo, S. A., & Celano, G. (2003). Drought-induced variations of water relations parameters in *Olea europaea*. *Plant and Soil*, 257(2), 381-389.
- Dichio, B., Margiotta, G., Xiloyannis, C., Bufo, S. A., Sofo, A., & Cataldi, T. R. (2009). Changes in water status and osmolyte contents in leaves and roots of olive plants (*Olea europaea* L.) subjected to water deficit. *Trees*, 23(2), 247-256.
- Ehrenberger, W., Rüger, S., Rodríguez-Domínguez, C. M., Díaz-Espejo, A., Fernández, J. E., Moreno, J., ... & Zimmermann, U. (2012). Leaf patch clamp pressure probe measurements on olive leaves in a nearly turgorless state. *Plant Biology*, 14(4), 666-674.
- Ennajeh, M., Vadel, A. M., Cochard, H., & Khemira, H. (2010). Comparative impacts of water stress on the leaf anatomy of a drought-resistant and a drought-sensitive olive cultivar. *The Journal of Horticultural Science and Biotechnology*, 85(4), 289-294.
- Fernandes, R. D. M., Cuevas, M. V., Hernandez-Santana, V., Rodriguez-Dominguez, C. M., Padilla-Díaz, C. M., & Fernández, J. E. (2017). Classification models for automatic identification of daily states from leaf turgor related measurements in olive. *Computers and electronics in agriculture*, 142, 181-189.
- Fernandes, R. D. M., Cuevas, M. V., Diaz-Espejo, A., & Hernandez-Santana, V. (2018). Effects of water stress on fruit growth and water relations between fruits and leaves in a hedgerow olive orchard. *Agricultural Water Management*, 210, 32-40.
- Fernández, J. E., Díaz-Espejo, A., Infante, J. M., Durán, P., Palomo, M. J., Chamorro, V., ... & Villagarcía, L. (2006). Water relations and gas exchange in olive trees under regulated deficit irrigation and partial rootzone drying. *Plant and Soil*, 284(1-2), 273-291.
- Fernández, J. E., Torres-Ruiz, J. M., Díaz-Espejo, A., Montero, A., Álvarez, R., Jiménez, M. D., ... & Cuevas, M. V. (2011a). Use of maximum trunk diameter measurements to detect water stress in mature 'Arbequina' olive trees under deficit irrigation. *Agricultural Water Management*, 98(12), 1813-1821.
- Fernández, J. E., Rodríguez-Dominguez, C. M., Perez-Martin, A., Zimmermann, U., Rüger, S., Martín-Palomo, M. J., ... & Diaz-Espejo, A. (2011b). Online-monitoring of tree water stress in a hedgerow olive orchard using the leaf patch clamp pressure probe. *Agricultural Water Management*, 100(1), 25-35.
- Fernández, J. E. (2014). Plant-based sensing to monitor water stress: Applicability to commercial orchards. *Agricultural water management*, 142, 99-109.
- Fernández, J. E. (2017). Plant-based methods for irrigation scheduling of woody crops. *Horticulturae*, 3(2), 35.
- Girón, I. F., Corell, M., Galindo, A., Torrecillas, E., Morales, D., Dell'Amico, J., ... & Moriana, A. (2015). Changes in the physiological response between leaves and fruits during a moderate water stress in table olive trees. *Agricultural Water Management*, 148, 280-286.
- Gucci, R., Grimelli, A., Costagli, G., Tognetti, R., Minnocci, A., & Vitagliano, C. (2000, September). Stomatal Characteristics of Two Olive Cultivars "Frantoio" and "Leccino". In *IV International Symposium on Olive Growing* 586 (pp. 541-544).

- Jones, H. G. (2007). Monitoring plant and soil water status: established and novel methods revisited and their relevance to studies of drought tolerance. *Journal of experimental botany*, 58(2), 119-130.
- Karamanos, A. J. (1984). Ways of detecting adaptive responses of cultivated plants to drought. An agronomic approach. In *Being alive on land* (pp. 91-101). Springer, Dordrecht.
- Klein, T. (2014). The variability of stomatal sensitivity to leaf water potential across tree species indicates a continuum between isohydric and anisohydric behaviours. *Functional Ecology*, 28(6), 1313-1320.
- Lo Bianco, R., & Scalisi, A. (2017). Water relations and carbohydrate partitioning of four greenhouse-grown olive genotypes under long-term drought. *Trees*, 31(2), 717-727.
- Marino, G., Pernice, F., Marra, F. P., & Caruso, T. (2016). Validation of an online system for the continuous monitoring of tree water status for sustainable irrigation managements in olive (*Olea europaea* L.). *Agricultural Water Management*, 177, 298-307.
- Marino, G., Caruso, T., Ferguson, L., & Marra, F. P. (2018). Gas Exchanges and Stem Water Potential Define Stress Thresholds for Efficient Irrigation Management in Olive (*Olea europea* L.). *Water*, 10(3), 342.
- McCutchan, H., & Shackel, K. A. (1992). Stem-water potential as a sensitive indicator of water stress in prune trees (*Prunus domestica* L. cv. French). *Journal of the American Society for Horticultural Science*, 117(4), 607-611.
- Morandi, B., Manfrini, L., Zibordi, M., Noferini, M., Fiori, G., & Corelli Grappadelli, L. (2007). A low-cost device for accurate and continuous measurements of fruit diameter. *HortScience*, 42(6), 1380-1382.
- Moreno, F., Conejero, W., Martín-Palomo, M. J., Girón, I. F., & Torrecillas, A. (2006). Maximum daily trunk shrinkage reference values for irrigation scheduling in olive trees. *Agricultural Water Management*, 84(3), 290-294.
- Moriana, A., & Fereres, E. (2002). Plant indicators for scheduling irrigation of young olive trees. *Irrigation Science*, 21(2), 83-90.
- Moriana, A., Pérez-López, D., Prieto, M. H., Ramírez-Santa-Pau, M., & Pérez-Rodríguez, J. M. (2012). Midday stem water potential as a useful tool for estimating irrigation requirements in olive trees. *Agricultural Water Management*, 112, 43-54.
- Naor, A. (1999). Midday stem water potential as a plant water stress indicator for irrigation scheduling in fruit trees. In III International Symposium on Irrigation of Horticultural Crops 537 (pp. 447-454).
- Naor, A., Schneider, D., Ben-Gal, A., Zipori, I., Dag, A., Kerem, Z., ... & Gal, Y. (2013). The effects of crop load and irrigation rate in the oil accumulation stage on oil yield and water relations of 'Koroneiki' olives. *Irrigation Science*, 31(4), 781-791.
- Padilla-Díaz, C. M., Rodríguez-Domínguez, C. M., Hernández-Santana, V., Pérez-Martin, A., & Fernández, J. E. (2016). Scheduling regulated deficit irrigation in a hedgerow olive orchard from leaf turgor pressure related measurements. *Agricultural Water Management*, 164, 28-37.
- Parent, B., Hachez, C., Redondo, E., Simonneau, T., Chaumont, F., & Tardieu, F. (2009). Drought and abscisic acid effects on aquaporin content translate into changes in hydraulic conductivity and leaf growth rate: a trans-scale approach. *Plant physiology*, 149(4), 2000-2012.
- Patakas, A., & Noitsakis, B. (1997). Cell wall elasticity as a mechanism to maintain favorable water relations during leaf ontogeny in grapevines. *American Journal of*

- Enology and Viticulture, 48(3), 352-356.
- Rodriguez-Dominguez, C. M., Ehrenberger, W., Sann, C., Rüger, S., Sukhorukov, V., Martín-Palomo, M. J., ... & Zimmermann, U. (2012). Concomitant measurements of stem sap flow and leaf turgor pressure in olive trees using the leaf patch clamp pressure probe. *Agricultural water management*, 114, 50-58.
- Sade, N., Gebremedhin, A., & Moshelion, M. (2012). Risk-taking plants: anisohydric behavior as a stress-resistance trait. *Plant signaling & behavior*, 7(7), 767-770.
- Sade, N., & Moshelion, M. (2014). The dynamic isohydric–anisohydric behavior of plants upon fruit development: taking a risk for the next generation. *Tree physiology*, 34(11), 1199-1202.
- Savitzky, A., & Golay, M. J. (1964). Smoothing and differentiation of data by simplified least squares procedures. *Analytical chemistry*, 36(8), 1627-1639.
- Scalisi, A., Bresilla, K., & Simões Grilo, F., (2017). Continuous determination of fruit tree water-status by plant-based sensors. *Italus Hortus*, 24(2), 39-50.
- Schultz, H. R. (2003). Differences in hydraulic architecture account for near-isohydric and anisohydric behaviour of two field-grown *Vitis vinifera* L. cultivars during drought. *Plant, Cell & Environment*, 26(8), 1393-1405.
- Shackel, K. A., Ahmadi, H., Biasi, W., Buchner, R., Goldhamer, D., Gurusinge, S., ... & McGourty, G. (1997). Plant water status as an index of irrigation need in deciduous fruit trees. *HortTechnology*, 7(1), 23-29.
- Skelton, R. P., West, A. G., & Dawson, T. E. (2015). Predicting plant vulnerability to drought in biodiverse regions using functional traits. *Proceedings of the National Academy of Sciences*, 112(18), 5744-5749.
- Stocker, O. (1956). Die abhängigkeit der transpiration von den umweltafaktoren. In *Pflanze und Wasser/Water Relations of Plants* (pp. 436-488). Springer, Berlin, Heidelberg.
- Tardieu, F., & Simonneau, T. (1998). Variability among species of stomatal control under fluctuating soil water status and evaporative demand: modelling isohydric and anisohydric behaviours. *Journal of experimental botany*, 419-432.
- Tognetti, R., Raschi, A., Béres, C., Fenyvesi, A., & Ridder, H. W. (1996). Comparison of sap flow, cavitation and water status of *Quercus petraea* and *Quercus cerris* trees with special reference to computer tomography. *Plant, Cell & Environment*, 19(8), 928-938.
- Turner, N. C. (1988). Measurement of plant water status by the pressure chamber technique. *Irrigation science*, 9(4), 289-308.
- Xiloyannis, C., Dichio, B., & Nuzzo, V. (1993). Meccanismi di risposta dell'olivo alla carenza idrica. *Atti Convegno " Tecniche, norme e qualita'in Olivicoltura"*. Potenza, Italy, 15-17.
- Zimmermann, D., Reuss, R., Westhoff, M., Geßner, P., Bauer, W., Bamberg, E., ... & Zimmermann, U. (2008). A novel, non-invasive, online-monitoring, versatile and easy plant-based probe for measuring leaf water status. *Journal of Experimental Botany*, 59(11), 3157-3167.

4. NECTARINE TREE WATER RELATIONS

Preliminary test of fruit- and leaf-based sensors in high-density nectarine orchards. A caste study: “Continuous detection of new plant water status indicators in stage I of nectarine fruit growth”

Based on the paper:

Scalisi A., O’Connell M., Lo Bianco R., Stefanelli D. Continuous detection of new plant water status indicators in stage I of nectarine fruit growth. Accepted by Acta Horti (August 2018, presented at Water and Nutrient Relations and Management of Horticultural Crops, IHC 2018, Istanbul, Turkey).

ABSTRACT

Conventional irrigation management is often inefficient in responding to seasonal changes of tree water needs. The use of leaf- and fruit-based sensors might provide helpful insights on tree water status, although they have been poorly investigated so far. Fruit gauges and leaf patch clamp pressure (LPCP) probes were tested during stage I of nectarine fruit growth to evaluate if leaf turgor pressure and fruit size may serve as indicators of water deficit. The experiment was carried out in the 2017/18 season. During stage I four different irrigation levels were applied to ‘September Bright’ nectarine trees: 100, 40, 20 and 0% of crop evapotranspiration (ET_c). Tree size, fruit bearing habit, leaf chlorophyll concentration, plant water status, fruit diameter and canopy light interception were measured. Fruit gauges and LPCP probes were mounted on trees for a week interval in the second half of fruit growth stage I. Sensor outputs were expressed as fruit diameter and attenuated pressure of leaf patches (p_p). At the end of stage I, fruit diameter was lower in deficit irrigated trees but no differences in light interception among treatments were found. As expected, stomatal conductance (g_s) and stem water potential (Ψ_{stem}) were related to irrigation inputs. Continuous fruit diameter and p_p were found to be both sensitive to water deficit, although they require different analytical approaches for data interpretation. Results of this study suggest that nectarine fruit growth and leaf turgor pressure can be used independently as continuous indicators of plant water status.

Keywords: automation, fruit size, irrigation, *Prunus persica* (L.) Batsch, turgor pressure, water potential.

INTRODUCTION

Climate changes are leading to shortages of water worldwide, affecting traditional horticultural management strategies. Improved understanding of crop water

requirements, coupled with irrigation automation, play a key role for water saving and orchard management efficiency. However, although automated, current irrigation strategies are often neither efficient nor timely in responding to seasonal changes of tree water needs. In this regard, precision horticulture is moving towards the use of plant-based sensors for the real-time continuous assessment of water requirements (Scalisi et al., 2017). Leaf and fruit-based sensors provide helpful insights on tree water status, although they have been poorly adopted as a tool for irrigation management.

The intrinsic fragility of leaves in most fruit trees typically discourages growers from using continuous sensors on these organs as they are likely to end up damaging cells, compromising sensors' output. Nevertheless, in recent times, the use of leaf patch clamp pressure (LPCP) probes (Zimmermann et al., 2008) has been associated with water status assessment in olive (Ehrenberger, 2012), clementine (Ballester et al., 2015), persimmon (Martínez-Gimeno et al., 2017) and other fruit crops. LPCP probe outputs are expressed in attenuated pressure of leaf patches (p_p) in response to clamp pressure (p_{clamp}), whose values are inversely related to cell turgor pressure (p_c) (Zimmermann et al., 2008). According to several authors (Fernández et al., 2011; Ehrenberger et al., 2012, Rodriguez-Dominguez et al., 2012; Marino et al., 2016; Padilla-Díaz et al., 2016), a reversal of the p_p curve is found at low turgor pressure values, indicating a threshold below which trees enter water stress.

Daily fruit growth rate decreases with midday stem water potential (Ψ_{stem}) (Naor et al., 1997), as it depends on xylem, phloem and transpiration (Morandi et al., 2007a). Thus, fruit gauges for the continuous determination of daily fruit-size fluctuations (DFF) may provide valuable insights on water deficit. Midday Ψ_{stem} represents the most valuable tool for plant water status determination, but the automation of its measurements has never been accomplished (Scalisi et al., 2017). Klepper (1968), used a machinist's dial gauge on pears to estimate fruit growth responses to Ψ_{stem} . Afterwards, many sensors mainly based on linear variable displacement transducers have been adopted to determine DFF.

This study aimed to test leaf and fruit-mounted sensors at stage I of nectarine fruit growth (cell division) to evaluate leaf turgor pressure and fruit size dynamics as indicators of water deficit. Spot measurements of vegetative growth, fruit bearing habit, leaf chlorophyll, stomatal conductance (g_s), Ψ_{stem} and fruit diameter were measured to support results.

MATERIALS AND METHODS

The experiment was conducted at the research station of Agriculture Victoria, Tatura (36.43°S, 145.28°E, elev. 114 m), Australia, in summer 2017/18 using four-year-old ‘September Bright’ nectarine (late season) trees trained to an open Tatura system (2222 tree/ha). Four irrigation treatments were applied as fractions of crop evapotranspiration (ET_c) at stage I of fruit growth: control (100% of ET_c), deficit irrigation at 40% of ET_c (DI_40), deficit irrigation at 20% of ET_c (DI_20) and rainfed (no irrigation, DI_0). Trees were selected and labelled according to a randomized block design (6 blocks). Each plot consisted of three adjacent rows of six trees per row. The central two trees of each plot were used for measurements. Trunk cross-sectional area (TCSA) and the number of multiple and single fruitlets on 1-year-old shoots were recorded at the beginning of stage I. Leaf g_s and Ψ_{stem} were measured with a Delta-T AP4 dynamic porometer (Delta-T Devices LTD., Cambridge, UK) and a 3000 Scholander Plant Water Status Consol (ICT International, Armidale, AU), respectively. Fruit diameter was measured weekly using a Calibit digital calliper (HK Horticultural Knowledge srl, Bologna, Italy) equipped with memory for data storage. Vegetative growth was estimated with light interception measurements halfway and at the end of stage I using a Sunfleck PAR ceptometer (Decagon Devices Inc., Pullman, US) and a light trolley (Tranzflo NZ Ltd, Palmerston North, New Zealand). Effective area of shade (EAS) was calculated using the method described by Goodwin et al. (2006). Leaf chlorophyll concentration was expressed as SPAD index (Rodriguez and Miller, 2000) and measured with a SPAD 502 plus chlorophyll meter (Konica Minolta Inc., Osaka, JP) at the end of stage I.

Fruit gauges described by Morandi et al. (2007b) were used to assess DFF, whereas dynamics in leaf turgor pressure were determined with LPCP probes (Yara International, Oslo, NO). Dynamics in leaf turgor pressure and DFF were monitored on trees from one block for a week interval (48 to 54 DAFB) in the second half of fruit growth stage I. Sensors’ raw data were smoothed by the Savitzky and Golay (1964) method, and then converted into fruit diameter and p_p z-scores (standard scores) to allow comparison among treatments with different initial values of the measured variable.

Hourly weather data were retrieved from a weather station located at the research station. Crop data were analysed with analysis of variance, Tukey’s multiple comparison

and linear regression analysis using SYSTAT 13.1 (Systat software Inc., Chicago, Illinois, USA) procedures and results were plotted using SigmaPlot 12.5 (Systat software Inc., Chicago, Illinois, USA).

RESULTS AND DISCUSSION

Stage I of fruit growth was tracked for 36 days, from October 10 to November 14, 2017 (28 to 63 days after full bloom, DAFB). Temperatures and vapour pressure deficit (VPD) dropped in the middle of stage I (Fig. 4.1A) due to cloudy days. Concurrently, high precipitations occurred at 46 and 48 DAFB (Fig. 4.1B), leading to an increased crop water supply (CWS, i.e. rainfall + irrigation). Therefore, irrigation in the subsequent days was withheld accordingly. In the second half of stage I, temperature and VPD rose again.

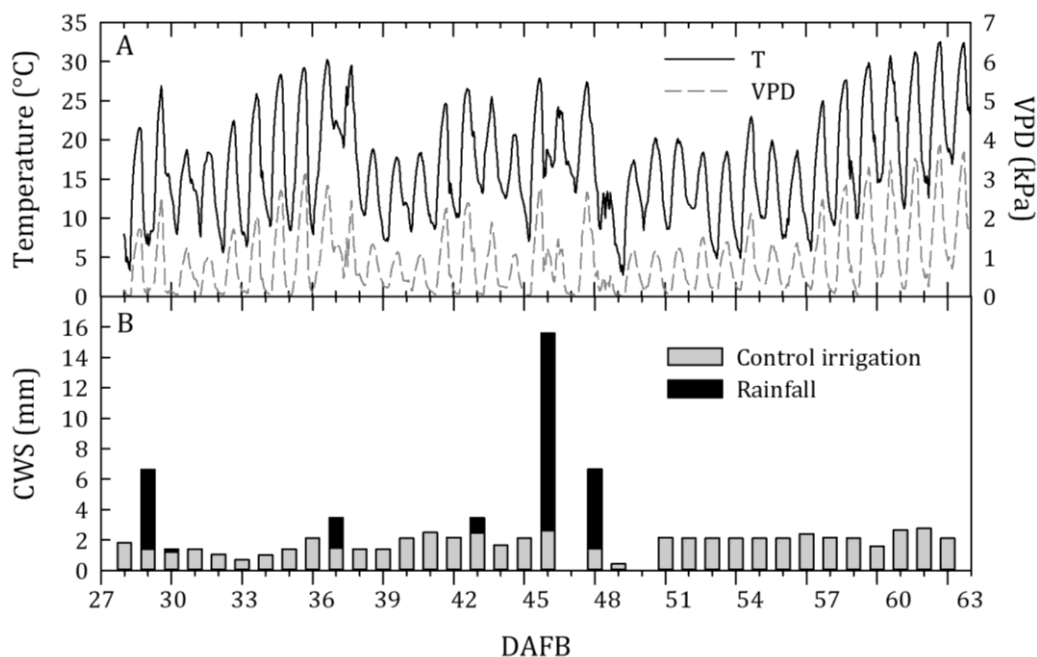


Figure 4.1. Temperature and vapour pressure deficit (VPD) trends (A), and daily crop water supply (CWS, B) in control trees (100% of ET_c) of ‘September Bright’ nectarines at growth stage I (28 to 63 days after full bloom, DAFB).

TREE SIZE, FRUIT BEARING HABIT AND LEAF CHLOROPHYLL CONCENTRATION

Tree size was estimated prior the beginning of stage I by determining TCSA. Although the four different irrigation strategies were already imposed to all trees in the previous year, no significant TCSA differences were found among treatments (Tab. 4.1). Moreover, following shuck fall, the ratio between multiple and single fruitlets in 1-year-old shoots (fruit bearing habit) was not affected by previous-year irrigation. Nevertheless, control and DI_40 trees appeared to bear the highest number of multiple

fruitlets (Tab. 4.1). This finding is in contrast with the effect of water stress on peach fruit doubling (Patten et al., 1988), which, on the other hand, considered all-season deficit irrigation, suggesting that there is a stage-related response to water deficit. High levels of deficit irrigation in stage I caused an expected decrease of the SPAD index (Tab. 4.1), in accordance with previous findings in grapes (Fanizza et al., 1991).

Table 4.1. Trunk cross-sectional area (TCSA), multiple/single fruitlet ratio per shoot, and leaf SPAD index of ‘September Bright’ nectarine trees under different irrigation levels. Data represent means \pm standard errors. Analysis of variance was followed by Tukey’s pairwise comparison (different letters indicate significant differences at $P \leq 0.05$).

Irrigation treatment	TCSA (cm²)	Multiple/single fruitlets	SPAD index
Control	35.8 \pm 1.85	0.65 \pm 0.10	42.1 \pm 0.44 ab
DI_40	32.3 \pm 1.88	0.74 \pm 0.11	42.8 \pm 0.79 a
DI_20	35.3 \pm 2.68	0.40 \pm 0.10	40.5 \pm 0.51 b
DI_0	36.4 \pm 2.33	0.41 \pm 0.09	40.5 \pm 0.51 b
P-value	n.s.	n.s.	<0.05

PLANT WATER STATUS

Mid-morning leaf g_s measurements provided insights on plant stomatal aperture mechanisms, emphasizing how significant responses to deficit irrigation were only found in the second half of stage I (Fig. 4.2). Indeed, at 44 DAFB, no significant differences among irrigation treatments were found, whereas at 63 DAFB, DI_20 and DI_0 trees significantly reduced their mid-morning g_s compared to Control and DI_40 trees (Fig. 4.2), implying that plants were protecting themselves from excessive water loss by transpiration.

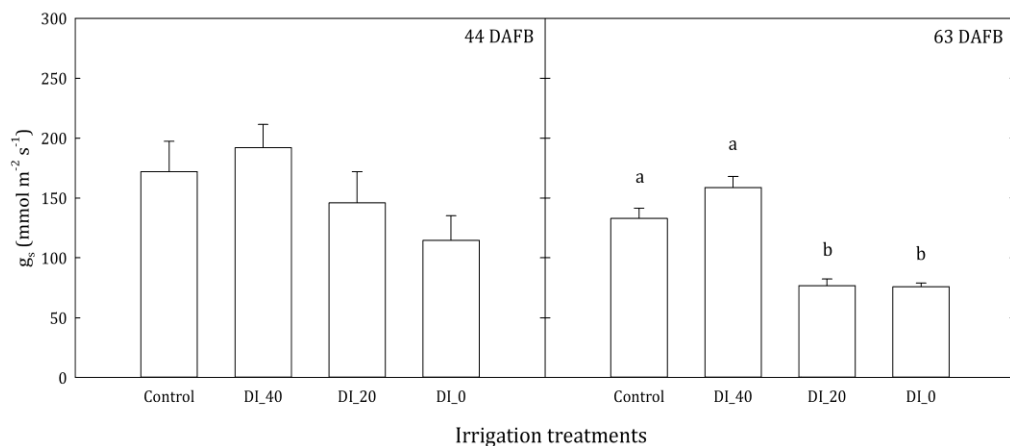


Figure 4.2. Mid-morning leaf stomatal conductance (g_s) of ‘September Bright’ nectarines under four different irrigation levels, at 44 and 63 days after full bloom (DAFB). Means ($n=6$) and standard errors are shown. Different letters indicate significant differences determined with analysis of variance and Tukey’s pairwise comparison ($P \leq 0.05$).

On the contrary, Ψ_{stem} decreases were already observed in DI_0 and DI_20 starting at 44 DAFB, whereas Ψ_{stem} of DI_40 remained similar to control until 50 DAFB (Fig. 4.3). These trends indicate that nectarine trees under water deficit preferred to keep stomata open (Fig. 4.2) and lose water at relatively low Ψ_{stem} suggesting a relevant osmotic component. Weather conditions in the last week of fruit growth stage I (Fig. 4.1) led to an overall drop of Ψ_{stem} (Fig. 4.3). In control trees Ψ_{stem} plummeted at 64 DAFB (-1.75 MPa) but its value was still significantly higher than the other treatments.

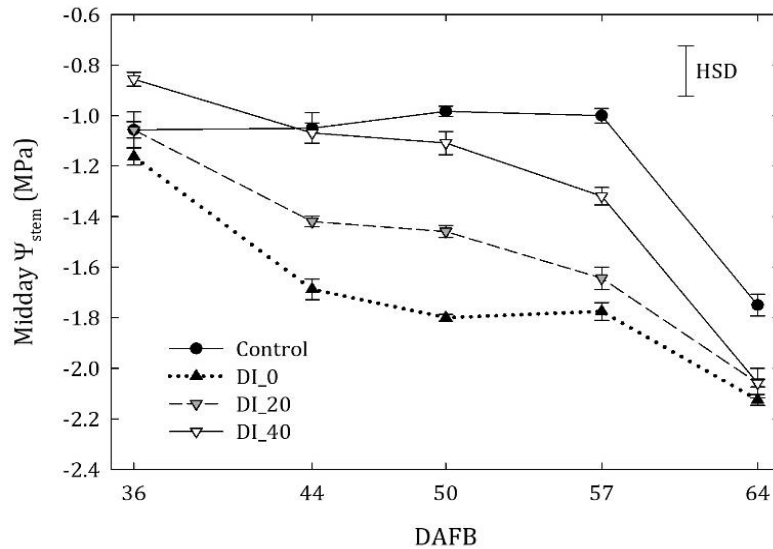


Figure 4.3. Midday stem water potential (Ψ_{stem}) of 'September Bright' nectarines under four different irrigation levels at fruit growth stage I. Means ($n=8$) and standard errors are shown. Statistically significant differences determined with analysis of variance and Tukey's Honest Significant Difference (HSD, $P \leq 0.05$).

FRUIT AND VEGETATIVE GROWTH

Irrigation treatments began to affect significantly fruit growth in the second half of stage I (Fig. 4.4), during a high temperature and no rainfall period (Fig. 4.1) and several days after irrigation treatments had a significant effect on midday Ψ_{stem} (Fig. 4.3). Fruit growth at stage I is characterized by cell division and, as expected, this process is reduced by water deficit, affecting final fruit size.

The values of f_{APAR} were not significantly different among irrigation treatments calculated at noon, noon - 3.5 h and noon + 3.5h, in the first (35 DAFB) and second half (57 DAFB) of fruit growth stage I. Nevertheless, an overall increase of EAS due to vegetative growth was observed from 35 to 57 DAFB (0.50 and 0.61, respectively). These results emphasize how deficit irrigation during stage I of 'September Bright' nectarine does not seem to affect light interception, in contrast with results found in peach by Li et al. (1989).

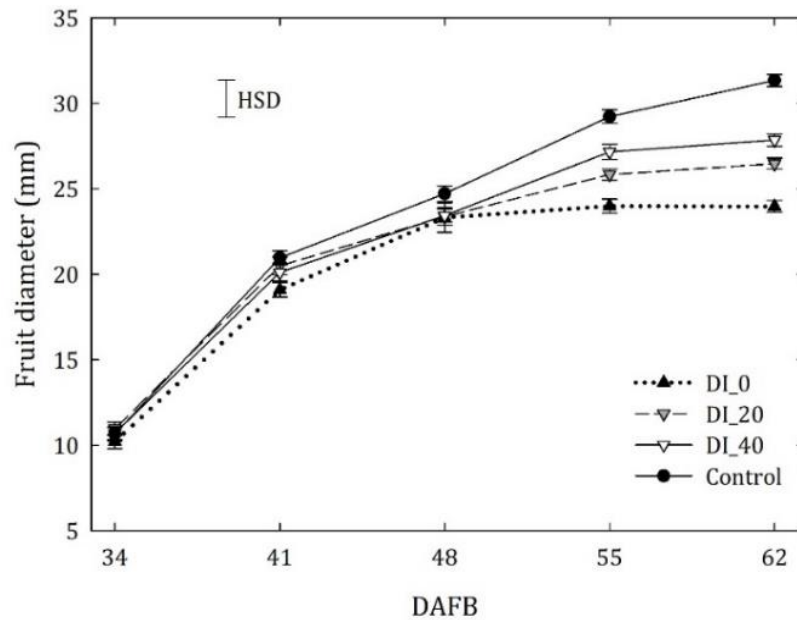


Figure 4.4. Fruit diameter during stage I of 'September Bright' nectarines under four different irrigation levels. Means ($n=36$) and standard errors are shown. Statistically significant differences determined with analysis of variance and Tukey's Honest Significant Difference (HSD, $P < 0.05$).

CONTINUOUS MEASUREMENTS OF FRUIT SIZE AND LEAF TURGOR PRESSURE

In the period from 48 to 54 DAFB, an overall linear increase in fruit diameter was observed (Fig. 4.5A). The 24-hour fruit diameter increases (Δ diameter) in DI_0 trees started decreasing from day 51, whereas in control trees, it was delayed by one-day (Fig. 4.5C), due to more favourable tree water status. Similar trends were not observed when 24-hour p_p absolute differences $|\Delta p_p|$ of control and DI_0 trees were compared (Fig. 4.5D). Indeed, p_p fluctuations (Fig. 4.5B) seem to be more influenced by environmental variables, as shown at 48 DAFB, where p_p 24-hour fluctuations follow the same pattern of T and VPD (Fig. 4.1). Yet, $|\Delta p_p|$ seem to follow trends of daily maximum VPD. This is expected as stomatal aperture in leaves is, at least in part, regulated by external VPD. The lack of different responses of p_p to irrigation treatments may indicate either that the level of water content in leaf tissues did not reach critical levels, or that LPCP probes are not appropriate sensors to determine when nectarine trees experience severe dehydration. The first hypothesis is more likely, as a prolonged period of irrigation reduction in deficit-irrigated trees might have led to a quicker stomatal closure during the day, implying a change in p_p dynamics. On the other hand, the deceleration of diel fruit size increases (Fig. 4.5C) may be associated with a threshold at which plants enter a higher water deficit condition.

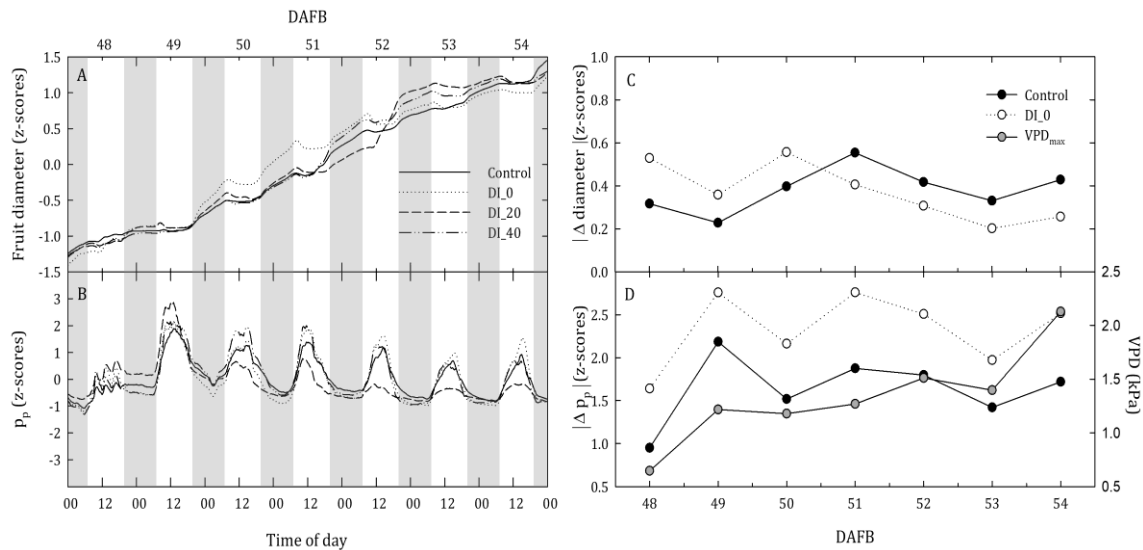


Figure 4.5. Fruit diameter (A) and attenuated pressure of leaf patches (p_p , B) weekly trends in ‘September Bright’ nectarines under four different irrigation levels, at fruit growth stage I. Grey and white areas emphasize night and day hours, respectively. Panels C and D show 24-hour absolute changes in fruit diameter ($|\Delta \text{diameter}|$) and p_p ($|\Delta p_p|$), respectively, for the Control and DI_0 treatments, and daily maximum VPD (VPD_{max}).

A further step towards the understanding of fruit diameter and p_p responses to water deficit may be done by analysing diel fluctuations. When a single day (50 DAFB) was taken into account, the Ψ_{stem} daily curve showed the typical inverted-bell shape, with a gradual and significant differentiation among treatments, especially around noon (Fig. 4.6A). However, fruit diameter and p_p did not show differences among treatments in a similar fashion to Ψ_{stem} (Fig. 4.6B and C). The unexpected higher increase of fruit diameter observed in DI_0 (Fig. 4.6B) is likely to be due to the heavy rain at 46 and 48 DAFB. Indeed, the rainfall led to higher recall of water from fruit of DI_0 trees that had a deeper water deficit. When fruit diameter and p_p data were regressed vs Ψ_{stem} using pooled data from all irrigation treatments, a significant inverse relationship between p_p and Ψ_{stem} was found, whereas no relationship was found between fruit diameter and Ψ_{stem} (Fig. 4.6D and E). The diel association between p_p and Ψ_{stem} may provide an important tool for real-time prediction of tree water status.

The inversion of the p_p curve observed in olive (Fernández et al., 2011) was never detected in this study, not even in DI_0 trees. This may be either because trees in this trial did not reach a critical level of water deficit, or because nectarine and olive have different leaf morphology and use different physiological mechanisms in response to drought (Larsen et al., 1989).

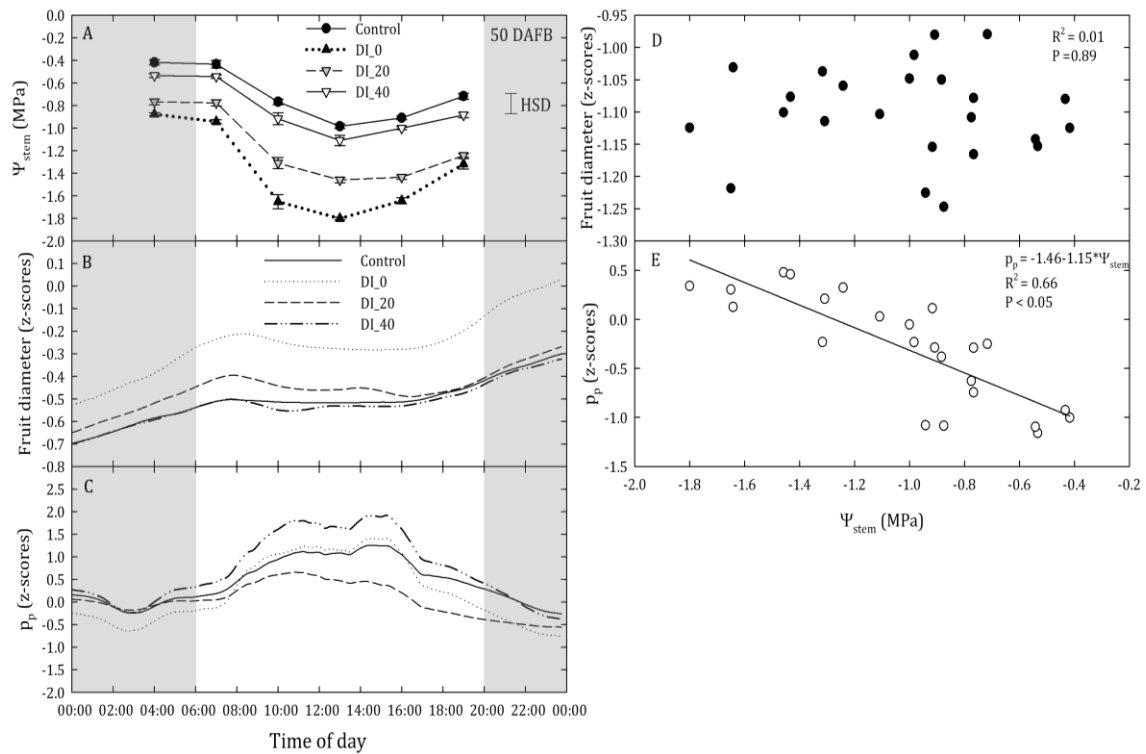


Figure 4.6. Stem water potential (Ψ_{stem} , A), fruit diameter (B) and attenuated pressure of leaf patches (p_p , C) diel trends in ‘September Bright’ nectarines under four different irrigation levels, at 50 days after full bloom (DAFB). Grey and white areas emphasize night and day hours, respectively. In panel A, significant differences determined with analysis of variance and Tukey’s Honest Significant Difference (HSD) at $p \leq 0.05$. Panels D and E, show linear regression analysis of fruit diameter and p_p vs Ψ_{stem} , respectively.

CONCLUSIONS

In this study, continuous data from fruit- and leaf-mounted sensors provided useful information on the responses of ‘September Bright’ nectarine trees to water deficit. The findings obtained from the analysis of weekly and diel trends suggest that both the sensors under study may represent valuable tools for determining plant water deficit in nectarine trees, although data from the two sensors require different analytical approaches. In future studies, all fruit growth stages need to be addressed to test if sensor outputs can confirm present results. Derivatives of fruit diameter and p_p data, and separate diurnal and nocturnal responses are to be further considered to determine the best indices for continuous plant water status determination.

LIST OF REFERENCES

Ballester, C., Castiella, M., Zimmermann, U., Ruger, S., Martnez Gimeno, M.A., and Intrigliolo, D.S. (2015). Usefulness of the ZIM-probe technology for detecting water stress in clementine and persimmon trees. *Acta Hort.* 1150, 105-112.

doi:10.17660/ActaHortic.2017.1150.15

- Ehrenberger, W., Rüger, S., Rodríguez-Domínguez, C.M., Díaz-Espejo, A., Fernández, J.E., Moreno, J., Zimmermann, D., Sukhorukov, V.L., and Zimmermann, U. (2012). Leaf patch clamp pressure probe measurements on olive leaves in a nearly turgorless state. *Plant Biol.*, 14(4), 666-674. doi:10.1111/j.1438-8677.2011.00545.x
- Fanizza, G., Ricciardi, L., and Bagnulo, C. (1991). Leaf greenness measurements to evaluate water stressed genotypes in *Vitis vinifera*. *Euphytica*, 55(1), 27-31. doi:10.1007/bf00022556
- Fernández, J.E., Rodríguez-Domínguez, C.M., Perez-Martin, A., Zimmermann, U., Rüger, S., Martín-Palomo, M.J., Torres-Ruiz, J.M., Cuevas, M.V., Sann, C., Ehrenberger, W., et al. (2011). Online-monitoring of tree water stress in a hedgerow olive orchard using the leaf patch clamp pressure probe. *Agric. Water Manag.*, 100(1), 25-35. doi:10.1016/j.agwat.2011.08.015
- Goodwin, I., Whitfield, D.M., & Connor, D.J. (2006). Effects of tree size on water use of peach (*Prunus persica* L. Batsch). *Irr. Sci.*, 24(2), 59-68. doi:10.1007/s00271-005-0010-z
- Klepper, B. (1968). Diurnal pattern of water potential in woody plants. *Plant Phys.*, 43(12), 1931-1934.
- Larsen, F.E., Higgins, S.S., and Al Wir, A. (1989). Diurnal water relations of apple, apricot, grape, olive and peach in an arid environment (Jordan). *Sci. Hortic.*, 39(3), 211-222. doi:10.1016/0304-4238(89)90134-9
- Li, S.H., Huguet, J.G., Schoch, P.G., and Orlando, P. (1989). Response of peach tree growth and cropping to soil water deficit at various phenological stages of fruit development. *J. Hortic. Sci.*, 64(5), 541-552. doi:10.1080/14620316.1989.11515989
- Marino, G., Pernice, F., Marra, F.P., and Caruso, T. (2016). Validation of an online system for the continuous monitoring of tree water status for sustainable irrigation managements in olive (*Olea europaea* L.). *Agric. Water Manag.*, 177, 298-307. doi:10.1016/j.agwat.2016.08.010
- Martínez-Gimeno, M.A., Castiella, M., Rüger, S., Intrigliolo, D.S., and Ballester, C. (2017). Evaluating the usefulness of continuous leaf turgor pressure measurements for the assessment of Persimmon tree water status. *Irr. Sci.*, 35(2), 159-167. doi:10.1007/s00271-016-0527-3
- Morandi, B., Rieger, M., and Corelli Grappadelli, L. (2007a). Vascular flows and transpiration affect peach (*Prunus persica* Batsch.) fruit daily growth. *J. Exp. Botany*, 58(14), 3941-3947. doi:10.1093/jxb/erm248
- Morandi, B., Manfrini, L., Zibordi, M., Noferini, M., Fiori, G., and Corelli Grappadelli, L. (2007b). A low-cost device for accurate and continuous measurements of fruit diameter. *HortScience*, 42(6), 1380-1382.
- Naor, A., Klein, I., Doron, I., Gal, Y., Ben-David, Z., and Bravdo, B. (1997). The effect of irrigation and crop load on stem water potential and apple fruit size. *J. Hort. Sci.*, 72(5), 765-771. doi:10.1080/14620316.1997.11515569
- Padilla-Díaz, C.M., Rodríguez-Domínguez, C.M., Hernandez-Santana, V., Perez-Martin, A., and Fernández, J.E. (2016). Scheduling regulated deficit irrigation in a hedgerow olive orchard from leaf turgor pressure related measurements. *Agric. Water Manag.*, 164, 28-37. doi:10.1016/j.agwat.2015.08.002
- Patten, K., Nimr, G., and Neuendorff, E. (1988). Fruit doubling of peaches as affected by water stress. *Acta Hortic.* 254, 319-322. doi:10.17660/ActaHortic.1989.254.53
- Rodríguez, I.R., and Miller, G.L. (2000). Using a chlorophyll meter to determine the

- chlorophyll concentration, nitrogen concentration, and visual quality of St. Augustine grass. *HortScience*, 35(4), 751-754.
- Rodriguez-Dominguez, C.M., Ehrenberger, W., Sann, C., Rüger, S., Sukhorukov, V., Martín-Palomo, M.J., Diaz-Espejo, A., Cuevas, M.V., Torres-Ruiz, J.M., Perez-Martin, A., et al. (2012). Concomitant measurements of stem sap flow and leaf turgor pressure in olive trees using the leaf patch clamp pressure probe. *Agric. Water Manag.*, 114, 50-58. doi:10.1016/j.agwat.2012.07.007
- Savitzky, A. and Golay, M.J. (1964). Smoothing and differentiation of data by simplified least squares procedures. *Analytical chemistry*, 36(8), 1627-1639. doi:10.1021/ac60214a047
- Scalisi, A., Bresilla, K., and Simões Grilo F. (2017). Continuous determination of fruit tree water-status by plant-based sensors. *Italus Hortus*, 24 (2), 39-50. doi:10.26353/j.itahort/2017.2.3950
- Zimmermann, D., Reuss, R., Westhoff, M., Geßner, P., Bauer, W., Bamberg, E., Bentrup F-W., and Zimmermann, U. (2008). A novel, non-invasive, online-monitoring, versatile and easy plant-based probe for measuring leaf water status. *J. Exp. Botany*, 59(11), 3157-3167. doi:10.1093/jxb/ern171

The combined use of leaf turgor pressure probes and fruit diameter sensors as an indicator of tree water status

Based on the paper:

Scalisi A., O'Connell M., Stefanelli D., Lo Bianco R. "Fruit and leaf sensing for continuous detection of nectarine water status", ready for submission to *Frontiers of Plant Science*.

ABSTRACT

Continuous assessment of plant water status indicators might provide the most precise information for irrigation management and automation, as plants are the interface between soil and atmosphere. This study investigates the relationship of plant water status to continuous fruit diameter (FD) and inverse leaf turgor pressure rates (p_p) in nectarine trees [*Prunus persica* (L.) Batsch] throughout fruit development. The influence of deficit irrigation treatments on stem (Ψ_{stem}) and leaf water potential, leaf relative water content, leaf hydraulic conductance, fruit and vegetative growth was studied across the stages of double-sigmoidal fruit development in 'September Bright' nectarines. Fruit relative growth rate (RGR) and leaf pressure change rate (RPCR) were derived from FD and p_p to represent rates of water in- and outflows in the organs, respectively. Continuous RGR and RPCR dynamics were independently and combinedly related to plant water status and environmental variables. The independent use of RGR and RPCR yielded significant associations with midday Ψ_{stem} , the most representative index of tree water status in anisohydric species. However, the combined use of nocturnal fruit and leaf parameters unveiled an even more significant relationship with Ψ_{stem} , suggesting a different fruit-to-leaf water balance in response to pronounced water deficit. In conclusion, we highlight the suitability of a multi-organ sensing approach for improved prediction of tree water status.

Keywords: fruit growth, irrigation, precision horticulture, *Prunus persica* (L.) Batsch, turgor pressure, water potential.

INTRODUCTION

Precision irrigation is becoming a crucial management approach for environmentally and economically sustainable fruit tree production. The vast majority of fruit crops need irrigation supply, as rainfall does not match crop water requirements (Scalisi et al., 2017). In most cases of fruit crops cultivated in dry areas, rainfed agriculture is not sustainable and deficit irrigation (DI) is a reasonable tool to improve water use efficiency. Fereres and Soriano (2007) highlighted the benefits of regulated

deficit irrigation (RDI) as a strategy to reduce agricultural water use. The main purpose of RDI is to reduce irrigation at specific developmental stages of the crop with no or limited effects on yield. The use of DI in different phenological stages of fruit crops started in the 80's by Chalmers et al. (1981; 1986). Today, water supply for DI treatments is often calculated as a fraction of crop evapotranspiration (ET_c) (Naor, 2006; Paço et al., 2006) or weather-based modelling crop water requirements. Additional approaches, on the other hand, rely on soil- or plant-based sensing.

Plant physiological indicators of water deficit are predominantly subjected to changes in tissue water content and status rather than to soil water dynamics (Jones, 2004; Steppe et al., 2008). Moreover, to represent adequately soil spatial variability and wetted and non-wetted zones in irrigated crops, soil-based sensing requires the use of many sensors, making this approach costly and difficult. Therefore, a continuous assessment of plant water status (PWS) indicators might provide the most precise information for irrigation management and automation. The advantage of plant-based methods over soil-based techniques resides in the fact that plants are an interface between soil and atmosphere (Fernández, 2017), being in the middle of the soil-plant-atmosphere continuum (SPAC). Therefore, precise automated irrigation management is likely to be highly associated to direct or indirect measurements of plant physiological indicators.

Midday stem water potential (Ψ_{stem}) is one of the most widely used indicators of plant water status for irrigation scheduling in anisohydric plants (McCutchan and Shackel, 1992; Shackel et al., 1997; Naor, 1999). Conversely, Blanco-Cipollone et al. (2017) suggested the adoption of pre-dawn leaf water potential (Ψ_{leaf}) as a suitable parameter for irrigation scheduling in isohydric species such as grapevine. Leaf relative water content (RWC) can also be used as a water deficit indicator (Lo Bianco and Scalisi, 2017; Mossad et al., 2018), although, differently from water potential it does not give indication of water energy status (Jones, 2007). Indicators of leaf water status may not be very useful in the early detection of plant water deficit in isohydric species (Jones, 2004), as their preventive stomatal closure preserves leaf turgor and leaf RWC.

A completely automated model for irrigation management in fruit crops is difficult to achieve, as responses to water deficit not only depend on environmental variables and soil water availability, but on fruit tree phenology as well. In stone fruits (e.g. peach, nectarines, plums), tree water status and sink-source relationships differ in the three stages of the typical double sigmoidal fruit growth model (Connors, 1919; Chalmers

and van den Ende, 1975), as shown in peach by DeJong and Goudriaan (1989). Therefore, DI applied at each of the stages of peach fruit growth differently affects vegetative and fruit growth, causing changes in final fruit size and composition (Li et al., 1989a). Fruit water exchanges are driven by transpiration, phloem and xylem with different mechanisms linked to fruit growth stages (Marsal and Girona, 1997; Morandi et al., 2007a; Morandi et al., 2010a). In peach, drought induces a relatively lower reduction of fruit growth in the early stages of fruit development, compared to final stages, when cell enlargement occurs (Li et al., 1989a; Génard and Huguet, 1996).

A direct automated and continuous estimation of Ψ_{stem} , Ψ_{leaf} or leaf RWC is not feasible yet and the use of indirect plant-based technologies might represent a viable solution for PWS determination. Trunk-based sensing such as sap-flow methods and dendrometry have been used for irrigation scheduling in peach and several other fruit crops (Fernández, 2017). Li et al. (1989b), Simonneau et al. (1993) and Goldhamer et al. (1999) successfully associated peach tree water status to stem diameter fluctuations obtained by dendrometers built on linear variable displacement transducers (LVDTs). In addition, Conejero et al. (2007) studied peach maximum trunk daily shrinkage and sap-flow signals for irrigation scheduling, suggesting that the former represents a more sensitive indicator of plant water status. Nevertheless, the use of stem diameter variations and sap flow for irrigation scheduling is questionable. Trunk diameter fluctuations are affected by plant age and size, crop load and growth patterns (Fernández, 2017), whereas sap flow rates reflect transpiration dynamics, which are dependent on stomatal closure/aperture and environmental variables (Jones, 2004).

The use of fruit- and leaf-based sensors to study tree water relations has also been reviewed in the literature (Jones, 2004; Fernández, 2017; Scalisi et al., 2017). The combined study of fruit and leaf water relations by continuous sensors may represent an innovative approach to determine sensitive indicators to water deficit. Changes in peach fruit water content in response to drought may be assessed with a model developed by Génard and Huguet (1996). The most common type of fruit-based sensor used to determine when trees enter water deficit conditions are based on LVDT technologies. Lang (1990) used LVDT sensors to emphasise the role of phloem, xylem and transpiration in ruling apple fruit changes in size over time. Similar sensors were used by Morandi et al. to study vascular flows in peach (2007a; 2010a), kiwifruit (2010b) and pear (2014). Fruit growth dynamics are definitely a good indirect indicator of fruit water status (Fernandes e al., 2018), as dry matter accumulation is negligible on a daily

scale (Blanke and Lenz, 1989). Fruit growth dynamics however can be influenced by growth stage and crop load. In peach, fruit water dynamics vary across the season, with maximum transpiration at fruit cell enlargement (Morandi et al., 2010a). As a consequence, the use of fruit gauges alone may not be a reliable indicator of whole plant water energy status.

Leaf-based sensing technologies mainly adopt leaf thickness sensors and pressure probes. The continuous outputs of the former were related to leaf RWC (Búrquez, 1987), although their long-term use is not feasible as they commonly injure leaves after short time (Zimmermann et al., 2008). As a consequence, recently a less invasive leaf pressure probe for the continuous determination of leaf water status (Zimmermann et al., 2008) has taken hold. These so-called leaf patch clamp pressure (LPCP) probes can be used to assess plant water status for irrigation scheduling, as they respond to leaf turgor pressure dynamics. Most of the initial studies with LPCP probes were carried out on olive (Fernández et al., 2011; Ehrenberger et al., 2012; Rodríguez-Dominguez et al., 2012; Padilla-Díaz et al., 2016) because the thick leaves of this species suit better the prolonged use of sensors. Olive is cultivated in dry or semi-dry regions with limited or no irrigation water supply. LPCP probes were also related to plant water status in other fruit crops, such as banana (Zimmermann et al., 2010), grapevine (Rüger et al., 2010), clementine (Ballester et al., 2015) and persimmon (Ballester et al., 2015; Martínez-Gimeno et al., 2017). However, as for fruit sensors, the use of LPCP probes alone can only give partial information on whole plant water status, unless many sensors are used on a tree. This is particularly due to different leaf initial conditions depending on age (especially in evergreen species) and exposure to light within the canopy. Even accepting the goodness of the data, a further need to test LPCP probes on species with thinner leaves (e.g. stone fruits) arises, as their prolonged use might damage leaf cuticle and alter readings (Scalisi et al., 2017). As mentioned above, the use of a single type of sensors can only provide partial information on tree water status. Most of C3 fruit trees exchange water with the surrounding atmosphere by means of transpiring fruit and leaves.

This study aims at investigating the relationship of plant water status to continuous fruit size and leaf turgor pressure dynamics in nectarine trees [*Prunus persica* (L.) Batsch] subjected to DI at each of the individual stages of fruit growth. The main hypothesis is that the combined information from fruit and leaves (i.e. the transpiring organs) provides more powerful information than individual indicators to

determine plant water status on a continuous basis for adoption of precision irrigation management.

MATERIALS AND METHODS

EXPERIMENTAL DESIGN

The experiment was carried out in summer 2017/18 on late ripening 'September Bright' nectarine trees grafted on 'Elberta' rootstock at the research station of Agriculture Victoria, Tatura, Australia (36°26'7.2" S and 145°16'8.4" E, 113 m a.s.l.). Within the experimental site, 144 four-year-old trees trained to an open Tatura system with 4.5 × 1 m spacing (i.e. 2222 trees/ha) were selected. Trees were disposed along N-to-S oriented rows. The soil was a clay-loam and trees were regularly fertigated according to conventional protocols. Fruit thinning and summer pruning were carried out at 43 and 125 days after full bloom (DAFB), respectively.

The typical double-sigmoidal fruit growth pattern was characterized by measurements of fruit diameter in control trees at weekly intervals from shuck fall to harvest. Growth stages were divided as follows: a cell division stage (I), a pit hardening stage (II), and a cell expansion stage (III). Stage III was further subdivided into two phases of about a month each, with the first (IIIa) starting when fruit cells re-established a strong sink power after stage II, and the second being the final period of sugar accumulation and chlorophyll degradation (stage IIIb). Four different DI levels, namely 100% of crop evapotranspiration (ET_c , control), 40% of ET_c (DI-40), 20% of ET_c (DI-20) and 0% of ET_c (DI-0) were applied at each of the fruit growth stages by drip irrigation. The experimental design included six replications in a randomised complete block design, each with two tree orientations (East and West) per treatment and fruit growth stage; measurement trees were separated by buffer trees and rows. At stage IIIb, the DI-40 treatment was not included, due to limited number of trees available. Canopy orientation was also included in the design, including West- and East-oriented trees of the open Tatura system. This was particularly helpful to explain different responses among trees due to light interception in different times of the day.

Meteorological data were collected using a weather station located in the experimental field. Reference evapotranspiration (ET_0) and vapour pressure deficit (VPD) were calculated using the methods described by Allen et al. (1998). ET_c was estimated by weighing ET_0 with nectarine effective area of shade (EAS) as shown by Goodwin et al. (2006).

LIGHT INTERCEPTION AND FRUIT SIZE

Canopy light interception was measured in all the fruit growth stages, at three different times of the day: solar noon, solar noon -3.5 h and solar noon +3.5 h. Noon measurements of photosynthetically active radiation (PAR) were carried out with a Sunfleck PAR ceptometer (Decagon Devices Inc., Pullman, US), whereas morning and afternoon data were collected using a custom-built PAR trolley equipped with a CR-1000 data logger (Campbell scientific, Inc., Logan, US). The total fraction of absorbed PAR (f_{APAR}) was estimated from both ceptometer (i.e. noon measurements) and PAR trolley data (i.e. morning and afternoon measurements). Subsequently, EAS was derived by averaging f_{APAR} data from the three diurnal measurements, as described by Goodwin et al. (2006).

Fruit diameters were regularly measured at weekly intervals during all the stages using a Calibit digital calliper (HK Horticultural Knowledge srl, Bologna, Italy).

TREE WATER RELATIONS AND LEAF FLUORESCENCE

Water potential

A pressure chamber (3000 Scholander Plant Water Status Consol, ICT International, Armidale, AU) was used for the measurements of Ψ_{stem} and Ψ_{leaf} according to Turner (1988). Midday Ψ_{stem} was determined at weekly intervals in all the stages of fruit growth on three leaves of the two trees (East- and West-oriented) per treatment in one of the six blocks. Daily curves from pre-dawn to 19.00h were plotted using Ψ_{stem} and Ψ_{leaf} data collected at three-hour intervals (Ψ_{leaf} was only measured at stage IIIa and IIIb of fruit growth).

Leaf relative water content

Leaf RWC was obtained using the method described by Barrs and Weatherley (1962). Mature leaves similar to those used for Ψ_{stem} were collected, sealed in plastic bags and transported to the laboratory for fresh weight (FW) determination. Turgid weight (TW) was obtained after immersing leaves in deionized water for 24 h at 4 °C. Subsequently, leaves were dried in an oven at 60 °C until constant weight (2-3 days) to estimate dry weight (DW). Leaf RWC was calculated as shown in Eq. 4.1.

$$RWC = (FW - DW) / (TW - DW) \times 100 \quad (\text{Eq. 4.1})$$

Leaf RWC was determined at three-hour intervals on the same days and trees as Ψ_{stem} and Ψ_{leaf} determination.

Leaf hydraulic conductance

A Delta-T AP4 dynamic porometer (Delta-T Devices LTD, Cambridge, UK) was used to determine leaf hydraulic conductance (g_l). Mid-morning (10 to 11am) measurements of g_l were undertaken at weekly intervals, whereas stage-related g_l daily curves were obtained for the same days and trees as Ψ_{stem} , Ψ_{leaf} and leaf RWC.

Leaf fluorescence

Leaf fluorescence was measured with a LI-6400XT portable photosynthesis system equipped with a 6400-40 leaf chamber fluorometer (LI-COR, Inc, Lincoln, US). Mid-morning data were collected at the end of stages I, IIIa and IIIb from the same trees as Ψ_{stem} , Ψ_{leaf} and leaf RWC, and expressed in terms of PSII efficiency (Φ_{PSII}).

FRUIT DIAMETER AND LEAF TURGOR PRESSURE CONTINUOUS SENSING

Fruit diameter (FD) was determined continuously with the LVDT-based fruit gauges described by Morandi et al. (2007b) connected to CR-1000 data loggers (Campbell scientific, Inc., Logan, US). Concurrently, leaf-mounted LPCP probes (Yara International, Oslo, NO) were used to track leaf turgor pressure dynamics using the attenuated pressure of leaf patches (p_p), an index which is inversely related to leaf cell turgor pressure (p_c), as described by Zimmermann et al. (2008). Data from both sensors were recorded at 15-minute intervals for a week period at each of the growth stages in one of the blocks within the experimental orchard. Two fruit gauges and LPCP probes were mounted on each West- and East-oriented tree, at medium canopy height and in nearby positions. Prior the actual week of measurements, a preliminary three-day comparison test between East- and West-oriented trees was carried out to verify if canopy orientation had an effect on sensors' outputs. Data from East and West trees were compared using daily relative standard deviations (RSD), mean, sum, max and min.

Raw data obtained from fruit gauges and LPCP probes were smoothed using a 15-point convoluted spline function (Savitzky and Golay, 1964). Subsequently, FD and p_p values were standardized by using z-scores (i.e. $z = (x - \text{mean}) / \text{standard deviation}$) to permit the possible comparison among fruits or leaves, respectively, which had different characteristics when the sensors were attached (i.e. fruit diameter and leaf turgor

pressure). This allowed averaging more sensors' output on the same tree and compare different treatments. Furthermore, the second derivatives of fruit diameter and p_p were calculated to determine fruit relative growth rate (RGR) and leaf relative pressure change rate (RPCR), as shown in Eqs. 4.2 and 4.3, respectively. Second derivatives were not standardised as they were calculated based on the previous FD and p_p , consenting possible comparisons among outputs from different sensors.

$$\text{RGR} = [\ln(\text{FD}_2) - \ln(\text{FD}_1)] / t_2 - t_1 \quad (\text{Eq. 4.2})$$

$$\text{RPCR} = [\ln(p_{p2}) - \ln(p_{p1})] / t_2 - t_1 \quad (\text{Eq. 4.3}),$$

where FD_2 and FD_1 correspond to FD at time 2 (t_2) and 1 (t_1), and p_{p2} and p_{p1} correspond to p_p at time 2 (t_2) and 1 (t_1), respectively.

Diel, diurnal and nocturnal variance of sensors' outputs was expressed as relative standard deviation ($\text{RSD} = \text{standard deviation} / |\text{mean}|$), to allow comparison among variances of different units (i.e. FD / p_p and RGR / RPCR). In addition, also diel, diurnal and nocturnal statistical parameters from data series were calculated for the variables considered (i.e. maximum, minimum and sum values) in order to find the best predictor of midday Ψ_{stem} .

Data from sensors that either caused damage to leaves or fruit or that were displaced by strong wind were not considered in the analysis.

STATISTICAL ANALYSIS

Statistical analysis was carried out using SYSTAT procedures (Systat software Inc., Chicago, US). Analysis of variance was performed when comparing irrigation treatments, canopy orientation and time factors, and, when appropriate, means were compared by Tukey's multiple range test and honestly significant difference (HSD). Sigmaplot procedures (Systat software Inc., Chicago, US) were used for linear and multiple linear regression analyses in order to associate continuous sensors' output to plant water status indicators.

RESULTS AND DISCUSSION

FRUIT DEVELOPMENTAL STAGES, WEATHER CONDITIONS AND CROP WATER SUPPLY

The typical double sigmoidal fruit development pattern was observed and Stages I, II, IIIa and IIIb lasted 35, 50, 29 and 31 days, respectively (Fig. 4.7).

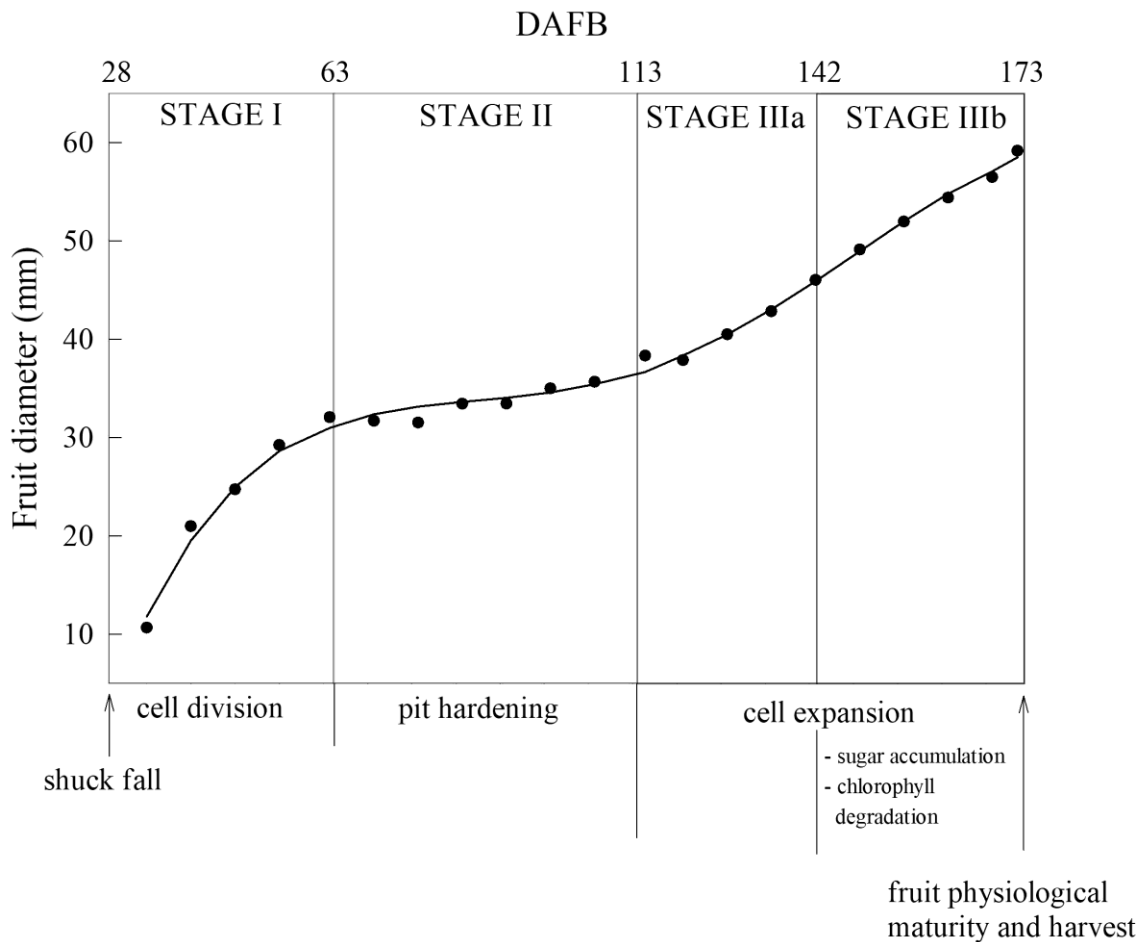


Figure 4.7. Fruit diameter during each fruit growth stages of 'September Bright' nectarines under control irrigation. Time series expressed in days after full bloom (DAFB).

Temperature (T), relative humidity (RH), ET_0 and VPD recorded from 27 to 173 days DAFB are shown in Figure 4.8. The gap in the data from 106 to 110 DAFB was due to a battery discharge. In stage I and at the beginning of stage II, frequent and abundant precipitations (Tab. 4.2) led to relatively low T (Fig. 4.8B) and high RH (Fig. 4.8C) (i.e. from 78 to 89 DAFB). Maximum ET_0 occurred in stage IIIa (Fig. 4.8A), driven by a combination of high T and low RH which caused a rise in VPD (Fig. 4.8D).

Precipitations progressively decreased towards the end of stage IIIb (Tab. 4.2). The highest crop water supply (CWS, i.e. rainfall + irrigation) found in stage II was likely to be due to its longer duration compared to other stages (Tab. 4.2).

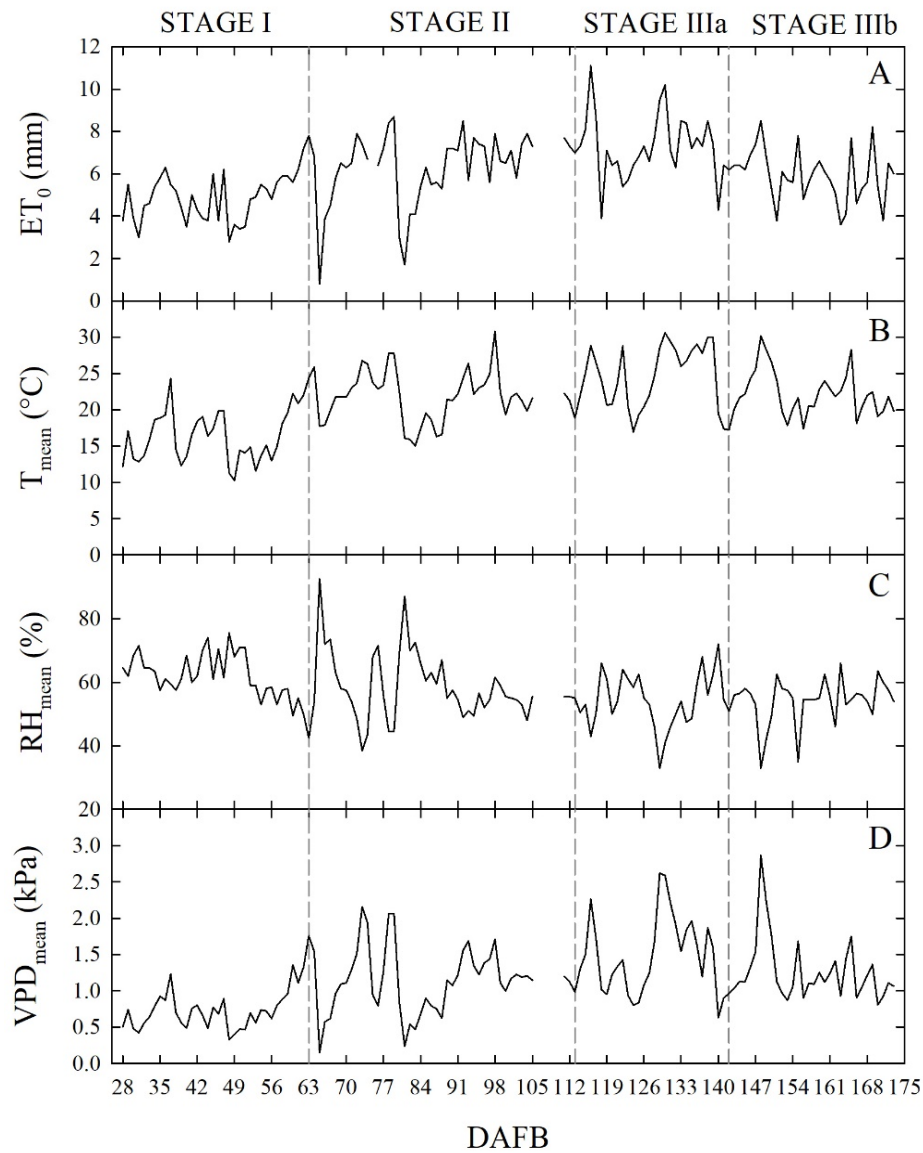


Figure 4.8. Daily total reference evapotranspiration (ET_0 , A), mean temperature (T_{mean} , B), mean relative humidity (RH_{mean} , C) and mean vapour pressure deficit (VPD_{mean} , D) along the considered four stages of fruit growth in days after full bloom (DAFB). Missing data from 106 to 110 DAFB.

Table 4.2. Total rainfall, full irrigation to control irrigated trees (FI) and crop water supply to control trees (CWS, i.e. rainfall + irrigation) at each of the fruit growth stages.

Fruit growth stage	Duration (No. days)	Rainfall (mm)	FI (mm)	CWS (mm)
I	36	64	73	137
II	50	141	78	219
IIIa	29	35	81	116
IIIb	31	3	83	86
Total	146	243	315	559

LIGHT INTERCEPTION AND FRUIT SIZE

The daily pattern of f_{APAR} was in line with expectations for an open Tatura system, combining West- and East-oriented trees. Tree canopies intercepted the highest amount of light in the morning and in the afternoon, while they reached a minimum absorption at noon (Fig. 4.9). A similar behaviour was observed in all the fruit growth stages and in all irrigation treatments. Data from West- and East-oriented trees were pooled together.

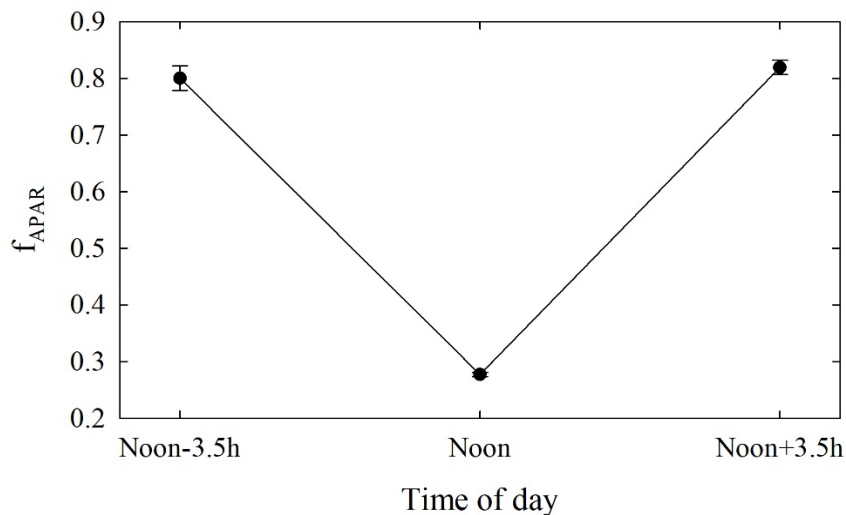


Figure 4.9. Fraction of absorbed photosynthetically active radiation (f_{APAR}) in control irrigated trees during a clear sky day at fruit growth stage I (57 DAFB). Error bars represent standard errors of means ($n = 36$).

An overall increase of EAS from stage I to stage II was observed, following the natural vegetative growth pattern (Fig. 4.10). Deficit irrigation in stage I did not significantly affect canopy size. On the other hand, a gradual decrease of EAS occurred along with RDI treatments in stage II, with significant lower values in DI-20 and DI-0 when compared to control trees (Fig. 4.10). Significant reduction of vegetative growth by application of DI in stage II were consistent with previous results in peach (Li et al., 1989a; Girona et al., 2005). Summer pruning was carried out in the very last days of stage II, causing a restoration of similar EAS among irrigation treatments in stage IIIa and IIIb. In stage III, DI did not have any significant influence on EAS.

No significant difference in fruit size was found between East- and West-oriented trees, thus data from the two sides were pooled together. At stage I, fruit diameter was significantly reduced by DI at 55 DAFB, with DI-20 and DI-40 inducing similar reductions and intermediate between the control and DI-0 (Fig. 4.11A). At stage II, during pit hardening, fruit diameter was only slightly affected by DI treatments, and significant differences only emerged at the end of the stage between control and DI-0

trees (Fig. 4.11B). At stage IIIa, DI induced fruit diameter reductions similar to those at stage I, with all DI treatments showing similar reductions compared to the control. Finally, DI caused the highest reduction of fruit growth at stage IIIb (Fig. 4.11D). Results from DI in stages I, II, IIIa and IIIb are in line with findings in peach from Li et al. (1989a) and Génard and Huguet (1996), and in nectarines from Naor et al. (1999; 2001).

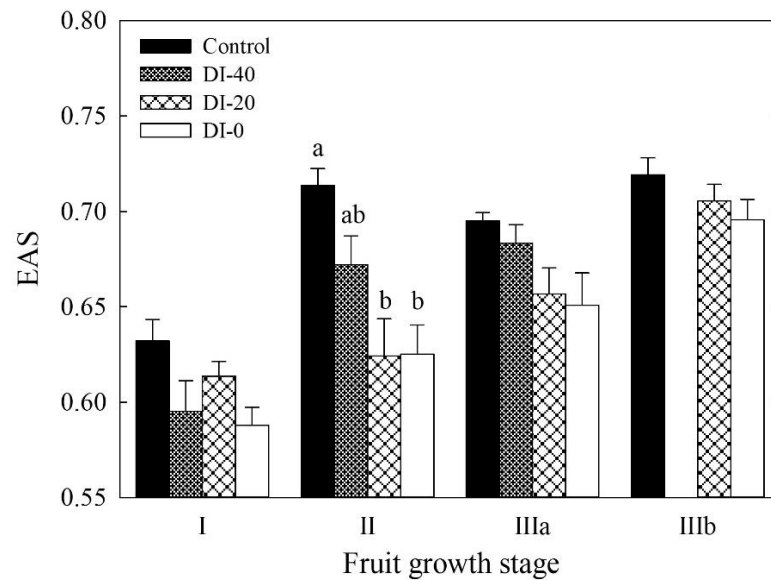


Figure 4.10. Effective area of shade (EAS) at fruit growth stages I, II, IIIa and IIIb of 'September Bright' nectarine. Error bars represent standard errors of means ($n = 36$) and different letters indicate significant differences within each stage determined with analysis of variance and Tukey's pairwise comparison ($P < 0.05$).

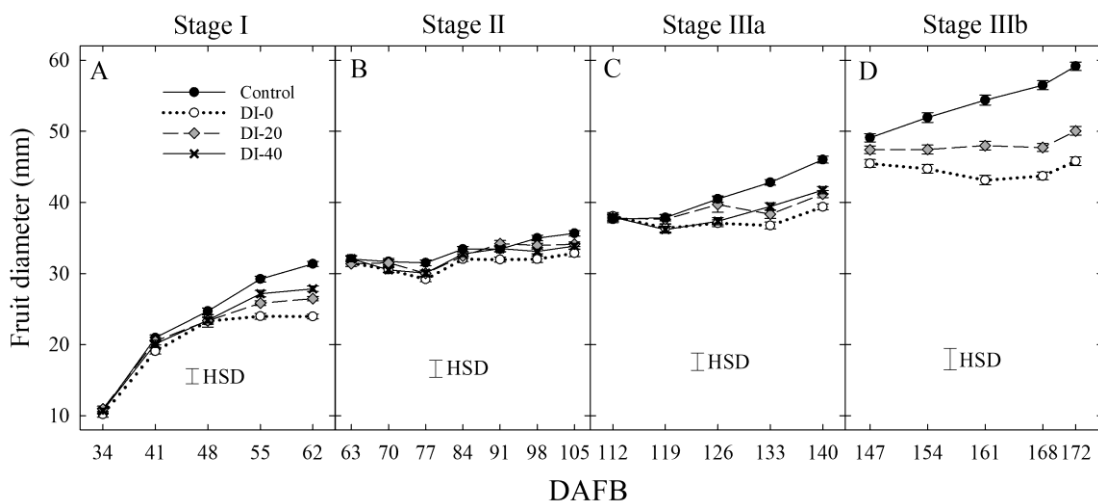


Figure 4.11. Fruit diameter at stage I (A), II (B), IIIa (C) and IIIb (D) of 'September Bright' nectarine fruit growth. Timeline expressed in days after full bloom (DAFB). Error bars represent standard errors of means ($n = 36$). Significant differences determined with analysis of variance and Tukey's Honest Significant Difference (HSD, $P < 0.05$).

TREE WATER RELATIONS AND LEAF FLUORESCENCE

Water potential

When water potentials from East- and West-oriented trees were compared, no statistically significant differences were found, thus data from the two sides were pooled together. Daily curves of Ψ_{stem} highlighted a relevant and gradual separation among irrigation treatments at solar noon measurements, except for stage II (Fig. 4.12), a further evidence of the suitability of midday Ψ_{stem} as an indicator of plant water deficit, as previously shown by Naor et al. (1999). The lack of an effect of DI on Ψ_{stem} at stage II might be related to the abundant precipitations which occurred during this phase (Tab. 4.2). Similarly, when weekly midday Ψ_{stem} was considered, the effect of DI treatments increased gradually with fruit growth, reaching the most marked reductions at the end of stage IIIb (Fig 4.13). Even in this case, minor or no effects were found at stage II, although in the second half, decreasing precipitations (data not shown) unveiled a drop of midday Ψ_{stem} in DI-0 trees (Fig. 4.13B). A steeper decrease of midday Ψ_{stem} at stage II was also found by Fereres and Soriano in peach (2006).

Daily measurements of Ψ_{leaf} carried out only in stage IIIa and IIIb (Fig. 4.14A and B), and concomitantly with Ψ_{stem} , showed typical patterns with lowest values around solar noon. As expected, Ψ_{leaf} resulted in slightly lower values than Ψ_{stem} , in accordance with the water potential gradient along the SPAC. DI-0 trees reached the lowest Ψ_{leaf} of -3.82 and -3.75 MPa in stage IIIa and IIIb, respectively (Fig. 4.14).

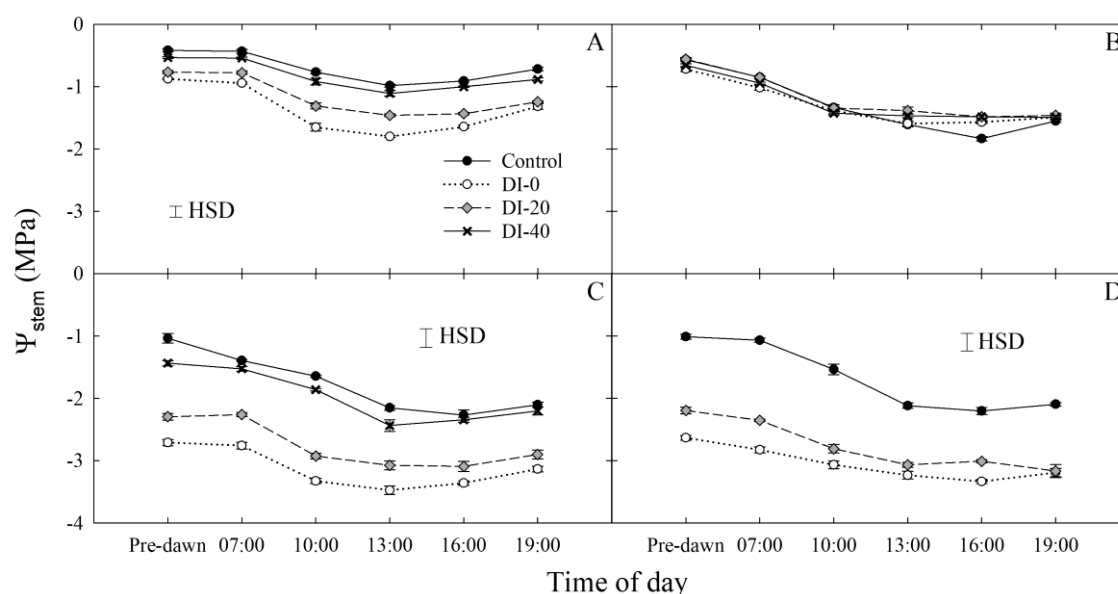


Figure 4.12. Daily curves of stem water potential (Ψ_{stem}) at stages I (A), II (B), IIIa (C) and IIIb (D) of 'September Bright' nectarine fruit growth. Error bars represent standard errors of means ($n = 6$). Significant differences determined with analysis of variance and Tukey's Honest Significant Difference (HSD, $P < 0.05$).

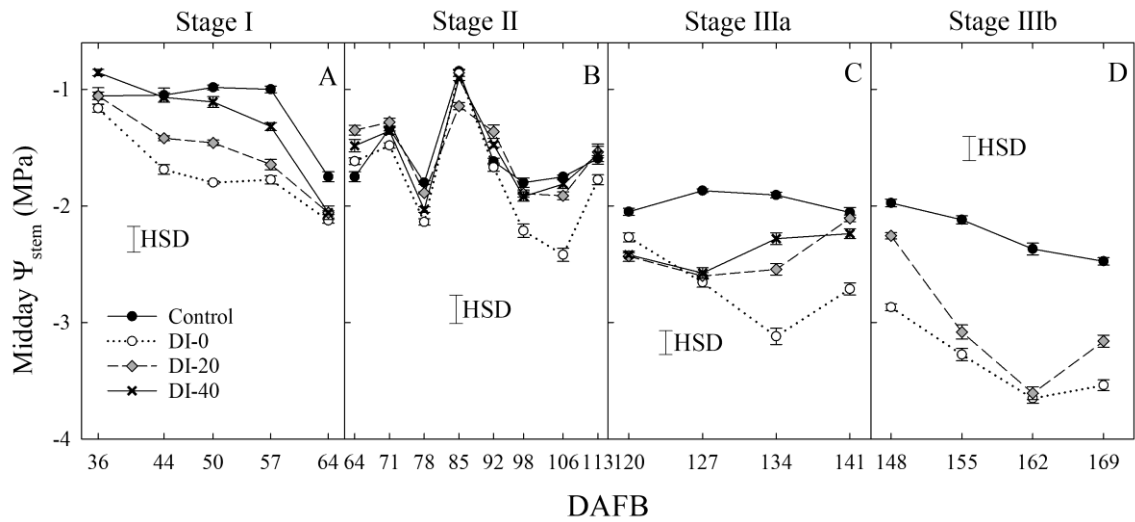


Figure 4.13. Midday stem water potential (Ψ_{stem}) at fruit growth stages I (A), II (B), IIIa (C) and IIIb (D) in 'September Bright' nectarines. Timeline expressed in days after full bloom (DAFB). Error bars represent standard errors of means ($n = 6$). Significant differences determined with analysis of variance and Tukey's Honest Significant Difference (HSD, $P < 0.05$).

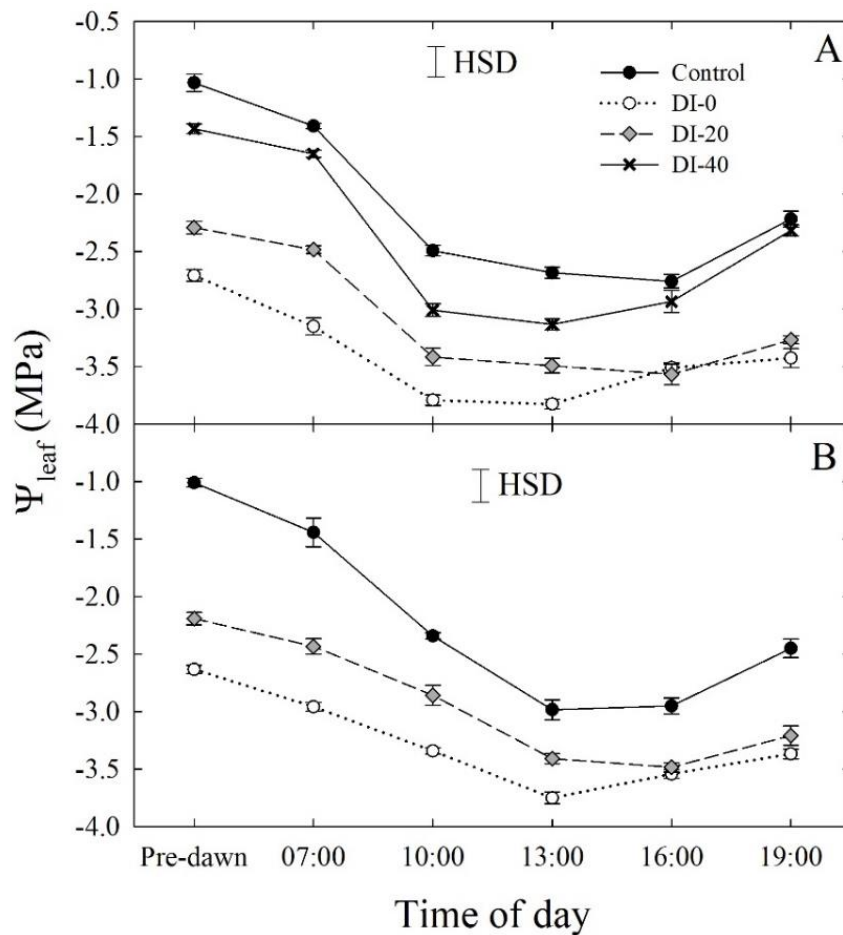


Figure 4.14. Daily curves of leaf water potential (Ψ_{leaf}) at stages IIIa (A) and IIIb (B) of 'September Bright' nectarine fruit growth. Error bars represent standard errors of means ($n = 6$). Significant differences determined with analysis of variance and Tukey's Honest Significant Difference (HSD, $P < 0.05$).

Leaf relative water content

Daily curves of leaf RWC obtained from measurements carried out at all the fruit development stages and on all the irrigation treatments did not highlight differences among West- and East-oriented trees (data not shown), thus data from the two sides were pooled together. At stage I, leaf RWC varied greatly showing erratic effects of DI (Fig. 4.15A). At stage II, irrigation treatment and time of day had no significant effect on leaf RWC (Fig. 4.15B). Nevertheless, leaf RWC was found gradually lower along the irrigation treatment gradient at stage IIIa (Fig. 4.15C), where the maximum differences between the two extreme treatments, control and DI-0, occurred at mid-morning and mid-afternoon. Ultimately, at stage IIIb, differences among treatments were once again non-significant, except for the measurement at 19.00h (Fig. 4.15D). Therefore, leaf RWC cannot be considered as sensitive as Ψ_{stem} and Ψ_{leaf} for nectarine water status determination, mainly because the variability of RWC among leaves is high and results in non-significant effects of DI (i.e. HSD in Figure 4.15).

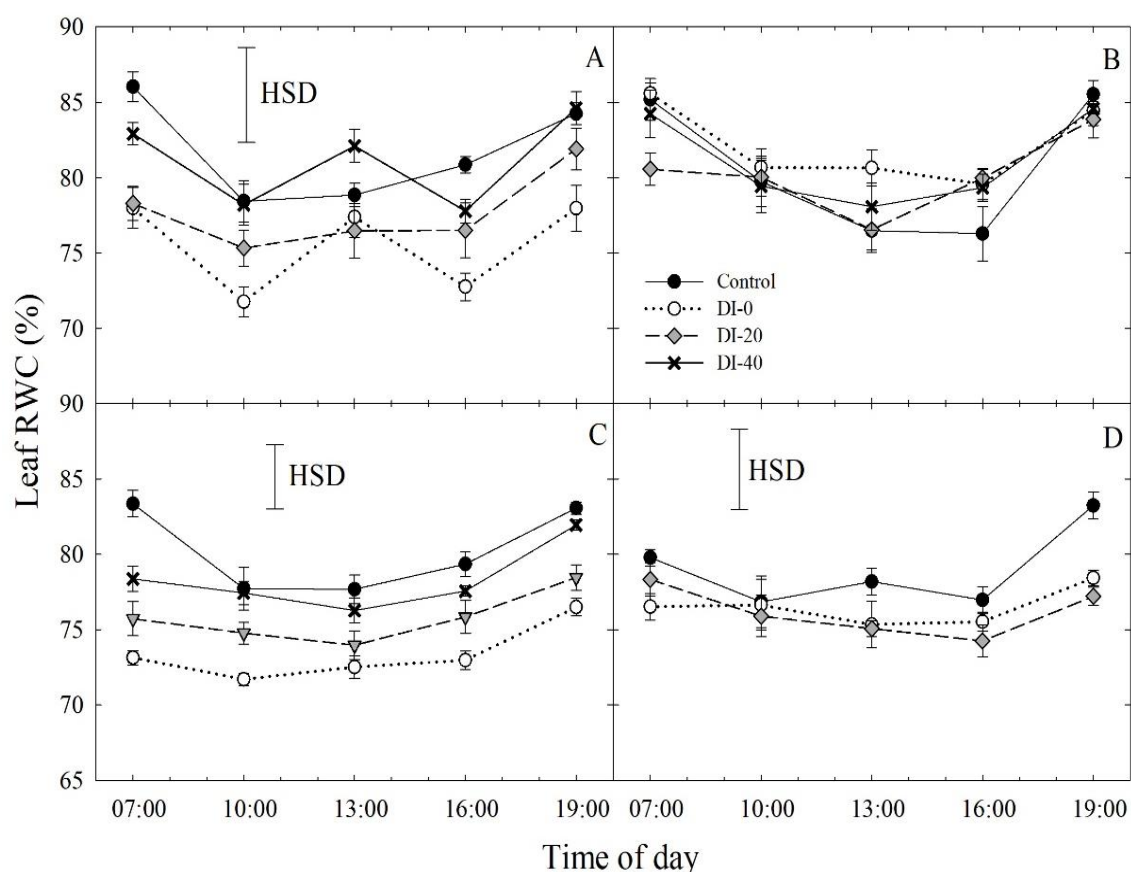


Figure 4.15. Daily curves of leaf relative water content (RWC) at stages I (A), II (B), IIIa (C) and IIIb (D) of 'September Bright' nectarine fruit growth. Error bars represent standard errors of means ($n = 6$). Significant differences determined with analysis of variance and Tukey's Honest Significant Difference (HSD, $P < 0.05$).

Leaf hydraulic conductance and fluorescence

Data of g_l at stage I are not available due to instrument malfunctioning. At stage II, no significant differences in daily g_l were found among irrigation treatments (Fig. 4.16A). When maximum stomatal aperture occurred (mid-morning) there was a significant influence of canopy orientation, resulting in higher g_l in leaves of West-oriented trees (Fig. 4.16B), as they intercepted greater PAR than East trees. After noon, an overall partial closure of stomata induced a consequential reduction of g_l in all the treatments. At stage IIIa, control irrigated trees expressed a g_l higher than $300 \text{ mmol m}^{-2} \text{ s}^{-1}$ in the morning, whereas DI-0 trees barely opened their stomata (about $10 \text{ mmol m}^{-2} \text{ s}^{-1}$) in response to high water deficit conditions (Fig. 4.16C). Differently from stage I, no differences were found between West- and East-oriented trees, because measurements were done on a cloudy day (Fig. 4.16D). At stage IIIb, leaves of control trees had higher g_l compared to DI-20 and DI-0 trees, which instead showed similar g_l levels (Fig. 4.16E). In addition, even in the case of stage IIIb daily curve, a cloudy morning concealed the effect of canopy orientation, and the increase of photosynthetic photon flux density (PPFD) caused by the disappearance of clouds after solar noon was not sufficient to show differences between West- and East-oriented trees (Fig. 4.16F).

When measured at weekly intervals, g_l showed no differences among irrigation treatments at stage II (Fig. 4.17A), whereas DI treatments reduced mid-morning stomatal aperture in the second half of stage IIIa (Fig. 4.17B). Only at stage IIIb, leaves from control trees consistently kept their g_l higher than leaves from DI-20 and DI-0 trees (Fig. 4.17C). At this stage, after reaching a severe water deficit, DI-0 and DI-20 trees limited their gas exchanges and photoassimilation to minimal levels, and likely DI induced a reduction of phloemic flows towards fruit. Therefore, a reduction of leaf gas exchanges might partially explain the poor, non-significant increase of fruit size observed in DI-0 (Fig. 4.11D). Overall, g_l data at mid-morning were found to be representative indicator of plant water deficit, as that is the time of highest leaf transpiration and maximum evidence of partial stomatal closure in response to water deficit.

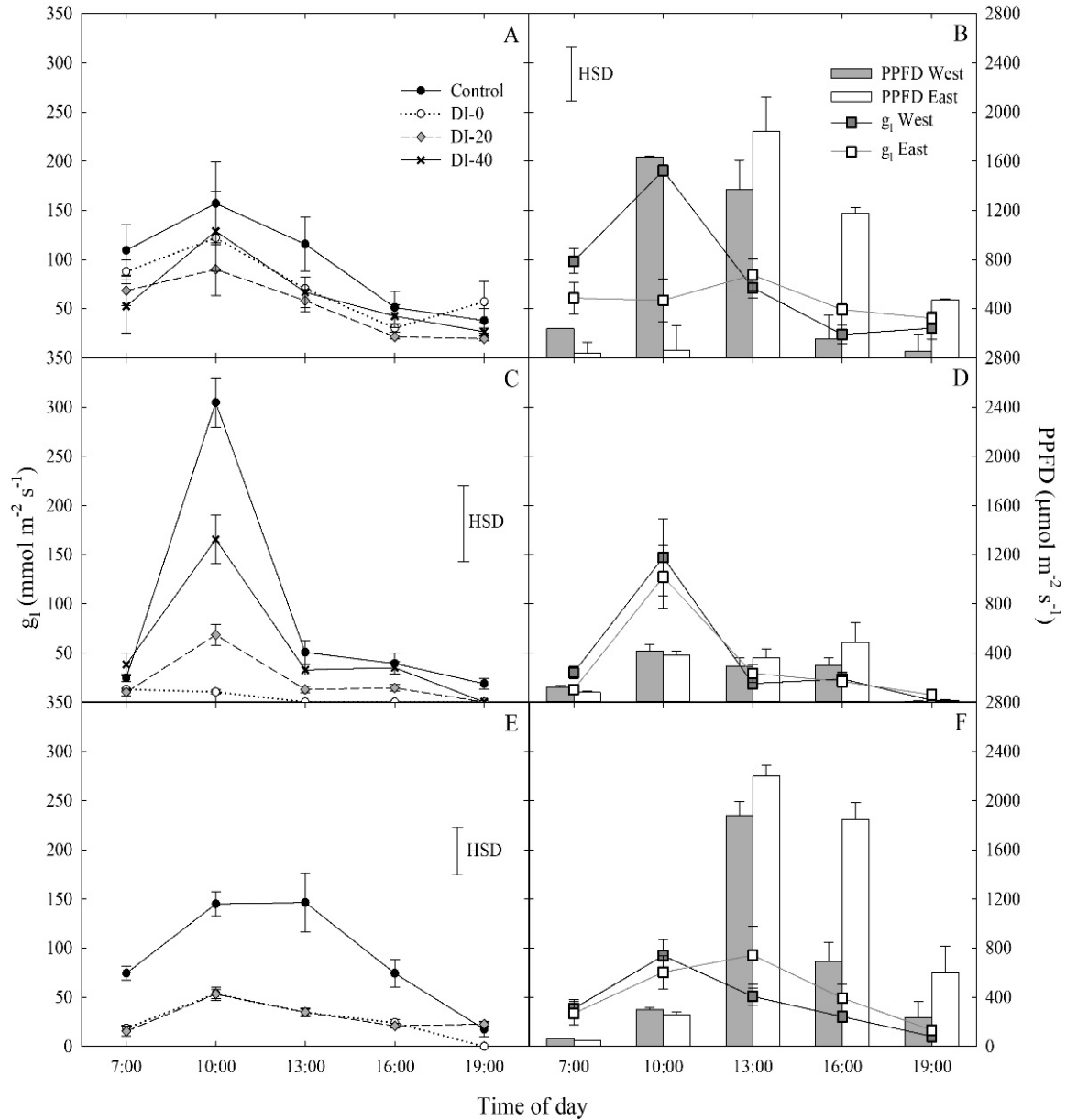


Figure 4.16. Daily curves of leaf hydraulic conductance (g_l) in control, DI-40, DI-20 and DI-0 trees at stages II (A), IIIa (C) and IIIb (E) of 'September Bright' nectarine fruit growth, and in West- and East-oriented trees (Stage II = B, IIIa = D, IIIb = F). Bars in panels B, D and F show means of photosynthetic photon flux density (PPFD) for West and East trees. Bars represent standard errors of means (irrigation treatment $n = 6$; canopy orientation $n = 12$). Significant differences determined with analysis of variance and Tukey's Honest Significant Difference (HSD, $P < 0.05$). The HSD bar in panel B highlights only differences in g_l , and not in PPFD.

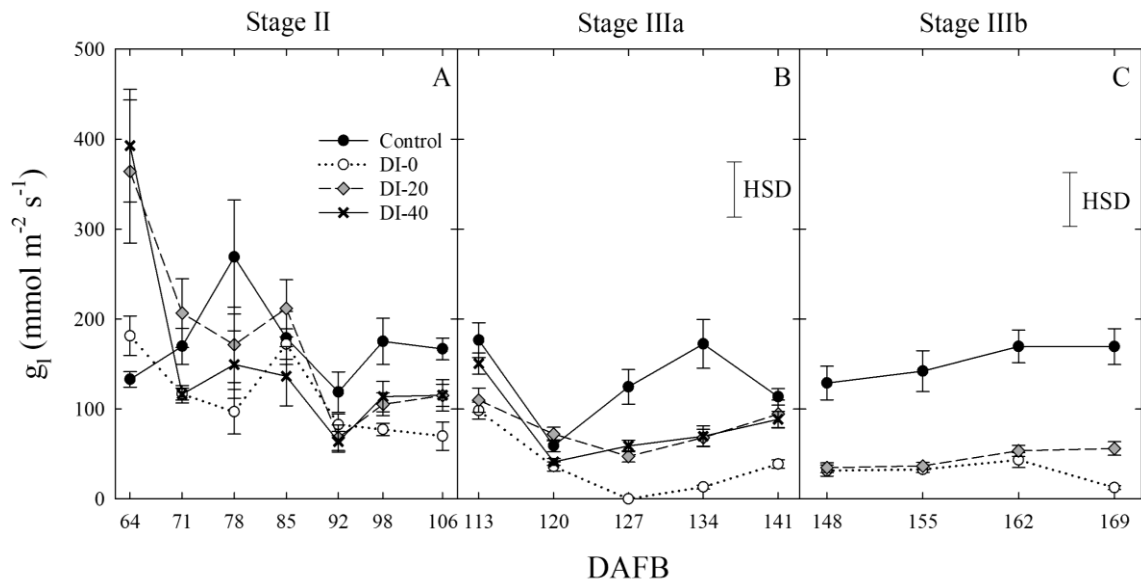


Figure 4.17. Mid-morning leaf hydraulic conductance (g_l) at stages II (A), IIIa (C) and IIIb (D) of 'September Bright' nectarine fruit growth. Error bars represent standard errors of means ($n = 6$). Significant differences determined with analysis of variance and Tukey's Honest Significant Difference (HSD, $P < 0.05$).

Imposed DI treatments did not influence Φ_{PSII} in measurements carried out at the end of fruit growth stage I (Fig. 4.18). No data were collected at the end of stage II as the equipment was under maintenance. However, it is legitimate to propose that DI treatments did not influence Φ_{PSII} also at the end of stage II, since g_l did not show any differences (Fig. 4.18A) and weather conditions were not likely to damage PSII. At the end of stage IIIa, despite a general drop of Φ_{PSII} , a partial but significant effect of DI treatments was observed, with higher values in control trees. At the end of stage IIIb, Φ_{PSII} of control leaves increased to 0.22, while Φ_{PSII} of DI-20 and DI-0 trees remained low (Fig. 4.18). Low Φ_{PSII} values in DI-20 and DI-0 agree with findings of Ψ_{stem} (Fig. 4.13) and g_l (Fig. 4.17), and suggest a possible damage of PSII after severe water deficit, as also found by Losciale et al. (2011) in peach.

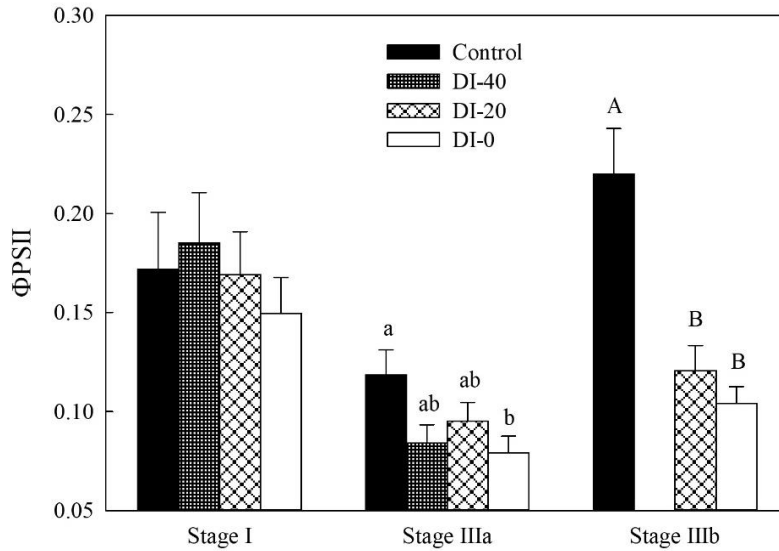


Figure 4.18. Efficiency of PSII (Φ_{PSII}) at the end of fruit growth stages I, IIIa and IIIb of 'September Bright' nectarine. Error bars represent standard errors of means ($n = 36$). When present, different letters indicate significant differences within each stage determined with analysis of variance and Tukey's pairwise comparison ($P < 0.01$).

The interdependency of plant water status indicators

Among the others, Ψ_{stem} is considered as the most sensitive indicator of plant water status in nectarines, and it is strictly connected to other water status indices along the SPAC (e.g. Ψ_{leaf} and external VPD) and to the regulation of stomatal opening, expressed in terms of g_l . Leaf RWC has also been linked to Ψ_{stem} as shown by Koide et al. (1989), although results of this study were not always in line. Indeed, leaf RWC was not found to be a sensitive measurement to highlight differences among irrigation treatments, especially at stage I, II and IIIb of fruit development (Fig. 4.15A, B and D). In our case, the strongest association between leaf RWC and Ψ_{stem} occurred at pre-dawn, when water potential and water content were in equilibrium (data not shown).

The combined interdependency of VPD, Ψ_{leaf} , g_l and leaf RWC with Ψ_{stem} was tested analysing data extrapolated from daily curves from all the fruit growth stages. Data were pooled together and associated to Ψ_{stem} through a multiple linear regression model. Stomatal aperture and closure dynamics are known to be regulated by Ψ_{leaf} among other factors, which in turn is influenced by VPD and strictly related to Ψ_{stem} . Leaf RWC is then adjusted responding to water potential gradients along the SPAC. Therefore, we expected to find the strongest association of Ψ_{stem} with Ψ_{leaf} , followed by decreasingly tight associations with g_l , VPD and leaf RWC, respectively. However, leaf RWC resulted to be non-significant in a first backward stepwise regression model ($P = 0.98$), and it was excluded from the final outcome. Minor leaf RWC changes on a daily

scale (Fig. 4.15) may explain the absence of a relationship with Ψ_{stem} . In the obtained multiple linear regression model, Ψ_{stem} was predicted from a linear combination of Ψ_{leaf} , g_l and VPD ($R^2 = 0.867$, $p < 0.001$, S.E. = 0.240), as shown in Eq. 4.4.

$$\Psi_{\text{stem}} = -0.311 + (0.882 \times \Psi_{\text{leaf}}) + (0.004 \times g_l) + (0.077 \times \text{VPD}) \quad (\text{Eq. 4.4})$$

Our results are in line with findings in nectarines and other woody species (Naor, 1998), where Ψ_{stem} was found to be related to leaf stomatal conductance (g_s) and Ψ_{leaf} .

Fruit diameter and leaf turgor pressure continuous sensing

The preliminary trial on FD, p_p , RGR and RPCR of East- and West-oriented trees did not show any significant effect of canopy orientation. As a consequence, at each of the fruit growth stages, FD and p_p data, as well as their derivatives (i.e. RGR and RPCR), from East- and West-oriented trees were pooled together. In control trees, FD showed an expected nocturnal increase with a diurnal lag phase (Fig. 4.19A). In the warmest hours of the day, p_p increased (Fig. 4.19B), being the inverse of p_c , as leaf turgor pressure was lost.

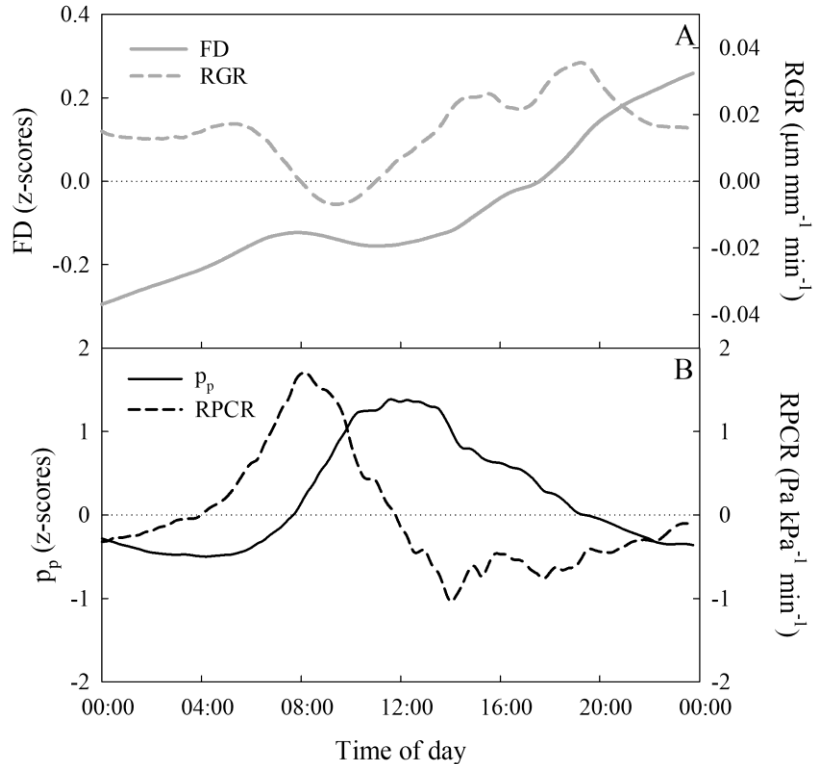


Figure 4.19. Diel trends of fruit diameter (FD, $n = 3$) and fruit relative growth rate (RGR, $n = 3$) (A), attenuated pressure of leaf patches (p_p) and leaf relative pressure change rate (RPCR) (B) in control irrigated trees at stage I (51 DAFB) of 'September Bright' nectarine fruit growth.

Initially, FD and p_p values, correspondent to the time of spot measurements of Ψ_{stem} , Ψ_{leaf} , g_l and leaf RWC from daily curves, were considered to determine whether any significant linear relationships occurred. Pearson's correlation analyses emphasised in most cases, no significance at all between FD and the water status indices, except for the association between FD and Ψ_{leaf} with a low correlation coefficient (Tab. 4.3). The inverse relationships with the highest correlation coefficients were found between p_p and leaf water status indices. Specifically, the highest coefficient corresponded to the p_p to Ψ_{leaf} correlation, due to the high influence of leaf turgor pressure on the total Ψ_{leaf} . The use of FD and p_p per se in association with plant water status indices is likely to hide information as there is an intrinsic delay in the adjustment of water in tissue in response to plant water deficit. Therefore, RGR and RPCR can be used to smooth delay of fruit and leaf responses to water deficit over time. Besides, the use of continuous data from leaves or fruit alone might not provide appropriate information on plant water status. Data from fruit diameter changes only are influenced by fruit development stage and fruit growth, while data of only leaf turgor pressure would ignore water balance in the other main organs capable of transpiration. Therefore, the association of RGR and RPCR dynamics can highlight leaf-to-fruit water exchanges, which in turn might reflect more precisely plant water status.

Table 4.3. Pearson's correlation coefficients for fruit diameter (FD) and attenuated leaf patch clamp pressure (p_p) vs plant water status (PWS) indicators: stem water potential (Ψ_{stem}), leaf water potential (Ψ_{leaf}), leaf hydraulic conductance (g_l) and leaf relative water content (RWC).

PWS indicator	FD (z-scores)	P-value	n	p_p (z-scores)	P-value	n
Ψ_{stem} (MPa)	-0.103	0.184	168	-0.320	<0.001	180
Ψ_{leaf} (MPa)	-0.296	0.009	78	-0.645	<0.001	84
RWC (%)	-0.156	0.066	140	-0.442	<0.001	150
g_l ($\text{mmol m}^{-2} \text{s}^{-1}$)	0.183	0.090	87	0.186	0.067	97

Subsequently, data of diel relationships (i.e. p_p vs FD and RPCR vs RGR) at 15-min intervals were plotted for a clear sky day at each stage of fruit development. Scatter plots in Figure 4.20 highlight anti-clockwise hysteretic relationships between RPCR and RGR. Similar trends were found for p_p vs FD associations (data not shown). Hysteresis among sensors' outputs and/or plant water status is common, especially when trunk or leaf indicators are considered (e.g. sap flow density, hydraulic conductance, diameter variations, Ψ_{leaf} , transpiration, etc.), and has been widely documented (Brough et al.,

1986; Cruziat et al., 1989; Granier et al., 1989; Ameglio and Cruziat, 1992; Tognetti et al., 1996; Fernández, 2017). The hysteretic behaviour was observed in all the fruit developmental stages, although it showed different patterns (Fig. 4.20). At stage I, there was a gradual increase of the hysteretic loop area as irrigation volume decreased, reaching its maximum size in the DI-0 treatment (Fig. 4.20A).

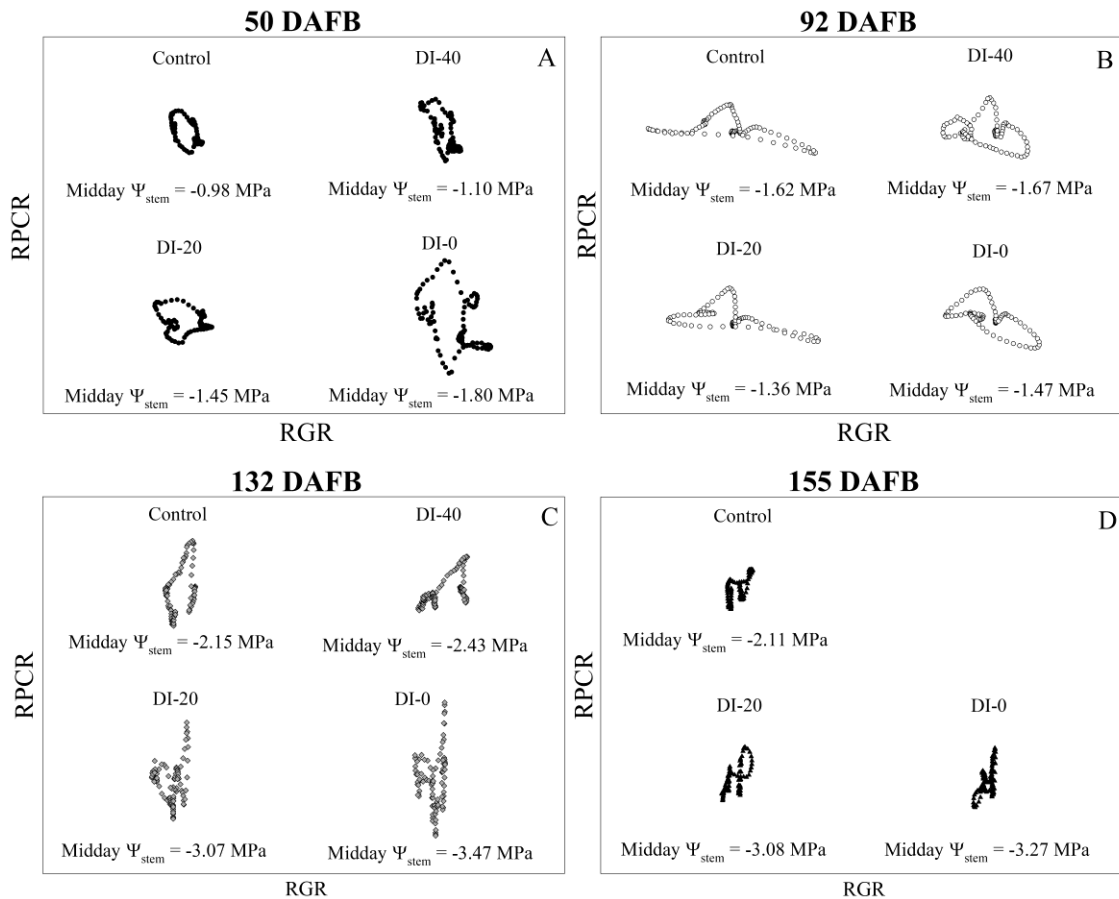


Figure 4.20. Scatter plots of diel leaf relative pressure change rate (RPCR) and fruit relative growth rate (RGR) in control, DI-40, DI-20 and DI-0 at stages I (A), II (B), IIIa (C) and IIIb (D) of 'September Bright' nectarine fruit growth. Midday Ψ_{stem} for each of the days considered is reported in its relative panel. Axis scales are equal in all panels and consequently omitted.

Nevertheless, a similar trend in loop area with higher levels of DI was not observed in the other stages, suggesting stage-dependent mechanisms of water regulation in fruits and leaves. In addition, the generally low midday Ψ_{stem} at stage IIIa and IIIb (i.e. always < -2.00 MPa) may have altered the hysteretic patterns. Hysteresis is likely to be caused by both a lag in tissue water de- and re-hydration, and nocturnal/diurnal inverted pattern of the RPCR to RGR association. Consequently, midday Ψ_{stem} was firstly associated with diel RGR and RPCR trends, and then with their diurnal (7.00 to 19.45h) and nocturnal (20.00 to 6.45h) subsets of data. The use of RGR

and RPCR was favoured over FD and p_p , as the former yielded the tightest associations with midday Ψ_{stem} . Diel, diurnal and nocturnal RGR and RPCR parameters (i.e. RSD, maximum, minimum, sum) from all the irrigation treatments were pooled together and their means were linearly regressed with midday Ψ_{stem} . Among all the significant ($P < 0.05$) regression models obtained, the highest R^2 were found when nocturnal maximum RGR (MAX_{RGR}) (Fig. 4.21A) and minimum diel RPCR (MIN_{RPCR}) (Fig. 4.21B) were related to midday Ψ_{stem} . The non-linear model in Figure 4.21A can be explained with the fact that a limited water deficit is needed for maximum fruit cell expansion due to rehydration (i.e. peak at -1.56 MPa). Oppositely, at Ψ_{stem} near -1.00 MPa, fruit cell turgor is higher and less water is drawn from nearby organs. When Ψ_{stem} reaches particularly low levels (~ -3.50 MPa) maximum RGR tends to zero.

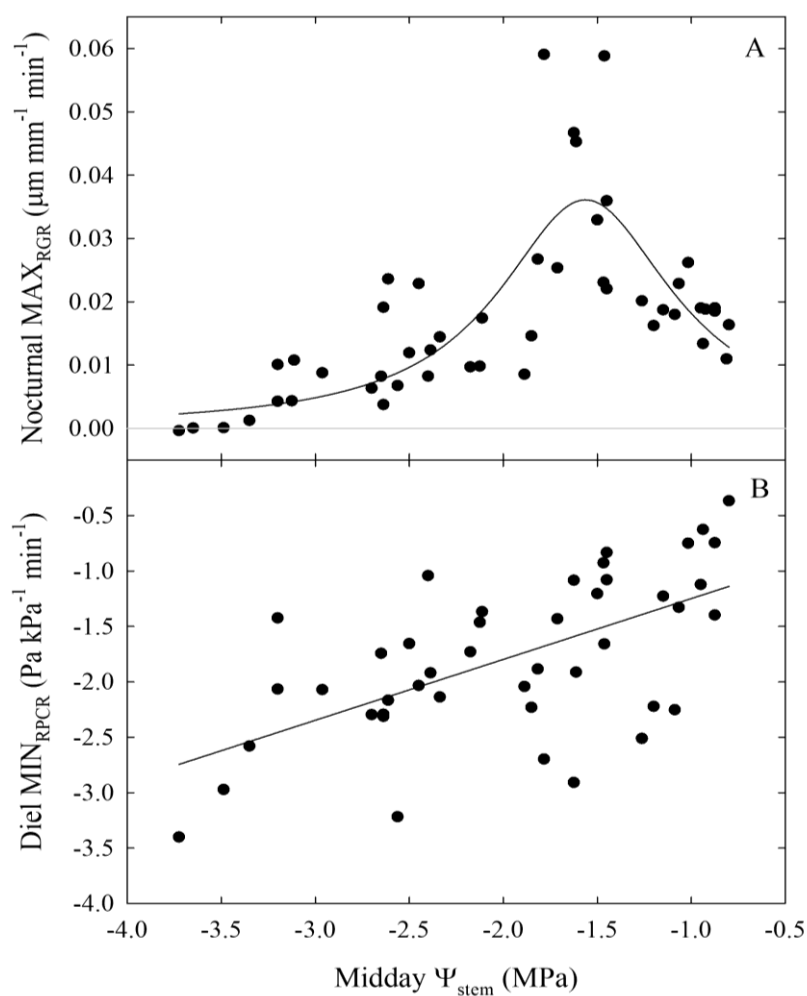


Figure 4.21. Maximum nocturnal fruit relative growth rate (MAX_{RGR}) vs midday Ψ_{stem} (A) and minimum diel leaf relative pressure change rate (MIN_{RPCR}) vs midday Ψ_{stem} (B). Nonlinear regression in panel A: $\text{MAX}_{\text{RGR}} = 0.04 / \{1 + [(\Psi_{\text{stem}} + 1.56) / 0.57]^2\}$, $R^2 = 0.597$, $P < 0.001$. Linear regression in panel B: $\text{MIN}_{\text{RPCR}} = -0.70 + 0.55 \times \Psi_{\text{stem}}$, $R^2 = 0.369$, $P < 0.001$. Data from all fruit growth stages included in the models.

The linear relationship between Ψ_{stem} and MIN_{RPCR} showed a loose but direct association (Fig. 4.21B), in contrast with findings in olive where Marino et al. (2016) instead found an inverse linear relationship. In our case, even the linear regression between p_p (the indicator used by Marino et al., 2016), rather than RPCR , and midday Ψ_{stem} resulted in a direct relationship, although with a lower R^2 (0.247) than the former (data not shown). The inverse relationship found by Marino et al. (2016) in olive was expected as p_p is the inverse of turgor pressure, which is instead directly related to Ψ_{stem} . In our case, MIN_{RPCR} indicates the speed at which dehydrating leaves draw water from nearby tissues. Therefore, the direct relationship between MIN_{RPCR} and Ψ_{stem} shows that such instantaneous water pulling force increases with water deficit, allowing leaves to maintain minimum hydration and escape desiccation and death. Indeed, a $\Psi_{\text{stem}} < 3.00$ MPa could be fatal for nectarine trees if a drought avoidance mechanism is not activated. On the other hand, olive can easily tolerate leaf dehydration at similar levels of Ψ_{stem} .

Insights from Figures 4.20 and 4.21 suggested that ratios of RGR to RPCR might be better indicators of midday Ψ_{stem} , by combining fruit and leaf water relations. More specifically, the changes in hysteretic patterns (Fig. 4.20) indicated that RGR/RPCR variance may be strictly related to midday Ψ_{stem} variations, as the shape of the loop changed along with increasing water deficit. However, hystereses were also likely to be shaped by intrinsic parameters of diel, diurnal and nocturnal variations, such as maximum, minimum and sum. As a consequence, linear regression models considered RGR -to- RPCR ratios for all these parameters regressed vs midday Ψ_{stem} . The only two linear models with $R^2 > 0.3$ were found for nocturnal data using the $\text{RSD}_{\text{RGR}}/\text{RSD}_{\text{RPCR}}$ ($R^2 = 0.346$) and $\text{MAX}_{\text{RGR}}/\text{MAX}_{\text{RPCR}}$ ($R^2 = 0.318$) ratios. The latter relationship was mostly derived from the significant association found in Figure 4.21A, as the response to midday Ψ_{stem} had a similar peak trend, but with a lower R^2 (0.405). Therefore, the $\text{MAX}_{\text{RGR}}/\text{MAX}_{\text{RPCR}}$ ratio was discarded.

Finally, stepping forward to the strongest association with midday Ψ_{stem} , the scatter plot showed an inverse non-linear association (Fig. 4.22C), suggesting that the model might be both composed by a linear phase at higher values of Ψ_{stem} and by an exponential phase at lower Ψ_{stem} . In accordance with our hypothesis, the diurnal regression tended to show an opposite trend, although no significant association was found (Fig. 4.22B). The diel regression reflected the unpredictable hysteretic behaviour seen in Figure 4.20, resulting in the weakest, non-significant association (Fig. 4.22A).

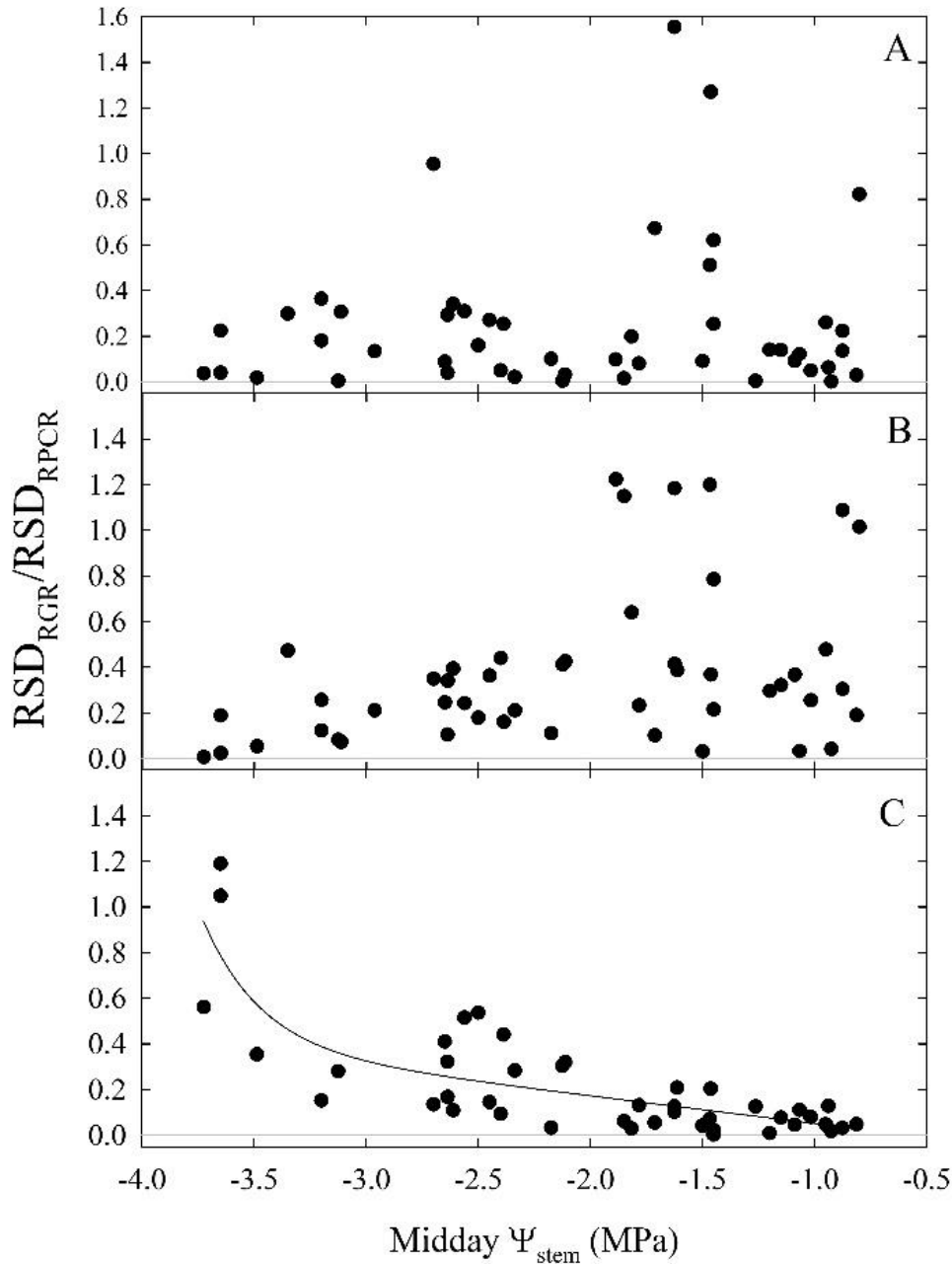


Figure 4.22. Diel (A), diurnal (B) and nocturnal ratios (C) of relative standard deviations of fruit relative growth rate (RSD_{RGR}) and leaf relative pressure change rate (RSD_{RPCR}) vs midday Ψ_{stem} . Expo-linear model in panel C: $RSD_{RGR}/RSD_{RPCR} = -0.07 + 2.88E-07 \times \exp(-3.89 \times \Psi_{stem}) - 0.12 \times \Psi_{stem}$, $R^2 = 0.650$, $P < 0.001$. Data from all fruit growth stages included in the model.

The association of nocturnal RSD_{RGR}/RSD_{RPCR} to Ψ_{stem} (Fig. 4.22C) shifted from linear to exponential at midday $\Psi_{stem} \cong -2.3$ MPa, suggesting that this water deficit level might be identified as a threshold under which late ripening 'September Bright' nectarine trees are significantly affected by drought. Below the level of -2.3 MPa the RSD of nocturnal fruit growth increases with respect to the one of leaf turgor pressure.

For instance, the slight decrease in fruit diameter occurring between 154 and 161 DAFB in DI-0 trees (Fig. 4.11D) induces an increase in nocturnal RSD_{RGR} while RSD_{RPCR} does not change, generating the observed increase of RSD_{RGR}/RSD_{RPCR} . At stage III, peach and nectarine stomata become dysfunctional (Chalmers et al., 1983) and high transpiration rates can overcome level of phloem and xylem inflows in fruits (Lescourret et al., 2001; Morandi et al., 2007a). This phenomenon generates particularly low fruit water potential and causes an increase in water potential difference between leaves and fruit (McFadyen et al., 1996), as found in olive by Fernandes et al. (2018). Therefore, the different regulation of water balance in fruits and leaves may provide a very useful parameter for real-time and continuous monitoring of plant water status.

The identified stage-independent threshold of midday $\Psi_{stem} = -2.3$ MPa might be used for irrigation management in commercial 'September Bright' nectarine orchards under environmental conditions similar to the ones of this study. However, it probably would not be effective at stage I, as trees exposed to DI at this stage never reached such low levels of Ψ_{stem} , despite yielding fruit with significantly lower final size compared to control irrigated trees (i.e. average fruit diameter at harvest equal to $53.3 \text{ mm} \pm 0.44$ vs $58.6 \text{ mm} \pm 0.81$ for DI and control, respectively). Hence, it is legitimate to think that, to some extent, trees adjust to water deficit levels throughout the season and different Ψ_{stem} thresholds should be considered at each fruit growth stage for irrigation management.

CONCLUSIONS

Overall, this work highlights the appropriateness of a multi-organ, fruit-to-leaf sensing approach for the quality of continuous monitoring of tree water status. On one side, the leaf sensing approach guarantees a fast and responsive signal based on leaf turgor pressure, which represents a pre-alarm forecast for irrigation management. On the other side, continuous fruit size sensing provides the exact information on the time lag and plant dehydration level to which deficit irrigation can be pushed before fruit growth and yield are significantly affected. Both together, leaf and fruit sensing provide a powerful and reliable tool that is not influenced by the fruit development stage and that can be continuously used to detect plant water status and irrigation thresholds. At this regard, further efforts should be made to develop new fruit and leaf sensing technologies that reduce the likelihood to damage organs during the period of data collection. Further investigations need also to be carried out considering fruit-to-leaf water balance, perhaps promoting models which considers together nocturnal to diurnal

shift within the diel hysteresis of fruit growth vs leaf turgor pressure, and the lag in time characterising the hysteretic loop.

ACKNOWLEDGEMENTS

The technical support and assistance of Dave Haberfield, Jim Selman, Athulya Jancy Benny, Andrew O'Connell and Cameron O'Connell, and the scientific support provided by Ian Goodwin, Des Whitfield, Subhash Chandra and Steve Green are gratefully acknowledged. The experiment was supported by a PhD project funded with a scholarship issued by the Italian Ministry of Education and the University of Palermo, and by the stone fruit experimental orchard project (SF17006 Summerfruit Orchard - Phase II) funded by Hort Innovation using Summerfruit levy and funds from the Australian Government with co-investment from Agriculture Victoria.

LIST OF REFERENCES

- Allen, R. G., Pereira, L. S., Raes, D., & Smith, M. (1998). Crop evapotranspiration-Guidelines for computing crop water requirements-FAO Irrigation and drainage paper 56. FAO, Rome, 300(9), D05109.
- Ameglio, T., & Cruziat, P. (1992). Daily variations of stem and branch diameter: short overview from a developed example. In *Mechanics of swelling* (pp. 193-204). Springer, Berlin, Heidelberg.
- Ballester, C., Castiella, M., Zimmermann, U., Rüger, S., Martínez Gimeno, M. A., & Intrigliolo, D. S. (2015, June). Usefulness of the ZIM-probe technology for detecting water stress in clementine and persimmon trees. In *VIII International Symposium on Irrigation of Horticultural Crops 1150* (pp. 105-112).
- Barrs, H. D., & Weatherley, P. E. (1962). A re-examination of the relative turgidity technique for estimating water deficits in leaves. *Australian Journal of Biological Sciences*, 15(3), 413-428.
- Blanco-Cipollone, F., Lourenço, S., Silvestre, J., Conceição, N., Moñino, M. J., Vivas, A., & Ferreira, M. I. (2017). Plant Water Status Indicators for Irrigation Scheduling Associated with Iso-and Anisohydric Behavior: Vine and Plum Trees. *Horticulturae*, 3(3), 47.
- Blanke, M. M., & Lenz, F. (1989). Fruit photosynthesis. *Plant, Cell & Environment*, 12(1), 31-46.
- Brough, D. W., Jones, H. G., & Grace, J. (1986). Diurnal changes in water content of the stems of apple trees, as influenced by irrigation. *Plant, Cell & Environment*, 9(1), 1-7.
- Burquez, A. (1987). Leaf thickness and water deficit in plants: a tool for field studies. *Journal of Experimental Botany*, 38(1), 109-114.
- Chalmers, D. J., & Ende, B. V. D. (1975). A reappraisal of the growth and development of peach fruit. *Functional Plant Biology*, 2(4), 623-634.
- Chalmers, D. J., Mitchell, P. D., & van Heek, L. (1981). Control of peach tree growth and productivity by regulated water supply, tree density, and summer pruning. *J. Amer. Soc. Hort. Sci.*, 106, 307-312.
- Chalmers, D. J., Olsson, K. A., & Jones, T. R. (1983). Water relations of peach trees and

- orchards. *Additional Woody Crop Plants*, 7, 197.
- Chalmers, D. J., Burge, G., Jerie, P. H., & Mitchell, P. D. (1986). The mechanism of regulation of 'Bartlett' pear fruit and vegetative growth by irrigation withholding and regulated deficit irrigation. *Journal of the American Society for Horticultural Science (USA)*.
- Conejero, W., Alarcón, J. J., García-Orellana, Y., Nicolás, E., & Torrecillas, A. (2007). Evaluation of sap flow and trunk diameter sensors for irrigation scheduling in early maturing peach trees. *Tree physiology*, 27(12), 1753-1759.
- Connors, C. H. (1919). Growth of fruits of peach. *New Jersey Agric. Exp. Stn. Annu. Rep.*, 40, 82-88.
- Cruziat, P., Granier, A., Claustres, J. P., & Lachaize, D. (1989). Diurnal evolution of water flow and potential in an individual spruce: experimental and theoretical study. In *Annales des Sciences Forestières (Vol. 46, No. Supplement, pp. 353s-356s)*. EDP Sciences.
- DeJong, T. M., & Goudriaan, J. (1989). Modeling peach fruit growth and carbohydrate requirements: reevaluation of the double-sigmoid growth pattern. *Journal of the American Society for Horticultural Science*, 114, 800-804.
- Ehrenberger, W., Rüger, S., Rodríguez-Domínguez, C. M., Díaz-Espejo, A., Fernández, J. E., Moreno, J., ... & Zimmermann, U. (2012). Leaf patch clamp pressure probe measurements on olive leaves in a nearly turgorless state. *Plant Biology*, 14(4), 666-674.
- Fereres, E., & Soriano, M. A. (2007). Deficit irrigation for reducing agricultural water use. *Journal of experimental botany*, 58(2), 147-159.
- Fernandes, R. D. M., Cuevas, M. V., Diaz-Espejo, A., & Hernandez-Santana, V. (2018). Effects of water stress on fruit growth and water relations between fruits and leaves in a hedgerow olive orchard. *Agricultural Water Management*, 210, 32-40.
- Fernández, J. E., Rodríguez-Domínguez, C. M., Perez-Martin, A., Zimmermann, U., Rüger, S., Martín-Palomo, M. J., ... & Diaz-Espejo, A. (2011). Online-monitoring of tree water stress in a hedgerow olive orchard using the leaf patch clamp pressure probe. *Agricultural Water Management*, 100(1), 25-35.
- Fernández, J. E. (2017). Plant-based methods for irrigation scheduling of woody crops. *Horticulturae*, 3(2), 35.
- Génard, M., & Huguet, J. G. (1996). Modeling the response of peach fruit growth to water stress. *Tree Physiology*, 16(4), 407-415.
- Girona, J., Gelly, M., Mata, M., Arbones, A., Rufat, J., & Marsal, J. (2005). Peach tree response to single and combined deficit irrigation regimes in deep soils. *Agricultural Water Management*, 72(2), 97-108.
- Goldhamer, D. A., Fereres, E., Mata, M., Girona, J., & Cohen, M. (1999). Sensitivity of continuous and discrete plant and soil water status monitoring in peach trees subjected to deficit irrigation. *Journal of the American Society for Horticultural Science*, 124(4), 437-444.
- Goodwin, I., Whitfield, D. M., & Connor, D. J. (2006). Effects of tree size on water use of peach (*Prunus persica* L. Batsch). *Irrigation Science*, 24(2), 59-68.
- Granier, A., Breda, N., Claustres, J. P., & Colin, F. (1989). Variation of hydraulic conductance of some adult conifers under natural conditions. In *Annales des Sciences Forestières (Vol. 46, No. Supplement, pp. 357s-360s)*. EDP Sciences.
- Jones, H. G. (2004). Irrigation scheduling: advantages and pitfalls of plant-based methods. *Journal of experimental botany*, 55(407), 2427-2436.
- Jones, H. G. (2007). Monitoring plant and soil water status: established and novel methods revisited and their relevance to studies of drought tolerance. *Journal of*

- experimental botany, 58(2), 119-130.
- Koide, R. T., Robichaux, R. H., Morse, S. R., & Smith, C. M. (1989). Plant water status, hydraulic resistance and capacitance. In *Plant physiological ecology* (pp. 161-183). Springer, Dordrecht.
- Lang, A. (1990). Xylem, phloem and transpiration flows in developing apple fruits. *Journal of Experimental Botany*, 41(6), 645-651.
- Lescourret, F., Génard, M., Habib, R., & Fishman, S. (2001). Variation in surface conductance to water vapor diffusion in peach fruit and its effects on fruit growth assessed by a simulation model. *Tree Physiology*, 21(11), 735-741.
- Li, S. H., Huguet, J. G., Schoch, P. G., & Orlando, P. (1989a). Response of peach tree growth and cropping to soil water deficit at various phenological stages of fruit development. *Journal of Horticultural Science*, 64(5), 541-552.
- Li, S. H., Huguet, J. G., & Bussi, C. (1989b). Irrigation scheduling in a mature peach orchard using tensiometers and dendrometers. *Irrigation and Drainage Systems*, 3(1), 1-12.
- Lo Bianco, R., & Scalisi, A. (2017). Water relations and carbohydrate partitioning of four greenhouse-grown olive genotypes under long-term drought. *Trees*, 31(2), 717-727.
- Losciale, P., Zibordi, M., Manfrini, L., Morandi, B., Bastias, R.M. and Corelli Grappadelli, L. (2011). Light management and photoinactivation under drought stress in peach. *Acta Hort.* 922, 341-347. DOI: 10.17660/ActaHortic.2011.922.44
- Marino, G., Pernice, F., Marra, F. P., & Caruso, T. (2016). Validation of an online system for the continuous monitoring of tree water status for sustainable irrigation managements in olive (*Olea europaea* L.). *Agricultural Water Management*, 177, 298-307.
- Marsal, J., & Girona, J. (1997). Relationship between leaf water potential and gas exchange activity at different phenological stages and fruit loads in peach trees. *Journal of the American Society for Horticultural Science*, 122(3), 415-421.
- Martínez-Gimeno, M. A., Castiella, M., Rüger, S., Intrigliolo, D. S., & Ballester, C. (2017). Evaluating the usefulness of continuous leaf turgor pressure measurements for the assessment of Persimmon tree water status. *Irrigation Science*, 35(2), 159-167.
- McCutchan, H., & Shackel, K. A. (1992). Stem-water potential as a sensitive indicator of water stress in prune trees (*Prunus domestica* L. cv. French). *Journal of the American Society for Horticultural Science*, 117(4), 607-611.
- McFadyen, L. M., Hutton, R. J., & Barlow, E. W. R. (1996). Effects of crop load on fruit water relations and fruit growth in peach. *Journal of Horticultural Science*, 71(3), 469-480.
- Morandi, B., Rieger, M., & Corelli Grappadelli, L. (2007a). Vascular flows and transpiration affect peach (*Prunus persica* Batsch.) fruit daily growth. *Journal of Experimental Botany*, 58(14), 3941-3947.
- Morandi, B., Manfrini, L., Zibordi, M., Noferini, M., Fiori, G., & Corelli Grappadelli, L. (2007b). A low-cost device for accurate and continuous measurements of fruit diameter. *HortScience*, 42(6), 1380-1382.
- Morandi, B., Manfrini, L., Losciale, P., Zibordi, M., & Corelli Grappadelli, L. (2010a). The positive effect of skin transpiration in peach fruit growth. *Journal of plant physiology*, 167(13), 1033-1037.
- Morandi, B., Manfrini, L., Losciale, P., Zibordi, M., & Corelli Grappadelli, L. (2010b). Changes in vascular and transpiration flows affect the seasonal and daily growth

- of kiwifruit (*Actinidia deliciosa*) berry. *Annals of botany*, 105(6), 913-923.
- Morandi, B., Losciale, P., Manfrini, L., Zibordi, M., Anconelli, S., Pierpaoli, E., & Corelli Grappadelli, L. (2014). Leaf gas exchanges and water relations affect the daily patterns of fruit growth and vascular flows in Abbé Fétel pear (*Pyrus communis* L.) trees. *Scientia Horticulturae*, 178, 106-113.
- Mossad, A., Scalisi, A., & Lo Bianco, R. (2018). Growth and water relations of field-grown 'Valencia' orange trees under long-term partial rootzone drying. *Irrigation Science*, 36(1), 9-24.
- Naor, A. (1998). Relations between leaf and stem water potentials and stomatal conductance in three field-grown woody species. *The Journal of Horticultural Science and Biotechnology*, 73(4), 431-436.
- Naor, A. (1999). Midday stem water potential as a plant water stress indicator for irrigation scheduling in fruit trees. In III International Symposium on Irrigation of Horticultural Crops 537 (pp. 447-454).
- Naor, A., Klein, I., Hupert, H., Grinblat, Y., Peres, M., & Kaufman, A. (1999). Water stress and crop level interactions in relation to nectarine yield, fruit size distribution, and water potentials. *Journal of the American Society for Horticultural Science*, 124(2), 189-193.
- Naor, A., Hupert, H., Greenblat, Y., Peres, M., Kaufman, A., & Klein, I. (2001). The response of nectarine fruit size and midday stem water potential to irrigation level in stage III and crop load. *Journal of the American Society for Horticultural Science*, 126(1), 140-143.
- Naor, A. (2006). Irrigation scheduling and evaluation of tree water status in deciduous orchards. *Horticultural reviews*, 32, 111-165.
- Paço, T. A., Ferreira, M. I., & Conceição, N. (2006). Peach orchard evapotranspiration in a sandy soil: Comparison between eddy covariance measurements and estimates by the FAO 56 approach. *Agricultural Water Management*, 85(3), 305-313.
- Padilla-Díaz, C. M., Rodriguez-Dominguez, C. M., Hernandez-Santana, V., Perez-Martin, A., & Fernández, J. E. (2016). Scheduling regulated deficit irrigation in a hedgerow olive orchard from leaf turgor pressure related measurements. *Agricultural Water Management*, 164, 28-37.
- Rodriguez-Dominguez, C. M., Ehrenberger, W., Sann, C., Rüger, S., Sukhorukov, V., Martín-Palomo, M. J., ... & Zimmermann, U. (2012). Concomitant measurements of stem sap flow and leaf turgor pressure in olive trees using the leaf patch clamp pressure probe. *Agricultural water management*, 114, 50-58.
- Rüger, S., Netzer, Y., Westhoff, M., Zimmermann, D., Reuss, R., Ovadiya, S., ... & Zimmermann, U. (2010). Remote monitoring of leaf turgor pressure of grapevines subjected to different irrigation treatments using the leaf patch clamp pressure probe. *Australian Journal of Grape and Wine Research*, 16(3), 405-412.
- Savitzky, A., & Golay, M. J. (1964). Smoothing and differentiation of data by simplified least squares procedures. *Analytical chemistry*, 36(8), 1627-1639.
- Scalisi, A., Bresilla, K., & Simões Grilo, F. (2017). Continuous determination of fruit tree water-status by plant-based sensors. *Italus Hortus*, 24(2), 39-50. doi:10.26353/j.itahort/2017.2.3950
- Shackel, K. A., Ahmadi, H., Biasi, W., Buchner, R., Goldhamer, D., Gurusinghe, S., ... & McGourty, G. (1997). Plant water status as an index of irrigation need in deciduous fruit trees. *HortTechnology*, 7(1), 23-29.
- Simonneau, T., Habib, R., Goutouly, J. P., & Hugué, J. G. (1993). Diurnal changes in stem diameter depend upon variations in water content: direct evidence in peach

- trees. *Journal of Experimental Botany*, 44(3), 615-621.
- Steppe, K., De Pauw, D. J., & Lemeur, R. (2008). A step towards new irrigation scheduling strategies using plant-based measurements and mathematical modelling. *Irrigation Science*, 26(6), 505.
- Tognetti, R., Raschi, A., Béres, C., Fenyvesi, A., & Ridder, H. W. (1996). Comparison of sap flow, cavitation and water status of *Quercus petraea* and *Quercus cerris* trees with special reference to computer tomography. *Plant, Cell & Environment*, 19(8), 928-938.
- Turner, N. C. (1988). Measurement of plant water status by the pressure chamber technique. *Irrigation science*, 9(4), 289-308.
- Zimmermann, D., Reuss, R., Westhoff, M., Geßner, P., Bauer, W., Bamberg, E., ... & Zimmermann, U. (2008). A novel, non-invasive, online-monitoring, versatile and easy plant-based probe for measuring leaf water status. *Journal of Experimental Botany*, 59(11), 3157-3167.
- Zimmermann, U., Rüger, S., Shapira, O., Westhoff, M., Wegner, L. H., Reuss, R., ... & Schwartz, A. (2010). Effects of environmental parameters and irrigation on the turgor pressure of banana plants measured using the non-invasive, online monitoring leaf patch clamp pressure probe. *Plant Biology*, 12(3), 424-436.

5. GENERAL CONCLUSIONS

Fruit- and leaf- based sensing represents a valuable tool for determining plant water deficit in high-density olive and nectarine orchards. While sensing leaf turgor pressure changes provides a pre-alarm forecast for irrigation management, detecting fruit size variations gives insights on the level of water deficit at which fruit growth and yield are significantly affected. Combined fruit-leaf sensing represents a high-quality approach for the continuous assessment of tree water status that can also be recommended for other fruit species of horticultural interest as predictor of plant water status. However, different modelling criteria need to be used in each species and even genotypes, as fruit and leaf responses to drought may differ sensibly, as described for the olive genotypes in Chapter 3 of this dissertation.

Modelling fruit and leaf responses to water deficit might provide the basis for a consequent automation of irrigation in response to pre-defined thresholds, being a tool of strategic help for growers who are trying to reach almost full mechanisation of farm operations. Nevertheless, the currently available sensing technologies for fruit and leaves are still not very easy to manage for unskilled workers. Therefore, there is an increasing need for support from specialised companies that can advise growers on the best moment to irrigate by accessing real-time data from the orchards. In addition, further efforts should be made to develop new fruit and leaf sensing technologies which reduce the likelihood to damage organs during the period of data collection. In future studies new technologies based on different sensing principles can be tested, in order to drastically reduce or almost cancel the influence of the probe on fruit and leaf physiological processes (e.g. photosynthesis, transpiration, light interception, etc.).

An integrated approach that considers the simultaneous use of sensors on fruit, leaf and other plant organs (e.g. trunk) is suggested to collect integrative information on plant water status. The development of whole-plant models that provide real-time information on water indicators based on continuous sensing is certainly a highly challenging goal for scientists, farmers and entrepreneurs who aim to an efficient total automation of fruit crop irrigation. Finally, our results can be used to stimulate a further understanding of fruit and leaf ecophysiological responses in dry and semi-dry environments, being increasingly relevant in areas that will be affected by reduced water availability as a consequence of climate changes.